DOKUZ EYLÜL UNIVERSITY
GRADUATE SCHOOL OF NATURAL AND APPLIED SCIENCES

MICROBIAL SUPPORT PARTICLE SELECTION FOR HYDROGEN GAS PRODUCTION IN AN IMMOBILIZED REACTOR SYSTEM BY DARK FERMENTATION

by
Pelin GÖKFİLİZ

July, 2014
İZMİR

MICROBIAL SUPPORT PARTICLE SELECTION FOR HYDROGEN GAS PRODUCTION IN AN IMMOBILIZED REACTOR SYSTEM BY DARK FERMENTATION

A Thesis Submitted to the
Graduate School of Natural and Applied Sciences of Dokuz Eylül University
In Partial Fulfillment of the Requirements for the Degree of Master of Science
in Biotechnology

by
Pelin GÖKFİLİZ

July, 2014
İZMİR

M.Sc THESIS EXAMINATION RESULT FORM

We have read the thesis entitled **"MICROBIAL SUPPORT PARTICLE SELECTION FOR HYDROGEN GAS PRODUCTION IN AN IMMOBILIZED REACTOR SYSTEM BY DARK FERMENTATION"** completed by **PELİN GÖKFİLİZ** under supervision of **PROF. DR. İLGİ KARAPINAR KAPDAN** and we certify that in our opinion it is fully adequate, in scope and in quality, as a thesis for the degree of Master of Science.

Prof. Dr. İlgi KARAPINAR KAPDAN

Supervisor

Prof. Dr. Yılmaz Büyüktaşoğlu

(Jury Member)

Prof. Dr. Leman Tarhan

(Jury Member)

Prof.Dr. Ayşe OKUR

Director

Graduate School of Natural and Applied Sciences

ACKNOWLEDGMENTS

I would like to express my special appreciation and thanks to my advisor Prof. Dr. İlgi KARAPINAR KAPDAN. I feel so lucky that I had a chance to study biohydrogen with her who is one of the pioneers of this field in Turkey. She was always so understanding, kind and supportive towards me during my Master Degree studies. I believe that her advice and experiences will guide me during my life.

I would also like to thank Prof. Dr. Leman TARHAN, Prof. Dr. Raziye ÖZTÜRK ÜREK and Asst. Prof. Serkan EKER for their contribution and guidance.

I wish to thank Hasan ÇETİN, Betül KIRLI and Onur BALCAN for their helps and friendships. I would like to give my sincere thanks to Sılay Aytaç KURT for her encouragement, insightful comments and patience during our endless phone call.

Lastly, a special thanks to my family; my father Mehmet GÖKFİLİZ and my mother Aycan GÖKFİLİZ. This thesis would not have been possible without their support and patience. They always encouraged me and believed in me. Their presence helped me to feel strong during my hard days and sleepless night. I love them.

Pelin GÖKFİLİZ

MICROBIAL SUPPORT PARTICLE SELECTION FOR HYDROGEN GAS PRODUCTION IN AN IMMOBILIZED REACTOR SYSTEM BY DARK FERMENTATION

ABSTRACT

The thesis aimed to determine the significant factors that affect hydrogen production by dark fermentation in immobilized systems. For this purpose, batch fermentation experiments were conducted to investigate effect of support particle type, size and number, also initial substrate concentration and temperature on hydrogen yield and production rate. Waste wheat was the substrate and hydrolyzed in diluted sulfuric acid at high temperature. Heat and acid pretreatment method was applied to anaerobic sludge to eliminate methanogens and select spore forming hydrogen producing bacteria like *Clostridium* sp. Total gas volume and hydrogen percentage in total gas were measured daily, total sugar and total volatile fatty acid concentration were determined at the beginning and end of the fermentation. Stainless steel scrubber, volcanic stone, tulle, polyester fiber, loofah sponge, plastic bath sponge, sea sponge and aquarium biological sponge were used as support materials in fermentation medium to investigate hydrogen production potentials of these particles. Experiments were conducted at different initial substrate concentration under thermophilic condition. Maximum hydrogen yield was obtained with polyester fiber and this particle was selected as support particle for further studies. In order to investigate effect of support particle size on hydrogen production, batch fermentation experiments were carried out with polyester fiber particles at different particle sizes. The highest hydrogen yield was obtained with the particles at zero point five centimeters in diameter. Finally, the effects of particle number, initial substrate concentration and temperature on hydrogen yield and production rate were evaluated by using Box–Wilson statistical experiment design method and optimum conditions were determined for the maximum hydrogen yield and rate of production.

Keywords: Biohydrogen, batch dark fermentation, immobilized system, support particle, Box–Wilson statistical design method.

İMMOBİLİZE REAKTÖR SİSTEMLERİNDE KARANLIK FERMENTASYONLA HİDROJEN GAZI ÜRETİMİ İÇİN MİKRORGANİZMA DESTEK TANECİĞİ SEÇİMİ

ÖZ

Tez çalışmasının amacı, bağlı büyümeli sistemlerde karanlık fermentasyon ile biyohidrojen üretimini etkileyen önemli faktörlerin belirlenmesidir. Bu amaçla, destek taneciği türünün, boyutunun, sayısının, başlangıç substrat derişiminin ve fermentasyon sıcaklığının hidrojen üretim verimi ve hızı üzerindeki etkisi kesikli fermentasyon deneyleri ile incelenmiştir. Öğütülmüş atık buğday karbon kaynağı olarak kullanılmış ve seyreltilmiş asit ve yüksek sıcaklıkta hidrolize edilmiştir. Anaerobik çamur mikrobiyal kültür olarak kullanılmış, metanojenleri elimine etmek ve *Clostridium* sp gibi spor oluşturan hidrojen üreten bakterileri seçmek amacıyla anaerobik çamura ısıl ve asit önişlemleri uygulanmıştır. Deneysel çalışmalarda toplam gaz hacmi ve hidrojen yüzdesi, toplam şeker tüketimi ve uçucu yağ asidi oluşumu izlenmiştir. Paslanmaz çelik bulaşık teli, volkanik taş, tül, elyaf, kabak lifi, plastik banyo süngeri, deniz süngeri ve biyolojik sünger mikroorganizma destek taneciği olarak kullanılmış ve bu parçacıklarla hidrojen üretim potansiyeli araştırılmıştır. Farklı substrat derişimlerinde ve termofilik şartlarda parçacık seçimi deneysel çalışmaları sonucunda en yüksek üretim verimi elyaf ile elde edilmiş ve bundan sonraki çalışmalarda destek taneciği olarak kullanılmıştır. Destek taneciği boyutunun hidrojen üretimi üzerindeki etkisini araştırmak amacıyla farklı boyutlardaki destek tanecikleri ile hidrojen üretimi çalışmaları yapılmış ve en yüksek verim sıfır nokta beş santimetre tanecik çapında gözlenmiştir. Son aşamada, Box–Wilson istatistiksel deney tasarım metodu kullanılarak parçacık sayısının, başlangıç substrat konsantrasyonunun ve sıcaklığın hidrojen verimi ve üretim hızı üzerine etkisi araştırılmış ve maksimum üretim verimi ve hızı için optimum şartlar belirlenmiştir.

Anahtar kelimeler: Biyohidrojen, kesikli karanlık fermentasyon, immobilize sistem, destek taneciği, Box–Wilson deneysel tasarım metodu.

CONTENTS

Page

THESIS EXAMINATION RESULT FORM ii
ACKNOWLEDGEMENTS iii
ABSTRACT iv
ÖZ v
LIST OF FIGURES ix
LIST OF TABLES xiv

CHAPTER ONE – INTRODUCTION 1

1.1 Bio-hydrogen Gas Production 1
1.2 Biochemical Aspects of Biohydrogen Production by Dark Fermentation 5
1.3 Major Challanges and Improvement Strategy in Biohydrogen Production by Dark Fermentation 8
1.3.1 Metabolic Pathways and End Products 8
1.3.2 Type of Substrates and Media Composition 9
1.3.3 Inoculum Type 10
1.3.4 Operating Conditions 11
1.3.5 Cultivation Type 12
1.4 Literature Review 16
1.5 Scope and Objective 19

CHAPTER TWO - MATERIALS AND METHODS 21

2.1 Batch Dark Fermentation 21
2.1.1 Organisms 21
2.1.2 Preparation of Acid Hydrolyzed Wheat Starch (AHWS) 21
2.1.3 Selection of Support Material 22
2.1.3.1 Support Material Preparation and Immobilization of Anaerobic Sludge 22
2.1.4 The Effect of Support Material Size on Biohydrogen Production 24

2.1.4.1 Support Material Preparation and Immobilization of Anaerobic Sludge 24
2.1.5 Box-Wilson Statistical Experiment Design 25
2.2 Analytical Methods 28
2.2.1 Sampling 28
2.2.2 Total Sugar Analysis 28
2.2.3 Total Vololite Fatty Acid (TVFA) Analysis 29
2.2.4 Total Gas Volume Measurement 29
2.2.5 H_2 Gas Measurements 29
2.2.6 pH and ORP Measurements 29
2.2.7 Calculations 29

CHAPTER THREE - RESULTS AND DISCUSSIONS 32

3.1 Selection of Support Material 32
3.1.1 The Effect of Initial Total Sugar Concentration 32
3.1.1.1 Control 32
3.1.1.2 Stainless Steel Scrubber 34
3.1.1.3 Volcanic Stone 35
3.1.1.4 Tulle 37
3.1.1.5 Polyester Fiber 38
3.1.1.6 Loofah Sponge 40
3.1.1.7 Plastic Bath Sponge 41
3.1.1.8 Sea Sponge 42
3.1.1.9 Aquarium Biological Sponge 44
3.1.1.10 Comparison 45
3.2 The Effect of Support Material Size 50
3.3 Box-Wilson Statistical Experiment Design 53
3.3.1 The Effect of Independent Variables on Hydrogen Yield 54
3.3.2 The Effect of Independent Variables on Hydrogen Production Rate 67

3.3.3 Optimization of Dark Fermentation Operating Conditions for Hydrogen Yield and Hydrogen Production Rate 75

CHAPTER FOUR – CONCLUSIONS AND RECOMMENDATIONS 76

REFERENCES 81

APPENDICES 89

LIST OF FIGURES

Page

Figure 1.1 Active site structures of the three hydrogenases: (a) [FeFe]-hydrogenase, (b) [NiFe]-hydrogenase, (c) [Fe]-hydrogenase 5

Figure 1.2 The major metabolic pathways in H_2 production by dark fermentation..... 8

Figure 1.3 Time-course of the change in the amount of biocatalytically active biomass present in a typical batch fermenter (●) and an immobilized cell reactor (■) 13

Figure 1.4 Basic methods of cell immobilization 14

Figure 1.5 Carrierless immobilization. 15

Figure 2.1 Different support materials used for particle selection. (a) stainless steel scrubber, (b) volcanic stone, (c) tulle, (d) polyester fiber, (e) loofah sponge, (f) plastic bath sponge, (g) sea sponge, (h) aquarium biological sponge. 23

Figure 2.2 Polyester fiber particles prepared with various sizes. The dimeter of the particles: (a) 0.5cm (b) 1 cm, (c) 2 cm, (d) 3 cm. 25

Figure 2.3 Points in Box-Wilson statistical experimental design where $k = 3$..... 26

Figure 3.1 Variation of cumulative hydrogen gas volume (CHV) with time for control at different initial total sugar concentrations (TS_o). TS_o: (—◆—) 13.17 ± 1.5 g/l, (—■—) 16.90 ± 2 g/l, (—▲—) 26.54 ± 4 g/l. 33

Figure 3.2 Variation of cumulative hydrogen gas volume (CHV) with time for stainless steel scrubber at different initial total sugar concentrations (TS_o). TS_o: (—◆—) 13.17 ± 1.5 g/l, (—■—) 16.90 ± 2 g/l, (—▲—) 26.54 ± 4 g/l. 34

Figure 3.3 Variation of cumulative hydrogen gas volume (CHV) with time for volcanic stone at different initial total sugar concentrations (TS_o). TS_o: (—◆—) 13.17 ± 1.5 g/l, (—■—) 16.90 ± 2 g/l, (—▲—) 26.54 ± 4 g/l. 36

Figure 3.4 Variation of cumulative hydrogen gas volume (CHV) with time for tulle at different initial total sugar concentrations (TS_o). TS_o: (—◆—) 13.17 ± 1.5 g/l, (—■—) 16.90 ± 2 g/l, (—▲—) 26.54 ± 4 g/l. 37

Figure 3.5 Variation of cumulative hydrogen gas volume (CHV) with time for polyester fiber at different initial total sugar concentrations (TS_o). TS_o: (◆) 13.17 ± 1.5 g/l, (■) 16.90 ± 2 g/l, (▲) 26.54 ± 4 g/l. 39

Figure 3.6 Variation of cumulative hydrogen gas volume (CHV) with time for loofah sponge at different initial total sugar concentrations (TS_o). TS_o: (◆) 13.17 ± 1.5 g/l, (■) 16.90 ± 2 g/l, (▲) 26.54 ± 4 g/l. 40

Figure 3.7 Variation of cumulative hydrogen gas volume (CHV) with time for plastic bath sponge at different initial total sugar concentrations (TS_o). TS_o:(◆) 13.17 ± 1.5 g/l, (■) 16.90 ± 2 g/l, (▲) 26.54 ± 4 g/l. 42

Figure 3.8 Variation of cumulative hydrogen gas volume (CHV) with time for sea sponge at different initial total sugar concentrations (TS_o). TS_o: (◆) 13.17 ± 1.5 g/l, (■) 16.90 ± 2 g/l, (▲) 26.54 ± 4 g/l. 43

Figure 3.9 Variation of cumulative hydrogen gas volume (CHV) with time for aquarium biological sponge at different initial total sugar concentrations (TS_o). TS_o: (◆) 13.17 ± 1.5 g/l, (■) 16.90 ± 2 g/l, (▲) 26.54 ± 4 g/l. 44

Figure 3.10 Hydrogen yield (Y_{H2}) for varied support materials with different initial total sugar concentrations (TS_o). TS_o: (■) 13.17 ± 1.5 g/l, (■) 16.90 ± 2 g/l, (■) 26.54 ± 4 g/l. 46

Figure 3.11 Variation of cumulative hydrogen gas volume (CHV) with time for polyester fiber with various sizes. The diameter of the particles: (◆) 0.5cm, (■) 1 cm, (▲) 2 cm, (●) 3 cm. 51

Figure 3.12 Hydrogen yield (Y_{H2}) for polyester fiber with various sizes. 53

Figure 3.13 The contour plot of response surface showing the variation of hydrogen yield (Y_{H2}, mol H_2/mol glucose) with particle number and initial substrate concentration at temperature, T= 35 ºC. 57

Figure 3.14 The three-dimensional response surface showing the variation of hydrogen yield (Y_{H2}, mol H_2/mol glucose) with particle number and initial substrate concentration at temperature, T=35 ºC. 57

Figure 3.15 The contour plot of response surface showing the variation of hydrogen yield (Y_{H2}, mol H_2/mol glucose) with particle number and initial substrate concentration at temperature, T= 45 ºC. 58

Figure 3.16 The three-dimensional response surface showing the variation of hydrogen yield (Y_{H2}, mol H_2/mol glucose) with particle number and initial substrate concentration at temperature, T= 45 ºC..... 58
Figure 3.17 The contour plot of response surface showing the variation of hydrogen yield (Y_{H2}, mol H_2/mol glucose) with particle number and initial substrate concentration at temperature, T= 55 ºC..... 59
Figure 3.18 The three-dimensional response surface showing the variation of hydrogen yield (Y_{H2}, mol H_2/mol glucose) with particle number and initial substrate concentration at temperature, T= 55 ºC..... 59
Figure 3.19 The contour plot of response surface showing the variation of hydrogen yield (Y_{H2}, mol H_2/mol glucose) with temperature and particle number at initial substrate concentration, TS_0 = 10 g/l..... 60
Figure 3.20 The three-dimensional response surface showing the variation of hydrogen yield (Y_{H2}, mol H_2/mol glucose) with temperature and particle number at initial substrate concentration, TS_0 = 10 g/l..... 61
Figure 3.21 The contour plot of response surface showing the variation of hydrogen yield (Y_{H2}, mol H_2/mol glucose) with temperature and particle number at initial substrate concentration, TS_0 = 20 g/l. 61
Figure 3.22 The three-dimensional response surface showing the variation of hydrogen yield (Y_{H2}, mol H_2/mol glucose) with temperature and particle number at initial substrate concentration, TS_0 = 20 g/l..... 62
Figure 3.23 The contour plot of response surface showing the variation of hydrogen yield (Y_{H2}, mol H_2/mol glucose) with temperature and particle number at initial substrate concentration, TS_0 = 30 g/l. 62
Figure 3.24 The three-dimensional response surface showing the variation of hydrogen yield (Y_{H2}, mol H_2/mol glucose) with temperature and particle number at initial substrate concentration, TS_0 = 30 g/l..... 63
Figure 3.25 The contour plot of response surface showing the variation of hydrogen yield (Y_{H2}, mol H_2/mol glucose) with temperature and initial substrate concentration at particle number, PN= 120..... 64

Figure 3.26 The three-dimensional response surface showing the variation of hydrogen yield (Y_{H2}, mol H_2/mol glucose) with temperature and initial substrate concentration at particle number, PN = 120. 64
Figure 3.27 The contour plot of response surface showing the variation of hydrogen yield (Y_{H2}, mol H_2/mol glucose) with temperature and initial substrate concentration at particle number, PN = 180. 65
Figure 3.28 The three-dimensional response surface showing the variation of hydrogen yield (Y_{H2}, mol H_2/mol glucose) with temperature and initial substrate concentration at particle number, PN = 180..... 65
Figure 3.29 The contour plot of response surface showing the variation of hydrogen yield (Y_{H2}, mol H_2/mol glucose) with temperature and initial substrate concentration at particle number, PN = 240. 66
Figure 3.30 The three-dimensional response surface showing the variation of hydrogen yield (Y_{H2}, mol H_2/mol glucose) with temperature and initial substrate concentration at particle number, PN = 240. 66
Figure 3.31 The contour plot of response surface showing the variation of hydrogen production rate (HPR, ml H_2/h) with particle number and initial substrate concentration at temperature, T = 38 ºC. 69
Figure 3.32 The three-dimensional response surface showing the variation of hydrogen production rate (HPR, ml H_2/h) with particle number and initial substrate concentration at temperature, T = 38 ºC..... 70
Figure 3.33 The contour plot of response surface showing the variation of hydrogen production rate (HPR, ml H_2/h) with particle number and initial substrate concentration at temperature, T= 45 ºC..... 70
Figure 3.34 The three-dimensional response surface showing the variation of hydrogen production rate (HPR, ml H_2/h) with particle number and initial substrate concentration at temperature, T= 45 ºC..... 71
Figure 3.35 The contour plot of response surface showing the variation of hydrogen production rate (HPR, ml H_2/h) with particle number and initial substrate concentration at temperature, T= 52 ºC. 71

Figure 3.36 The three-dimensional response surface showing the variation of hydrogen production rate (HPR, ml H_2/h) with particle number and initial substrate concentration at temperature, T = 52 ºC..... 72
Figure 3.37 The contour plot of response surface showing the variation of of hydrogen production rate (HPR, ml H_2/h) with temperature and particle number at initial substrate concentration, TS_0= 10 g/l. 73
Figure 3.38 The three-dimensional response surface showing the variation of hydrogen production rate (HPR, ml H_2/h) with temperature and particle number at initial substrate concentration, TS_0= 10 g/l..... 73
Figure 3.39 The contour plot of response surface showing the variation of of hydrogen production rate (HPR, ml H_2/h) with temperature and particle number at initial substrate concentration, TS_0= 30 g/l. 74
Figure 3.40 The three-dimensional response surface showing the variation of hydrogen production rate (HPR, ml H_2/h) with temperature and particle number at initial substrate concentration, TS_0= 30 g/l..... 74
Figure 3.41 Optimum operating conditions yielding the maximum hydrogen yield (Y_{H2}) and production rate (HPR). 75

LIST OF TABLES

Page

Table 1.1 Microorganisms for hydrogen generation 3
Table 1.2 Biohydrogen production process 4
Table 2.1 Coded and actual values of independent variables, where $|\alpha| = \sqrt{3}$ =1.73... 27
Table 2.2 Experimental conditions of the Box-Wilson statistical design 28
Table 3.1 Hydrogen production results of suspended culture at different TS_o concentration 34
Table 3.2 Hydrogen production results obtained by using stainless steel scrubber support particle at different TS_o concentration. 35
Table 3.3 Hydrogen production results obtained by using volcanic stone support particle at different TS_o concentration 37
Table 3.4 Hydrogen production results obtained by using tulle support particle at different TS_o concentration 38
Table 3.5 Hydrogen production results obtained by using polyester fiber support particle at different TS_o concentration 39
Table 3.6 Hydrogen production results obtained by using loofah sponge support particle at different TS_o concentration 41
Table 3.7 Hydrogen production results obtained by using plastic bath sponge support particle at different TS_o concentration 42
Table 3.8 Hydrogen production results obtained by using sea sponge support particle at different TS_o concentration 43
Table 3.9 Hydrogen production results obtained by using aquarium biological sponge support particle at different TS_o concentration 45
Table 3.10 Gompertz equation constants for varied support materials at different initial total sugar concentrations 48
Table 3.11 Variation of substrate utilization and TVFA formation for different support materials at TS_o = 13.17 ± 1.5 g/l 49
Table 3.12 Variation of substrate utilization and TVFA formation for different support materials at TS_o = 16.90 ± 2 g/l 49

Table 3.13 Variation of substrate utilization and TVFA formation for different support materials at TS_o = 26.54 $\pm$ 4 g/l 50
Table 3.14 Gompertz equation constants for polyester fiber with various sizes. 51
Table 3.15 Variation of substrate utilization and TVFA formation for polyester fiber with various sizes. 52
Table 3.16 Coefficients of the response functions for Y_{H2} 54
Table 3.17 Experimental and predicted values of $Y_{H2,}$ (R^2 = 0.89) 55
Table 3.18 Variance analysis for Y_{H2} (ANOVA, α=0.05). 55
Table 3.19 Coefficients of the response functions for HPR 67
Table 3.20 Experimental and predicted values of HPR (R^2=0.94) 68
Table 3.21 Variance analysis for HPR (ANOVA, α=0.05). 68
Table 4.1 Comparison of hydrogen yields of immobilized systems obtained from batch dark fermentation studies 79

CHAPTER ONE
INTRODUCTION

1.1 Bio-hydrogen Gas Production

Energy demand of world has increased during last decades sharply due to the growing global population and rapid economic development of countries. Fossil fuels, such as oil, natural gas and coal, are primary energy sources that supply this demand. However, combustion of the fossil fuels produces various gases (COx, SOx, NOx, CH) and many organic compounds. These lead to the global problems, such as the greenhouse effect, ozone layer depletion, acid rains and pollution (Veziroglu & Sahin, 2008). Moreover, nowadays, depletion of fossil fuel resources is a major concern of governments. Because of these problems, researchers have been investigating renewable energy sources if any of them can satisfy energy demands without damaging environment. Hydrogen seems to be a promising fuel of future because of its advantages over other carbon based energy sources.

Hydrogen (H_2) is the cleanest fuel which produces only heat and water upon combustion, releasing 286 kJ/mol of energy, and does not generate greenhouse gas emissions (Levin & Azbar, 2012). H_2 is the most abundant element in the universe but it is available on earth only in compounds; obtaining hydrogen from these compounds needs energy (Winter, 2009), so it requires expensive production methods (Kapdan & Kargı, 2006). Hydrogen can be produced from fossil resources, such as natural gas and coal or from renewable resources, like biomass and water. A variety of process technologies can be used, including chemical, biological, electrolytic, photolytic and thermo-chemical (International Energy Agency [IEA], 2006). Steam reforming and partial oxidation of natural gas, gasification of coal and water electrolysis are the most commonly industrial methods used for H_2 gas production. These processes occur at high- temperature and pressure and require high energy. So, these are neither environmentally-friendly nor cost effective methods. On the contrary, biological hydrogen production processes are operated under mild conditions (25-35 ºC, 1 atm) (Argun, Kargı, Kapdan & Oztekin, 2008).

Biohydrogen can be produced from water by algea and cynobacteria, from organic acids (acetic, lactic and butyric) by some photo-heterotrophic bacteria and from biomass or carbohydrate rich wastes by facultative or obligate anaerobic bacteria (Kapdan & Kargı, 2006). Algea and cynobacteria have capability to split water into hydrogen and oxygen by using sunlight as energy source. This prosess is called biophotolysis. One of the well-known hydrogen producing algea and cynobacteria is *Chlamydomonas reinhardtii* (Melis, 2002) and *Anabaena cylindrica* (Asada & Miyake, 1999), respectively. Another well studied biological hydrogen production method is photofermentation. Photosynthetic non-sulfur bacteria such as *Rhodobacter sp.* are used in biohydrogen production by photofermentation. Organic acids, such as acetic, lactic and butyric, are converted into H_2 and CO_2 under anaerobic conditions in the presence of light (Argun & Kargı, 2011). Dark fermentation is the third method used in biohydrogen production. In dark fermentation, H_2 is produced through the anaerobic digestion of carbohydrate containing wastes. Biomass is fermented by obligate anerob *Clostridium* species or facultative *Enterobacter* sp. in the absence of light. H_2, volatile fatty acids (VFAs) and CO_2 are the main products of dark fermentation. Hydrogenase and nitrogenase are two key enzymes responsible for the biochemical reactions in hydrogen production.

Several microorganisms used in biological hydrogen production, general reactions, advantages and disadvantages of bioprosses are summarized in Table 1.1 and Table 1.2 below.

Table 1.1 Microorganisms for hydrogen generation (Krishna, 2013)

Broad Classification	**Name of the microorganisms**
Green Algae	*Scenedesmus obliquus* *Chlamydomonas reinhardii* *C.moewusii*
Cyanobacteria Heterocystous	*Anabaena azollae* *Anabaena CA* *A.variabilis* *A.cylindrical* *Nostoc muscorum* *N.spongiaeforme* *Westiellopsis prolifica*
Cyanobacteria Nonheterocysous	*Plectonema boryanum* *Oscillotoria Miami BG7* *O.limnetica* *Synechococcus sp.* *Aphanothece halophytico* *Mastidocladus laminosus* *Phormidium valderianum*
Photosynthetic Bacteria	*Rhodobacter sphaeroides* *R. capsulatus* *R. sulidophilus* *Rhodopsuedomonas* *Sphaeroides* *R. palustris* *R. capsulata* *Rhodospirillium rubnum* *Chromatium sp.* *Miami PSB 1071*
Fermentative Bacteria	*Enterobacter aerogenes* *E. cloacae* *Clostridium butyricum* *C. pasteurianum* *Desulfovibrio vulgaris* *Magashaera elsdenii* *Citrobacter intermedius* *Escherichia Coli*

Table 1.2 Biohydrogen production process

Process	General reactions	Advantages	Disadvantages
Biophotolysis	$2H_2O + light \xrightarrow{Photosynthesis} 2H_2 + O_2$	Water utilization as a renewable resource CO_2 consumption as one of the air pollutants (Kapdan & Kargı, 2006)	Strong inhibition effect of generated oxygen on hydrogenase enzyme Low hydrogen production potential No waste utilization (Kapdan & Kargı, 2006)
Photo fermentation	$CH_3COOH + 2H_2O + light \longrightarrow 4\ H_2 + 2CO_2$	High theoretical conversion yields Ability to use wide spectrum of light Ability to consume organic substrates derivable from wastes (Das & Veziroglu, 2001)	Complex nutritional requirements (EDTA, Mo, Fe) of the *Rhodobacter* species Strict control requirements for environmental conditions Inhibitions caused by high concentrations of VFAs and NH_4-N (Argun, Kargı & Kapdan, 2009a)
Dark fermentation	$C_6H_{12}O_6 + 2\ H_2O \longrightarrow 4\ H_2 + 2\ CH_3COOH + 2\ CO_2$ (acetate) $C_6H_{12}O_6 \longrightarrow 2\ H_2 + 2\ CH_3CH_2CH_2COOH + 2\ CO_2$ (butyrate)	Continuous hydrogen production without light is possible A variety of carbon sources can be used as substrates including wastes/wastewater Valuable metabolites, i.e. butyric, lactic and acetic acids are produced There is no oxygen limitation problem since it is an anaerobic process (Keskin, Aksoyek & Azbar, 2011)	Relatively lower achievable yields of H_2 As yields increase H_2 fermentation becomes thermodynamically unfavourable Product gas mixture contains CO_2 which has to be separated (Sabaratnam & Hassan, 2012)

1.2 Biochemical Aspects of Biohydrogen Production by Dark Fermentation

Understanding the enzymes and pathways involved in biological H_2 production is important due to control microbial cell metabolism and to increase H_2 production. Biohydrogen production is dependent on the enzymes which catalyse the reduction of protons to dihydrogen (H_2), namely nitrogenase and hydrogenase (Carere & Levin, 2012).

$$2H^+ + 2e^- \longleftrightarrow H_2 \qquad (1.1)$$

Nitrogenase catalyzes the reduction of N_2 to ammonia under photo-heterotrophic conditions and H_2 is produced as a byproduct (D.H. Kim & M.S. Kim, 2011). Hydrogenase is found in a wide range of aerobic or anaerobic organisms (photosynthetic or non- photosynthetic) and it is responsible for hydrogen production during dark anaerobic fermentation (Tsygankov & Tekucheva, 2012).

Hydrogenases are complex metalloenzymes and classified into three groups according to the number and identity of the metals in their active site: iron-iron [FeFe]- , nickel-iron [NiFe]- and iron [Fe]-hydrogenases (Vardar-Schara, Maeda & Wood, 2008).

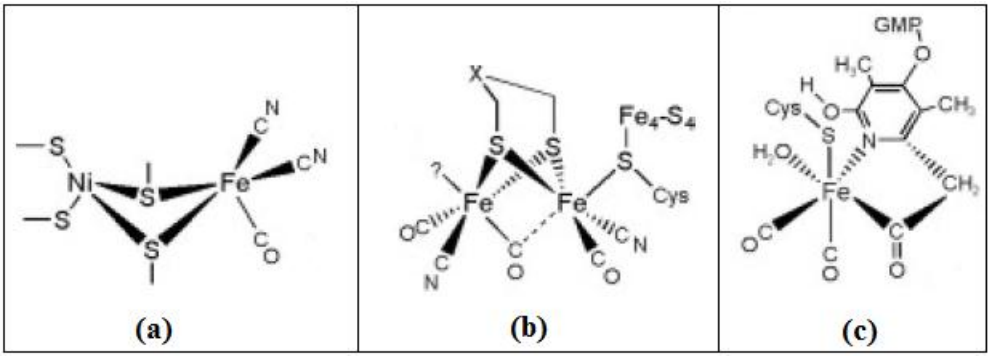


Figure 1.1 Active site structures of the three hydrogenases: (a) [FeFe]-hydrogenase, (b) [NiFe]-hydrogenase, (c) [Fe]-hydrogenase (Heinekey, 2009).

Biohydrogen production by dark fermentation starts with the conversion of substrate (glucose) to pyruvate by glycolysis producing ATP and reducing NAD^+ to $NADH+H^+$. $NADH+H^+$ is oxidized by producing reduced products (Hallenbeck & Ghosh, 2012).

$$Glucose \rightarrow 2Pyruvate + 2NADH + 2H^+ + 2ATP \quad (1.2)$$

There are three types of biochemical reactions which are currently known to produce H_2 in dark fermentation (Oh, Raj, Jung & Park, 2011).

The first one is typical in facultative anaerobes, such as *Escherichia coli* and Enterobacteriaceae. Pyruvate:formate lyase (PFL) and formate:hydrogen lyase (FHL) are two major enzymes in this pathway (Hallenbeck, 2005). Pyruvate is degraded to acetyl-CoA and formate by the activity of PFL and then, formate is split into H_2 and CO_2 by the FHL complex which possesses a [NiFe]-hydrogenase (Hallenbeck & Ghosh, 2012; Oh et al., 2011).

$$2\ Pyruvate + 2\ CoA \xrightarrow{PFL} 2\ Acetyl\text{-}CoA + 2\ Formate \quad (1.3)$$

$$2\ Formate \xrightarrow{FHL} 2\ H_2 + 2\ CO_2 \quad (1.4)$$

The maximum theoretical hydrogen yield obtained from the PFL pathway is 2 mol H_2/mol glucose (Hallenbeck & Ghosh, 2012). Besides formate; succinate, lactate, ethanol and acetate are generated as fermentation end products through the glucose metabolic pathway and these competing paths for obtaining NAD^+ for glycolysis from pyruvate lower the yield (Mathews & Wang, 2009; Vardar-Schara, Maeda & Wood, 2008).

In the second type of H_2 producing reaction, while pyruvate is converted to acetyl-CoA and CO_2, the electrons are transferred to oxidized ferredoxin (Fd_{ox}) through the action of pyruvate:ferredoxin oxidoreductase (PFOR). Then reduced ferredoxin (Fd_{rd}) transfers electrons to protons to form H_2 by Fd-dependent hydrogenase (HydA) which is a [FeFe]-hydrogenase (Hallenbeck, 2005; Hallenbeck & Ghosh,

2012; Oh et al., 2011). *Clostridium* species are responsible for this type of H_2 production (Mathews & Wang, 2009).

$$2\ \text{Pyruvate} + 2\ \text{CoA} + 4\ Fd_{ox} \xleftrightarrow{\text{PFOR}} 2\ \text{Acetyl-CoA} + 2\ CO_2 + 4\ Fd_{rd} \quad (1.5)$$

$$4\ Fd_{rd} + 4\ H^+ \xrightarrow{\text{HydA}} 4\ Fd_{ox} + 2\ H_2 \quad (1.6)$$

This pathway results in maximum 2 mol H_2/mol glucose (Vardar-Schara, Maeda & Wood, 2008).

In the third type of reaction, two additional moles of H_2 can be produced from the $NADH+H^+$ that is generated during glycolysis (Mathews & Wang, 2009; Vardar-Schara, Maeda & Wood, 2008). First, Fd_{ox} is reduced by $NADH+H^+$ by NADH:ferredoxin oxidoreductase (NFOR). Then the electrons are transferred to protons and H_2 is produced by HydA (Oh et al., 2011).

$$2\ \text{NADH} + 2H^+ + 4\ Fd_{ox} \xrightarrow{\text{NFOR}} 2\ NAD^+ + 4\ Fd_{rd} \quad (1.7)$$

$$4\ Fd_{rd} + 4\ H^+ \xrightarrow{\text{HydA}} 4\ Fd_{ox} + 2\ H_2 \quad (1.8)$$

It was suggested that to increase H_2 yield in dark fermentation, H_2 production pathway in microbial metabolism should be diverted to NFOR patway. However, NADH:Fd dependent route is significantly affected by several parameters like H^+ concentration, $NADH/NAD^+$ ratio, H_2 partial pressure and temperature (Oh et al., 2011).

The major metabolic pathways in H_2 production by dark fermentation is summarized in Figure 1.2 (Hallenbeck, Abo-Hashesh & Ghosh, 2012). Maximum 4 mol H_2/mol glucose could be obtained by dark fermentation, when only acetate is produced as the fermentation end-product. However, formation of lactate, ethanol, butanol or butyrate consumes NADH and results in lower hydrogen yield (Hallenbeck, 2012).

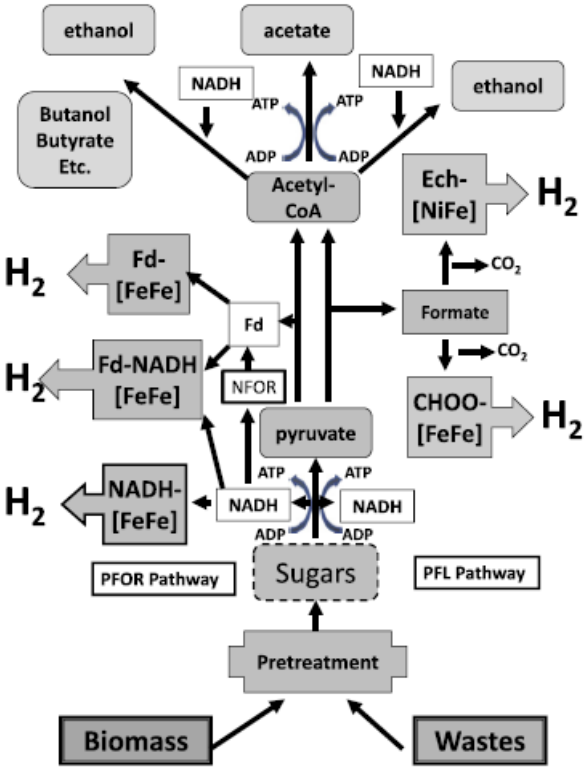


Figure 1.2 The major metabolic pathways in H_2 production by dark fermentation (Hallenbeck, Abo-Hashesh & Ghosh, 2012).

1.3 Major Challanges and Improvement Strategy in Biohydrogen Production by Dark Fermentation

Biohydrogen production by dark fermentation is adopted more advantageous method among other biological processes. However, it does not compete with the traditional hydrogen production methods due to low hydrogen yields obtained and unstable operation conditions. But there are many ongoing researches to overcome these obstacles and make hydrogen production by dark fermentation feasible at industrial scale.

1.3.1 Metabolic Pathways and End Products

Besides to hydrogen, VFAs; such as lactic acid, formic acid, acetic acid, propionic acid, butyric acid and alcohols; like ethanol, propanol, butanol are produced during

dark fermentation of organic substrate by anaerobic microorganisms. Thus, hydrogen yield depends on the methabolic pathway of the substrate degradation to these end products.

Theoretically, maximum 4 mol H_2 can be obtained per mol of glucose if the only end product is acetic acid. If it is butyric acid, hydrogen yield declines to 2 mol H_2/mol glucose. On the other hand, in propionic acid formation, 1 mol H_2 is consumed for each per mol of propionic acid produced. Lactic acid and ethanol fermentations do not result in H_2 formation or consumption (Argun & Kargi, 2011). However, in practice fermentation effluent contains a mixture of VFAs and alcohols. Also, glucose is used for microbial growth and maintenance besides hydrogen production (Argun & Kargi, 2011; Hay, Wu, Juan & Jahim, 2013). Thus, lower hydrogen yields are obtained. Microbial metabolic pathway should be diverted to acetic or butyric acid formation by controlling the operational conditions to increase the hydrogen yield and rate. Using two stage dark/photo fermentation system might be an alternative solution to maximize hydrogen production and to get additional hydrogen from the VFAs produced in dark fermentation by appliying photofermentation. In the first stage, VFAs are produced by dark fermentation and these are used as substrate by photosynthetic bacteria in the second stage. When dark and photo fermentations are operated simultaneously and if acetic acid is the only VFA produced, theoretically maximum 12 mol H_2/mol glucose can be obtained (Argun & Kargi, 2011).

1.3.2 Type of Substrates and Media Composition

Hydrogen can be produced from variety of feedstocks. The most important criteria affects the selection of raw material for biohydrogen production are its availability, carbohydrate content, fermentability and cost (Kapdan & Kargı, 2006). Biohydrogen production from simple sugars, such as glucose or sucrose, which are readiliy biodegradable, have been widely studied. However, glucose, sucrose or lactose are expensive feedstocks and using them as substrate increases biohdrogen production cost. On the other hand, starch or cellulose containing agricultural wastes and

carbohydrate rich industrial wastewater are not only cost effective but also renewable sources. These biomasses contain complex carbohydrates and most of the anaerobic bacteria are not able to ferment them directly to hydrogen gas. Therefore, different pre-treatment methods, such as physico-chemical or enzymatic, must be used to degrade these polymers into simple sugars prior to dark fermentation. It is reported that substrate pre-treatment enhances the hydrogen yield in dark fermentation (Gupta, Kumari, Reddy & Bux, 2013).

Biohydrogen production by dark fermentation is affected by media composition. Fermentaion medium requires additional nutrients such as nitrogen (N), phosphorous (P), iron (Fe) and sulfur (S). Fe is a cofactor of hydrogenase and Fe concentration affects the activity of this enzyme. N is an essential element in protein structure. Beside, both N and P are the building blocks of DNA (deoxyribonucleic acid). Thus, N and P need for microbial growth and maintenance. These nutrients should be at optimum concentrations because low or high concentrations of these nutrients may lead to obtain low hydrogen yields or production rates. It was suggested that N/C, P/C, Fe(II)/C ratios play a crucial role in biohydrogen production (Oztekin, Kapdan, Kargı & Argun, 2008).

1.3.3 Inoculum Type

Pure cultures or mixed cultures of bacteria can be used in biohydrogen production by dark fermentation. Hydrogen yields vary depending on the type of anaerobic bacteria used because metabolic pathways and the amount of VFAs differ depending on the type of bacteria (Argun, Kargı & Kapdan, 2009b). *Clostridium* and *Enterobacter* sp. are mostly preferred pure cultures as inoculum for biohydrogen production. Anaerobic sludge, municipal sewage sludge, compost and soil are widely used to obtain mixed cultures for biohydrogen production (Li & Fang, 2007). Mixed culture consists of different types of bacteria living symbiotically and H_2 is produced as a by-product during anaerobic digestion of wastes by these bacteria. Initially, biopolymers (protein, carbohydrate and lipid) are hydrolyzed into their monomers (aminoacids, sugars, long chain fatty acids and glycerol). These molecules are

converted into fatty acids during acidogenisis phase. Then, VFAs are used to produce acetate and hydrogen by acetogens and finally, methanogens produce methane by using acetate and hydrogen. To enrich spore forming hydrogen producing bacteria and inhibit methanogens, some pre-treatment methods are applied to mix cultures.

Different pretreatment methods, such as heat-shock, acid, base, aeration, freezing and thawing, chloroform, sodium 2-bromoethanesulfonate or 2 bromoethanesulfonic acid and iodopropane, were applied to anaerobic sludge to obtain hydrogen producing mixed cultures (Wang & Wan, 2008). The most approved method is the heat-shock (Li & Fang, 2007). The sludge is exposed to high temperature around 100 ºC for around one hour. The spore forming bacteria are selected while methanogens are inhibited. Heat treatment suppress the growth of H_2 consumers such as homoacetogens, nitrate and sulfate reducing bacteria as well (Argun & Kargi, 2011). Argun et al. (2009b) investigated hydrogen formation performances of different anaerobic bacteria in batch dark fermentation under the same experimental conditions. Pure cultures of *Clostridium acetobutylicum*, *Clostridium butyricum*, *Enterobacter aerogenes*, heat-treated anaerobic sludge and a mixture of those cultures were used in the study. The highest hydrogen yield was obtained with the heat-treated anaerobic sludge.

1.3.4 Operating Conditions

Biohydrogen yield in dark fermentation is highly related to environmental conditions. Important factors affecting H_2 production are pH, temperature and ORP (Oxidation-Reduction Potentials).

Kapdan & Kargı (2006) stated that H_2 production yield, biogas content, type of organic acids produced and the specific H_2 production rate are affected by medium pH. Medium pH decreases during dark fermentation because of the production of organic acids and this inhibits the hydrogen production because low pH values influence the activity of hydrogenase negatively (Azwar, Hussain & Abdul-Wahab, 2014; Kapdan & Kargı, 2006). Also at low pH, metabolic pathway shifts from VFAs

production to alcohol production (Argun & Kargı, 2011). Therefore it is reported that optimum pH range should be 5.5 and 6.5. Furthermore hydrogen consuming bacteria, like homoacetogens and methanogens can be inhibited by operating dark fermentation at optimal pH level (Hay et al., 2013). Therefore it is necessary to control medium pH during fermentation.

Another important parameter affects hydrogen yield and production rate is temperature. Hydrogen production by dark fermentation studies were conducted under mesophilic (25-40 ºC), thermophilic (40-65 ºC) or hyper-thermophilic (> 80 ºC) conditions. It is reported that optimum temperature for fermentative hydrogen production is not the same in the studies but it seems that mesophilic and thermophilic range are more effective for biohydrogen pruduction (Wang & Wan, 2009). Most of the studies have been carried out under mesophilic temperature range because of less energy requirement. However higher H_2 yield can be obtained with thermophilic operation due to limited growth of hydrogen consumers, destruction of pathogenic bacteria and faster metabolic activity of bacteria (Karadag, 2011; Ozmıhcı, Kargı & Cakır, 2011).

ORP value of fermentation medium is an important factor which must be controlled during hydrogen production by dark fermentation. Optimum oxidation-reduction potentials (ORP) for Clostridium sp. vary between -200 and -250 mV (Cai, Liu & Wei, 2004). Because (-)ORP value is an indicator which shows fermentation is carried out under anaerobic conditions. $_L$-cysteine–HCl.H_2O and Na-thioglycolate can be added to the medium to adjust the ORP lower than -150 mV and provide anaerobic conditions (Argun et al., 2009b; Oztekin et al., 2008).

1.3.5 Cultivation Type

Both suspended or immobilized cell culture can be used in biohydrogen production by dark fermentation. While cells are found in free form in suspended system, they are fixed in/on support matrixes in immobilized system. Free cells are not very stable and lose their catalytic activity after the ending of cell growth. However many industrial and academic research demonstrated that life of biocatalyst

can be extended by cell immobilization (Figure 1.3) (J Tampion & M.D. Tampion, 1987). Besides, high cell concentrations are provided by immobilization. Immobilized cells are reused in the fermenter and cells are easily seperated from the fermentation medium. Biomass washout problem is prevented at high dilution rates in continuous system. Also product stability and yield are improved by using immobilized cell system (Azbar & Kapdan, 2012). Entrapment within a porous matrix, attachment or adsorption on solid carrier surfaces, self-aggregation of cells (flocculation) and cell containment behind a barrier are basic methods for cell immobilization (Pilkington, Margaritis, Mensour, & Russel, 1998). These were shown in Figure 1.4.

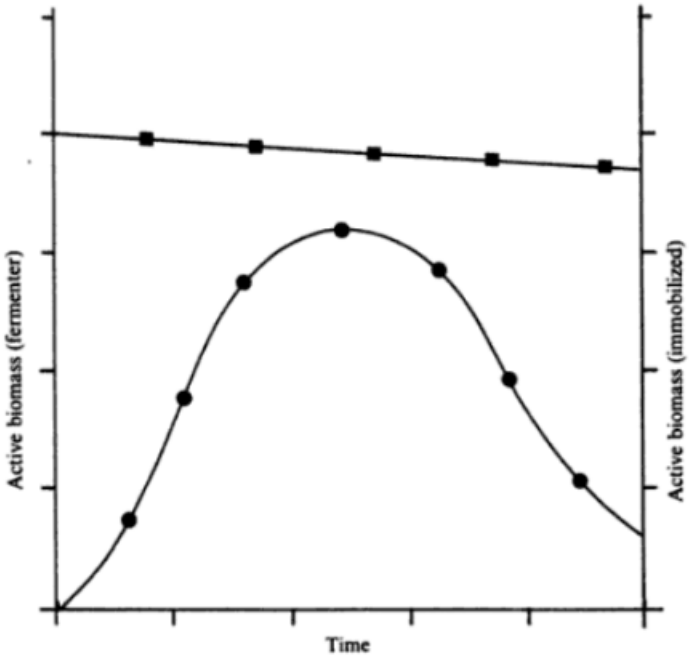


Figure 1.3 Time-course of the change in the amount of biocatalytically active biomass present in a typical batch fermenter (●) and an immobilized cell reactor (■) (J. Tampion & M.D. Tampion, 1987).

Entrapment is the most widely employed method of cell immobilization due to ease of operation and wide applicability (J. Tampion & M.D. Tampion, 1987). Cells are trapped within a matrix in this method. A variety of macro and micro porous materials (brick, ceramics, sintered glass, activated carbon, stainless steel wire, etc.) and porous polymers (agar, alginate, κ-carrageenan, polyacrylamid, chitosan, gelatin, collagen, etc.) could be used as matrix for the entrapment of cells (Azbar & Kapdan,

2012; Shuler & Kargı, 2002). This method provides cell protection from the shear force and high cell densities. However one of the drawback of this system is mass transfer limitations (Nedovic, Willaert, Cukalovic, Obradovic, & Bugarski, 2005).

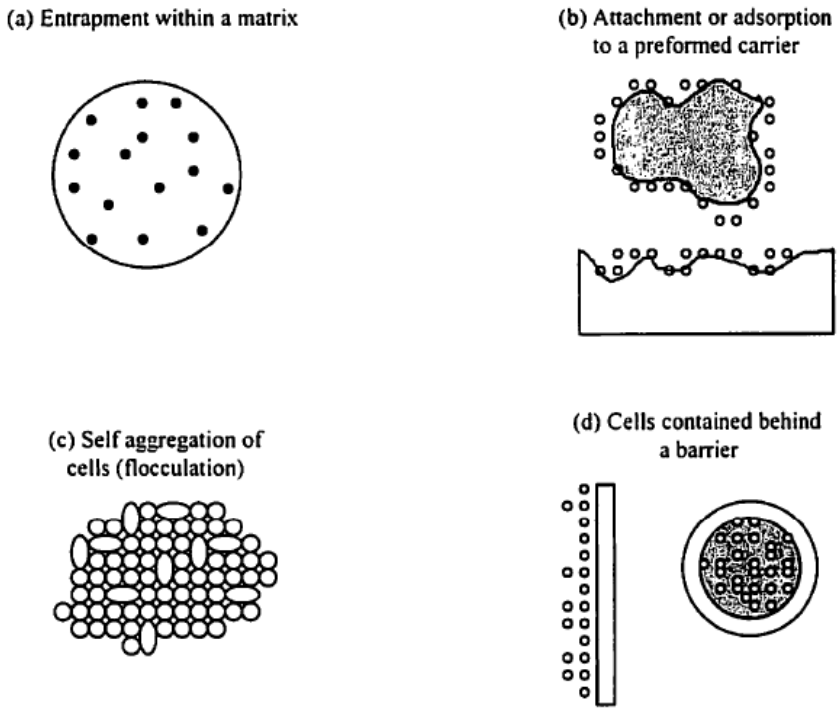


Figure 1.4 Basic methods of cell immobilization (Pilkington et al., 1998).

Cell immobilization by adsorption or attachment to a support material is a simple, cheap and fast method. Cells attach on an organic or inorganic support material spontaneously by Van der Waals forces, ionic bonds, hydrogen bridges or covalent interactions (Nedovic et al., 2005). Cell adsorption to solid surfaces is affected by various physical and chemical factors which include, the type of support (particle size, porosity, charge, composition), microorganisms (strain, age, surface charge) and environmental conditions (pH, temperature, liquid flow rate, and ionic strength) (Margaritis & Kilonzo, 2005). The disadvantage of this method is weakly bound biofilm detaches from the support easily due to the fluid shear force (Azbar & Kapdan, 2012).

Flocculation is a kind of carrierless immobilization technique in which cells aggregate naturally or by induced agents (Uemoto, 2005). Suspended free cells combine together in the fermentation medium and cell aggregates occur. The initial aggregates (embryonic granule) grow to matured granules, whose diameter is a few millimeters (Uemoto, 2005). Granules formation requires long time but they are stable during long term operation (Azbar & Kapdan, 2012).

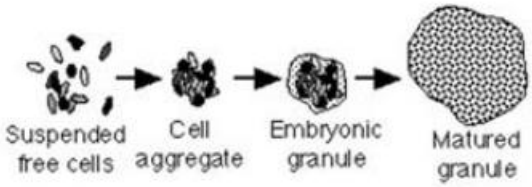


Figure 1.5 Carrierless immobilization (Uemoto, 2005).

Containment of cells behind a barrier can be achieved by the use of microporous membrane filters or by entrapment of cells in microcapsules (Verbelen, De Schutter, Delvaux, Verstrepen & Delvaux, 2006). Different kinds of polymers can be used to form microcapsules (nylon, collodion, polystyrene, acrylate, plylysine-alginate hydrogel, etc.) (Inui, Vertes & Yukawa, 2010). Immobilization by containment seems attractive in terms of productivity. Nevertheless it is not useful for low-added value fermentations because high-performance membranes are expensive (Verbelen et al., 2006).

Biohydrogen production by immobilized cell culture is a new approach. Aforementioned immobilization methods could be employed in biohydrogen production. Type and surface area of immobilization materials are important factor which affect hydrogen yields. When compared to suspended culture, higher hydrogen production rates and yields can be obtained by immobilized culture (Keskin, Giusti & Azbar, 2012).

1.4 Literature Review

A large amount of research has focused on biohydrogen production by immobilized culture due to the several advantages of this system over suspended culture. Immobilized cell system could be operated in batch, fed-batch and continuous mode. Both pure and mixed cultures are suitable for immobilization in biohydrogen production from simple sugars such as glucose, sucrose or carbohydrate rich wastes or wastewater.

Many batch immobilized fermentation studies were carried out to select the best support material for H_2 production. In addition, there are researches which the effect of properties of matrices (number, size, etc.) on biohydrogen production were evaluated.

Mohan et al. (2008) assessed self-immobilization of enriched acidogenic anaerobic mixed culture on different supporting materials including mesoporous silica material (SBA-15), granular activated carbon (GAC) and powdered activated carbon (PAC). Batch fermentation experiments were conducted to investigate H_2 production capacity and substrate degradation efficiency of these immobilized matrices under acidic conditions (pH= 5.5) and room temperature (28 ± 2 ºC). Composite chemical wastewater was used as substrate. Three of supporting materials were operated at four organic loading rates (OLRs), 0.83, 1.42, 2.32, 2.55 kg COD/m^3-day. H_2 production rates and yields varied with the particle types used for immobilization and OLR applied. Self-immobilization on SBA-15 showed the highest cumulative H_2 production and specific H_2 yield. While maximum cumulative H_2 production (53.89 mmol; 48h) was achieved at the highest OLR (2.55 kg COD/m^3-day), maximum specific H_2 yield (7.29 mol/kg COD_R-day) was obtained at the lowest OLR (0.83 kg COD/m^3-day). Maximum substrate degradation rate was observed for each material at the highest OLR; 0.96 kg COD/m^3-day with mesoporous (SBA-15) immobilization followed by 0.81 kg COD/m^3-day with GAC immobilization and 0.66 kg COD/m^3-day with PAC immobilization.

Batch H_2 production was carried out from sodium format (100 mM) using immobilized recombinant *Escherichia coli* SH5 at pH 6.5 and temperature 37 ºC by Seol et al. (2011). Agar, agarose and sodium alginate were used as immobilization matrix material and 716.0 ± 61.4 ml L^{-1} h^{-1} (agar), 682.9 ± 42.3 ml L^{-1} h^{-1} (agarose) and 676.1 ± 47.3 ml L^{-1} h^{-1} (alginate) of H_2 production rates were obtained. They, also, investigated the effect of agar concentrations on H_2 production using different agar concentrations in the range of 0.5% - 3.5%. Volumetric H_2 production rate was nearly same as 1500 ml L^{-1} h^{-1} at agar concentrations between 2% and 3.5%.

Ishikawa et al. (2006) studied the size effect of matrices on H_2 production using encapsulated *Escherichia coli* strain MC13-4 in alginate gel beads which were prepared 2, 4, 6, 8 mm in diameter. Each one of the immobilized cell culture was operated at 37 ºC using O.D. 100 cell density and 500mM glucose in batch mode. The optimum size of alginate beads was found 6 mm in diameter with the amount of produced hydrogen was 9.6 mL which was 1.2-fold higher than that of the total volume of hydrogen (8 mL) produced using 2mm gel beads.

Zhao et al. (2012) used biological mycelia pellets as matrix for immobilization of *Clostridium* sp. T2. They conducted batch experiments to optimize the best mycelia dosage (0.175-1.05 g/ 150 ml medium) and mycelia pellets size (0.5-3.5 mm) on hydrogen production. Mycelia pellets were formed in the process of *Aspergillus niger* Y3 fermentation. Varying mycelia dosage from 0.175 to 0.350 g/ 150 ml and mycelia pellets size from 0.5 to 1.5 mm resulted in an increase of H_2 yield but further increase of factors impacted H_2 production negatively. Maximum volumetric H_2 volume (1726 ml/ L) was obtained at 0.350 g/ 150 ml of mycelia dosage and 1.5 mm of mycelia pellets size.

Fritsch, Hartmeier & Chang (2008) operated column reactor containing various numbers of monoliths (square-structured ceramic fittings) in batch mode. *Clostridium butyricum* CGS2 was used as inoculum and reactor was fed with sucrose (20 g COD/l) containing medium. 217 ml of volumetric H_2 production and 0.70 mol H_2/ mol hexose of H_2 yield were obtained with one monolith experiment which was

lower than two or three monoliths experiments. However results were almost the same for two and three monoliths experiments (volumetric H_2 production = 278 ml with two monoliths, 280 ml with three monoliths; H_2 yield = 0.82 mol H_2/ mol hexose with two monoliths, 0.81 mol H_2/ mol hexose with three monoliths).

Other factors that affect biohydrogen production by immobilized system are temperature, pH and substrate concentration. Many studies have been conducted to optimize environmental conditions for H_2 production.

Wu & Chang (2007) investigated the effect of temperature, pH and carbon substrate concentration on H_2 production by using immobilized batch culture. Sucrose-based synthetic wastewater and acid pretreated anaerobic sludge were used as carbon source and seed culture. Polymethyl methacrylate (PMMA) was used to entrap biomass. Collagen and activated carbon were added to modify the physical properties of the immobilized cells. Firstly, batch systems containing PMMA-immobilized beads were operated at varying values of pH (5.5-7.0) and temperature (30-40 ºC) with 20 g COD l^{-1} of the initial sucrose concentration. Maximum volumetric H_2 production rate (238 $\pm$ 10 ml h^{-1} l^{-1}), total H_2 evolution (252 ml) and H_2 yield (2.25 $\pm$ 0.12 mol H_2 mol $sucrose^{-1}$) were obtained at pH 6.0 and 35 ºC. Then, immobilized batch tests were conducted to determine the best initial sucrose concentration (5-30 g COD l^{-1}) at the optimum pH (6.0) and temperature (35 ºC) value. It was found that the favorable conditions for batch H_2 fermentation using the PMMA immobilized cells were 35 ºC, pH 6.0 and an 20 g COD l^{-1} of sucrose, giving a H_2 production rate of 238 $\pm$ 5 ml h^{-1} l^{-1} and a H_2 yield of 2.25 $\pm$ 0.11 mol H_2 / mol sucrose.

Plangklang, Reungsang & Pattra (2012) immobilized pure culture of *Clostridium butyricum* TISTR 1032 on sugarcane bagasse (SCB) which is a porous cellulosic material to improve the H_2 production efficiency of batch fermentation. The effect of initial pH and sucrose concentration were investigated for free and immobilized *C. butyricum* by using sugarcane juice as substrate at 37 ºC. Batch experiments were conducted with the initial sucrose concentration of 25 g COD l^{-1} by varying the

initial pH in the range of 4.5-7.0 to obtain the optimum pH for H_2 production. After the determination of optimum pH, initial sucrose concentration of fermentation medium was varied between 20-40 g COD l^{-1} to assign the optimum initial sucrose concentration. Immobilized *C. butyricum* on SCB improved specific H_2 production rate approximately 1.5 times in comparison to free cells (438.16 mmol H_2/g dry cell-d with immobilized *C. butyricum* on SCB; 283.49 mmol H_2/g dry cell-d with free cell of *C. butyricum*). The maximum H_2 production rate (3.11 l H_2/ l) and H_2 yield (1.34 mol H_2/ mol hexose) were optained by immobilized *C. butyricum* on SCB at initial pH of 6.5 and initial sucrose concentration of 25 g COD l^{-1}.

Temperature effect on H_2 production was investigated using sewage sludge entrapped in ethylene-vinyl acetate copolymer (EVA) by Wu et al. (2005). Batch experiments were carried out with initial sucrose concentration of 20 g COD/l under a temperature of 30-45 ºC. H_2 volume and H_2 production rate ascended with the increase in temperature and reached a peak at 40 ºC (H_2 volume = 90 ml; H_2 production rate = 389 ml/h/gVSS; H_2 yield = 1.41 mol H_2/mol sucrose).

1.5 Scope and Objective

The major objective of this thesis is to investigate biohydrogen gas production potential of immobilized systems from acid hydrolyzed wheat starch (AHWS) by batch dark fermentation.

The specific objectives of the study can be summarized as follows;

- To investigate the effects of initial substrate (AHWS) concentration on biohydrogen gas production in batch dark fermentation operated with different support materials under thermophilic conditions,
- To select the most suitable microbial support material maximizing hydrogen gas yield and formation rate,
- To investigate the effect of particle size on hydrogen production and to determine the optimal size for forward studies,

- To investigate the effects of particle number, temperature and initial substrate concentration on hydrogen yield and hydrogen production rate by using Box-Wilson statistical experiment design method and determine interactions between the factors.

CHAPTER TWO
MATERIALS AND METHODS

2.1 Batch Dark Fermentation

2.1.1 Organisms

The mixed microbial culture was obtained from the acidogenic phase of anaerobic wastewater treatment plant of PAK MAYA Bakers Yeast Company in Izmir, Turkey. The anaerobic sludge was diluted by half with distilled water and was boiled at least for an hour at 100 ºC. pH of the sludge was adjusted to 5.9 by sulfuric acid (H_2SO_4). Spore forming hydrogen producing bacteria were selected and hydrogen consuming methanogens were inhibited by applying heat and acid treatment to anaerobic sludge. Heat treated sludge was directly used as inoculums without pre-fermentation.

2.1.2 Preparation of Acid Hydrolyzed Wheat Starch (AHWS)

Waste wheat was obtained from Soke Flour Compony in Soke, Izmir, Turkey. Firstly wheat was grounded and then the wheat powder was sieved down to 70 μm size (less than 200 mesh). In order to hydrolyze wheat starch to glucose and maltose, wheat powder solution was prepared by using 0.5 M H_2SO_4 (pH of the solution = 1.5-2) and autoclaved at 90 ºC for 15 minutes (min.). After acid and heat hydrolysis, wheat powder solution was centrifuged at 8000 g for 20 min. to remove solid phase. pH of the supernatant was adjusted to 7 by using 10 M NaOH solution. $(NH_4)_2SO_4$, KH_2PO_4 and $FeSO_4$ were added as nitrogen, phosphorus and iron source to overcome nutrient limitations. Optimum N/P/Fe/C ratio, which maximum H_2 yield was obtained by Oztekin et al. (2008), was 2/0.8/1.5/100 for acid hydrolyzed wheat starch. Lastly, total sugar concentration ([TS]) of the solution was analyzed by the acid-phenol spectrometric method.

2.1.3 Selection of Support Material

2.1.3.1 Support Material Preparation and Immobilization of Anaerobic Sludge

8 different porous synthetic or natural support materials were used to immobilize heat pre-treated anaerobic sludge. These were stainless steel scrubber, volcanic stone, tulle, polyester fiber, loofah sponge, plastic bath sponge, sea sponge and aquarium biological sponge. While stainless steel scrubber, volcanic stone, tulle, polyester fiber and plastic bath sponge were prepared as round shape (approximately 1.5 cm in diameter); loofah sponge, sea sponge and aquarium biological sponge were prepared as rectangular shape (approximately 2 x 1 x 1 cm). Polyester fiber and loofah sponge were surrounded with metal wire to prevent particles from dispersing. The pictures of support particles were given in Figure 2.1.

Repeated batch experiments were conducted in 610 ml serum bottles with 200 ml fermentation volume for entrapment of sludge into/onto the support materials. The volume of particles contained within bottles kept constant at 150 ml. Total particle numbers in the bottles were as follows; stainless steel scrubber N_1= 20, volcanic stone N_2= 60, tulle N_3= 45, polyester fiber N_4= 15, loofah sponge N_5= 40, plastic bath sponge N_6= 20, sea sponge N_7= 30 and aquarium biological sponge N_8= 25. Bottles containing support particles and 10 g/L AHWS were inoculated with 90 ml of heat treated sludge culture. Initial pH of fermentation medium was adjusted to 5.5-6. Silicone rubber stoppers and screw caps were used to avoid gas leakage from the bottles. Argon gas was passed through the cultivation media before incubation to maintain anaerobic conditions. Sludge, carbon source and immobilization material containing bottles were incubated at 55 ºC. A control experiment was conducted in parallel to immobilized repeated batch operation. Control bottles contained only sludge and fermentation medium without support particle. After 2 days of incubation, biomass was separated from the liquid phase by centrifugation. Then the biomass was re-suspended with fresh media and fed into the bottles. This process was repeated three times for every 2 days incubation. Biohydrogen production by batch

fermentation was started when biofilm formation was observed on the support particles.

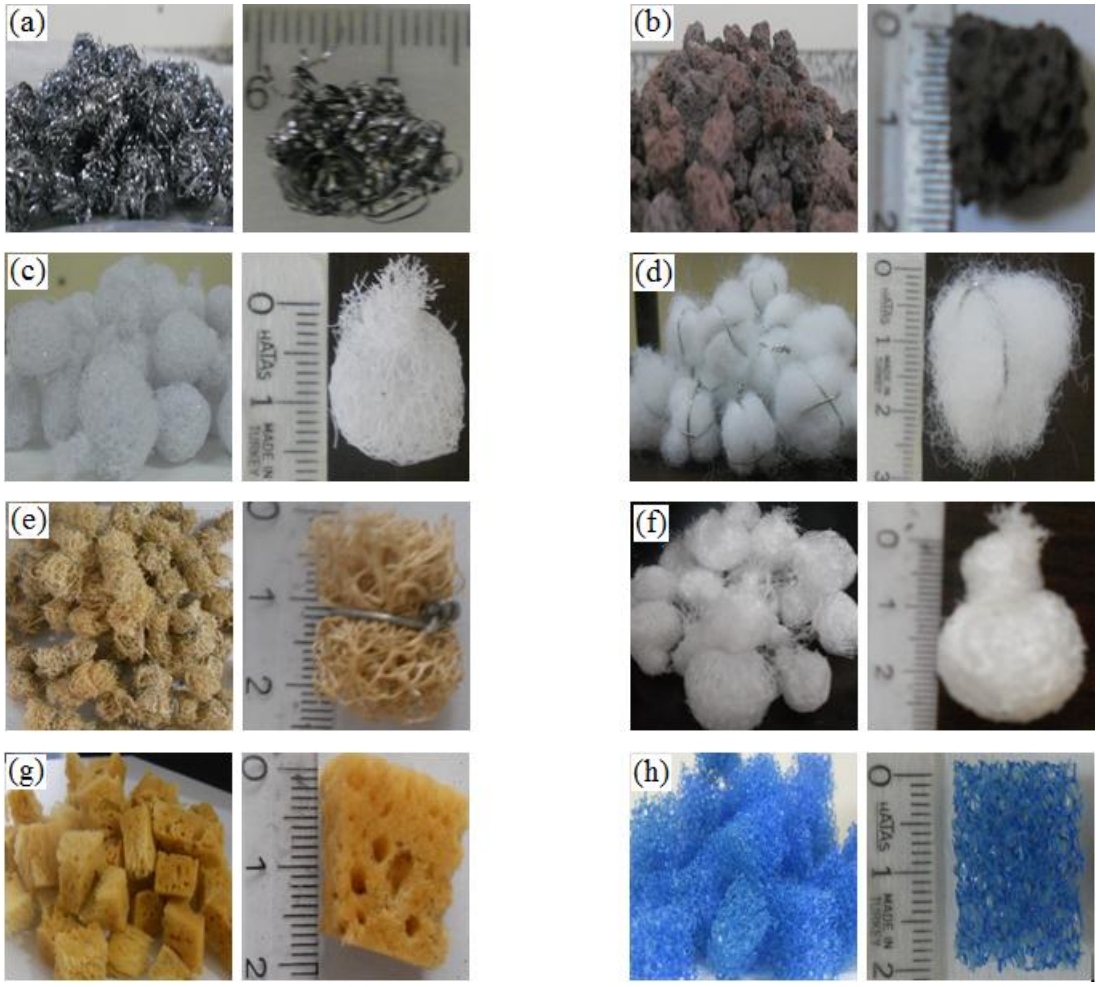


Figure 2.1 Different support materials used for particle selection. (a) stainless steel scrubber, (b) volcanic stone, (c) tulle, (d) polyester fiber, (e) loofah sponge, (f) plastic bath sponge, (g) sea sponge, (h) aquarium biological sponge.

The batch experiments for H_2 production by free and immobilized cell culture were conducted at varying initial total sugar concentration in the fermentation medium. At the end of the immobilization, biomass was separated from the liquid phase by centrifugation. Then, the bottles were reloaded with fresh media and with the biomass recovered after centrifugation. Initial total sugar concentrations of fermentation medium were 13.17 $\pm$ 1.5 g/l in the first set of batch experiments. Initial pH of fermentation medium was adjusted to 5.5-6. ORP was controlled under

-100 and -300 mV. The bottles were closed with silicone rubber stoppers and screw caps and were incubated at 55 ºC . The operation was terminated when cumulative hydrogen production volume remained almost constant. Argon gas was passed through the cultivation media every day. Aforementioned processes were repeated in the second and third set of batch experiments. Initial total sugar concentrations of fermentation medium were 16.90 $\pm$ 2 g/l in the second set of batch experiments and 26.54 $\pm$ 4 g/l in the third set of batch experiments. The support particle was selected based on the highest hydrogen yield obtained at different initial substrate concentrations.

2.1.4 The Effect of Support Material Size on Biohydrogen Production

2.1.4.1 Support Material Preparation and Immobilization of Anaerobic Sludge

Maximum hydrogen yield (mol H_2 / mol glucose) was obtained with polyester fiber. Therefore, this particle was selected as immobilization surface for hydrogen production from hydrolyzed wheat. The effect of particle size was investigated at constant substrate concentration. Polyester fiber particles were prepared at different sizes as 0.5, 1, 2, 3 cm in diameter. The pictures of polyester fiber particles were given in Figure 2.2. The total surface area of the particle would change with the diameter. On the other hand, the experiment should have been conducted at constant surface area. It was not possible to measure total surface area of a single particle including the inner particle surface. It was decided to neglect inner surface area, although it was significant, and consider the outer surface are of particles. Therefore, surface area of particles contained within bottles kept constant at almost 45 cm^2. Total particle numbers in the bottles were as follows; R = 0.5 cm, N_1= 241; R = 1 cm, N_2= 60; R = 2 cm, N_3= 15; R = 3 cm, N_4= 7. Bottles containing support particles and 10 g/l AHWS were inoculate with 90 ml of heat treated sludge culture. Initial pH of fermentation medium was adjusted to 5.5-6. The bottles were closed with silicone rubber stoppers and screw caps. Argon gas was passed through the cultivation media before incubation. The bottles were incubated at 55 ºC. Same immobilization procedure was applied as explained in part *2.1.3.1*. The batch experiments were

carried out as explained in part *2.1.3.1* with the initial total sugar concentration of 14.83 ± 0.5g/l.

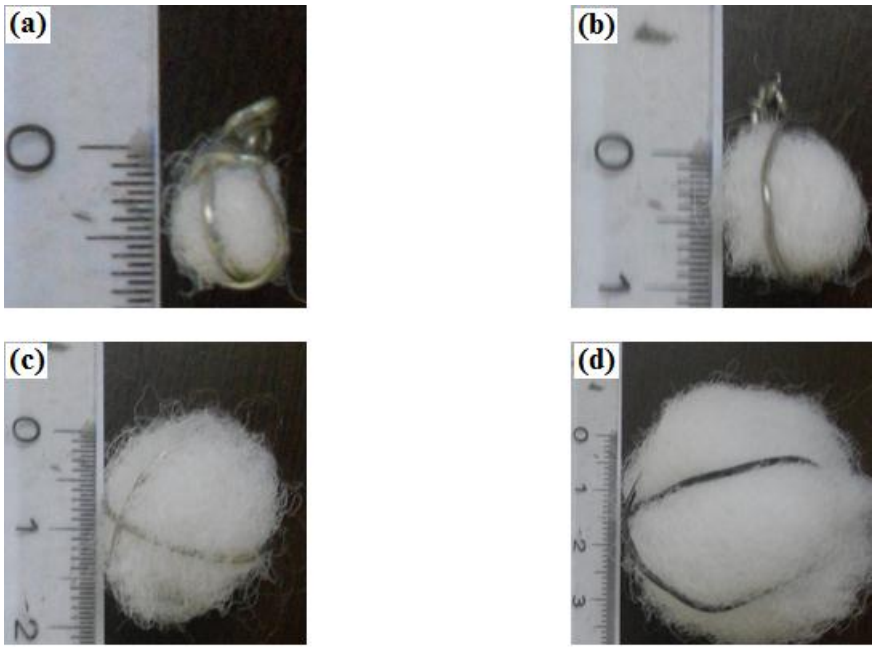


Figure 2.2 Polyester fiber particles prepared with various sizes. The dimeter of the particles: (a) 0.5cm (b) 1 cm, (c) 2 cm, (d) 3 cm.

2.1.5 Box-Wilson Statistical Experiment Design

The Box-Wilson statistical experimental design is a second order, response surface method used for evaluation of a dependent variable (response) as functions of independent variables (factors). One of the main objective of this method is optimizing the operating parameters of the process that yield a maximum or minimum response. Also, method provides an advantage to understand the interaction and quadratic effects among factors. Thus, this method is preferred when a peak or curvature is observed in the response. The following quadratic function is used for correlation of the response with independent three variables as X_1, X_2 and X_3. Schematic diagram of Box-Wilson experimental design is given in Figure 2.3

$$Y = b_0 + b_1X_1 + b_2X_2 + b_3X_3 + b_{12}X_1X_2 + b_{13}X_1X_3 + b_{23}X_2X_3 + b_{11}X_1^2 + b_{22}X_2^2 + b_{33}X_3^2 \quad (2.1)$$

where,

Y is the predicted response;

$\mathbf{b_0}$ is a constant;

$\mathbf{b_1}$, $\mathbf{b_2}$ and $\mathbf{b_3}$ are the linear coefficients;

$\mathbf{b_{12}}$, $\mathbf{b_{13}}$ and $\mathbf{b_{23}}$ are the coefficients of interactions among the variables;

$\mathbf{b_{11}}$, $\mathbf{b_{22}}$ and $\mathbf{b_{33}}$ are the quadratic coefficients.

The Box-Wilson statistical experimental design consists of three parts:

- Factorial points: 2^k factorial points, factors' levels are coded as -1, +1
- Axial points: $2k$ axial points, coded as $-\alpha$, $+\alpha$ where $|\alpha| = \sqrt{k}$ (2.2)
- Center points: nc center points (at least 3), coded as 0

where k is number of factors. The total number of design points is

$$N = 2^k + 2k + nc \quad (2.3)$$

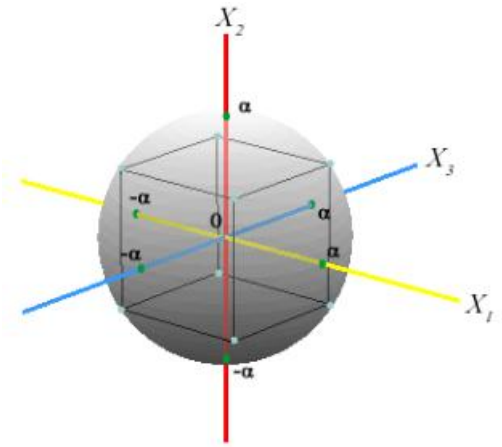


Figure 2.3 Points in Box-Wilson statistical experimental design where k = 3

This optimization process consists of the following major steps, performing the statistically designed experiments, estimating the coefficients in a mathematical model, and predicting the response and checking the adequacy of the model.

In this thesis, a Box–Wilson statistical experiment design method was used to determine the effects of particle number, initial substrate concentration and temperature on hydrogen yield (Y_{H2}, mol H_2/mol glucose) and hydrogen production rate (HPR, ml H_2/h). Particle number (X_1), initial substrate concentration (X_2) and temperature (X_3) were independent variables while the hydrogen yield and the HPR were the objective functions. Particle number (X_1) was varied between 120 and 240, initial substrate concentration (X_2) between 10 and 30 g/l and temperature (X_3) between 35 and 55 ºC. Coded and actual values of independent variables are shown in Table 2.1.

Table 2.1 Coded and actual values of independent variables, where $|\alpha| = \sqrt{3} = 1.73$

Variable	**Symbol**	**Levels**				
		–1	**–α**	**0**	**+α**	**+1**
Particle number	X_1	120	145	180	215	240
Initial substrate concentration (g/l)	X_2	10	14	20	26	30
Temperature (ºC)	X_3	35	39	45	51	55

The experiments consisted of six axial (A), eight factorial (F) and centre points (C). The centre point was repeated three times. The experimental data obtained from the experiments presented in Table 2.2 was used for determination of the coefficients in equation 2.1 using a Design Expert Trial version by regression analysis.

Table 2.2 Experimental conditions of the Box-Wilson statistical design

Experimental point	Coded value			Actual value		
	X_1	X_2	X_3	X_1	X_2	X_3
A_1	+α	0	0	215	20	45
A_2	-α	0	0	145	20	45
A_3	0	+α	0	180	26	45
A_4	0	-α	0	180	14	45
A_5	0	0	+α	180	20	51
A_6	0	0	-α	180	20	39
F_1	+1	+1	+1	240	30	55
F_2	+1	+1	-1	240	30	35
F_3	+1	-1	+1	240	10	55
F_4	+1	-1	-1	240	10	35
F_5	-1	+1	+1	120	30	55
F_6	-1	+1	-1	120	30	35
F_7	-1	-1	+1	120	10	55
F_8	-1	-1	-1	120	10	35
C_1	0	0	0	180	20	45
C_2	0	0	0	180	20	45
C_3	0	0	0	180	20	45

2.2 Analytical Methods

2.2.1 Sampling

Samples were removed from the fermentation medium at the beginning and at the end of the batch experiments were centrifuged at 8000 rpm. The clear supernatants were used for total sugar and total volatile fatty acid (TVFA) analysis.

2.2.2 Total Sugar Analysis

Total sugar concentrations were determined by the acid-phenol spectrometric method (Dubois et al., 1956).

2.2.3 Total Volatile Fatty Acid (TVFA) Analysis

TVFA analyses were carried out by using analytical kits (Spectroquant, 1.01763. 0001, Merck, Darmstadt, Germany) and a PC spectrometer (WTW Photolab S12).

2.2.4 Total Gas Volume Measurement

The total gas volume produced was determined by water displacement method everyday by using sulfuric acid (2%) and NaCl (10%) containing solution.

2.2.5 H_2 Gas Measurements

Hydrogen gas was sampled from the head space of the bottles by using gas-tight glass syringes. Hydrogen gas concentration in the gas phase and in the head space of the bottle after argon gas was passed through was measured by using a gas chromatograph (HP Agilent 6890). The column was Alltech, Hayesep D 80/100 6" × 1/8" × 085". Nitrogen gas was used as carrier with a flow rate of 30 ml min^{-1} and the head pressure was 22 psi. Temperatures of the oven, injection, detector, and filament were 35 ºC, 120 ºC, 120 ºC, 140 ºC, respectively.

2.2.6 pH and ORP Measurements

pH and ORP of the fermentation medium were monitored everyday by using a pH meter and ORP meter with relevant probes (WTW Sci., Germany). pH was maintained between 6.5 and 7.5 by manual pH control, using 5 M NaOH solution. ORP values varied between −100 and −300 mV, in general.

2.2.7 Calculations

The cumulative hydrogen gas volume (CHV, ml) was calculated by the following equation:

$$V_{H2}, i = V_{H2}, i\text{-}1 + V_W, i \times {}^1C_{H2}, i + V_G, i \left({}^1C_{H2}, i - {}^2C_{H2}, i\text{-}1 \right) \quad (2.4)$$

where

$\mathbf{V_{H2}, i}$; CHV (ml) calculated for the i^{th} measurement,

$\mathbf{V_{H2}, i\text{-}1}$; CHV (ml) calculated for the previous measurement of i^{th} ,

$\mathbf{V_{W}, i}$; total gas volume measured by the water displacement method (mL) for the i^{th} measurement,

$^{1}\mathbf{C_{H2}, i}$; the concentration of H_2 gas (%) in the total gas for the i^{th} measurement,

$\mathbf{V_{G}, i}$; the head space volume of the bottle for the i^{th} measurement,

$^{2}\mathbf{C_{H2}, i\text{-}1}$; the concentration of H_2 gas (%) in the head space of the bottle after argon gas was passed through for the $i\text{-}1^{th}$ measurement.

The moles of cumulative hydrogen was calculated by using ideal gas law equation:

$$PV = nRT \tag{2.5}$$

where:

P ;the absolute pressure of the gas (1 atm),

V ; CHV (L),

n ; the moles of CHV (mol),

R ; the ideal, or universal, gas constant, 0.082 (L atm / mol K),

T ; the absolute temperature of the gas (Kelvins ; 273 K = 0.00 ºC).

Hydrogen gas volumes were correlated to room temperature (25 ºC).

The moles of total sugar (glucose) consumed by microorganisms during batch fermentation was calculated as follow:

$$n = \frac{(TS_f - TS_0) \times V_0}{MW_{C_6H_{12}O_6}} \tag{2.6}$$

where:

n; the moles of total sugar (glucose) consumed (mol),

TS_f; final total sugar concentrations of the fermentation medium (g/l)

TS_0; initial total sugar concentrations of the fermentation medium (g/l),

V_0; the initial fermentation volume (l)

$MW_{C_6H_{12}O_6}$; molecular weight of glucose (180g/mol).

The hydrogen yield was calculated by using the following equation.

$$Y = \frac{\Delta H_2}{\Delta S} \qquad (2.7)$$

where:

Y; hydrogen yield (mol H_2/mol glucose)

$\Delta \mathbf{H_2}$; the moles of CHV (mol) calculated by the equation 2.5

$\Delta \mathbf{S}$; the moles of total sugar (glucose) consumed (mol) calculated by the equation 2.6

In batch fermentations, CHV versus time data were correlated with the Gompertz equation in equation 2.8 to determine the constants by regression analysis with Statistica 5. The Gompertz equation has the following form (Han & Shin, 2004):

$$H_{(t)} = P\, exp\left\{-exp\left[\left(\frac{R_m \times e}{P}\right)(\lambda - t) + 1\right]\right\} \qquad (2.8)$$

where,

$H_{(t)}$; CHV (ml) at any time,

P; the maximum potential hydrogen formation (ml),

R_m; the maximum rate of hydrogen formation, HPR (ml/h),

$\boldsymbol{\lambda}$; duration of the lag phase (h),

e; 2.718,

t; time (h).

CHAPTER THREE
RESULTS AND DISCUSSIONS

H_2 production studies by free and immobilized culture consist of three parts. In the first part of the study, the batch experiments were conducted with eight different support materials at varying the initial total sugar concentrations to select the most suitable support particle for hydrogen production. In the second part of the study, the effect of the support particle size (polyester fiber) on H_2 productivity was investigated. In the third part, a Box–Wilson statistical experiment design method was applied to determine the effects of particle number, initial substrate concentration and temperature on Y_{H2} and HPR and then an optimization of batch hydrogen production in an immobilized system was carried out.

3.1 Selection of Support Material

The effects of immobilization material type and initial total sugar concentrations on H_2 production were examined simultaneously. Batch dark fermentation experiments were carried out with stainless steel scrubber, volcanic stone, tulle, polyester fiber, loofah sponge, plastic bath sponge, sea sponge and aquarium biological sponge at initial total sugar concentrations of 13.17 $\pm$ 1.5 g/l, 16.90 $\pm$ 2 g/l, 26.54 $\pm$ 4 g/l. Control experiments (with no particles) were conducted under the same conditions in order to compare H_2 production capability of suspended and immobilized cell systems.

3.1.1 The Effect of Initial Total Sugar Concentration

3.1.1.1 Control

Figure 3.1 depicts variation of cumulative hydrogen gas volume (CHV) with time for control experiment at different initial total sugar concentrations (TS_o). The highest CHV (347.5 ml) was obtained at TS_o =13.17 $\pm$ 1.5 g/l. As indicated in Figure 3.1, CHV decreased when TS_o was increased. The lowest CHV (104.2 ml) was

obtained with the highest TS_o of 26.54 ± 4 g/l. That may be due to substrate inhibition in suspended culture.

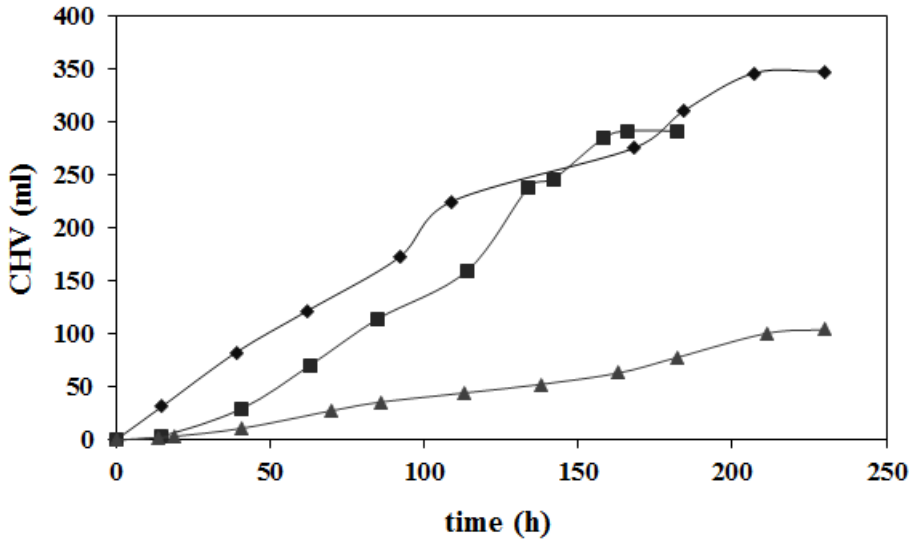


Figure 3.1 Variation of cumulative hydrogen gas volume (CHV) with time for control at different initial total sugar concentrations (TS_o). TS_o: (—◆—) 13.17 ± 1.5 g/l, (—■—) 16.90 ± 2 g/l, (—▲—) 26.54 ± 4 g/l.

Table 3.1 summarizes the yields and rates obtained from suspended culture batch experiments at different initial substrate concentration. The highest Y_{H2} (0.96 mol H_2/mol glucose) was obtained at TS_o of 13.17 ± 1.5 g/l while maximum HPR was 2.45 ml H_2/h when TS_o was 16.90 ± 2 g/l. However, both of them decreased sharply when TS_o was increased from 16.90 ± 2 g/l to 26.54 ± 4 g/l. $[TVFA]_{produced}$ increased from 3.35 g/l to 10.73 g/l as well in parallel to rise in substrate concentration. However, the increase in hydrogen production was not as much as in TVFA production. This result shows that TVFA accumulation in the fermentation medium caused product inhibition and resulted in decrease in Y_{H2} and HPR. Besides, % of substrate utilization decreased gradually with increase in TS_o either due to substrate inhibition or feed-back inhibition of organic acids.

Table 3.1 Hydrogen production results of suspended culture at different TS_o concentration.

TS_o (g/l)	CHV (ml)	Substrate utilization (%)	$[TVFA]_{produced}$ (g/l)	Y_{H2} (mol H_2/mol glucose)	HPR (ml H_2/h)
13.17 ± 1.5	347.5	95.6	3.35	0.96	2.10
16.90 ± 2	291.4	74.9	3.35	0.79	2.45
26.54 ± 4	104.2	57.3	10.73	0.24	0.56

([TVFA], TVFA concentration)

3.1.1.2 Stainless Steel Scrubber

Variation of cumulative hydrogen gas volume (CHV) with time for stainless steel scrubber support material at different initial total sugar concentrations (TS_o) is depicted in Figure 3.2. CHV was 537 ml for TS_o of 13.17 ± 1.5 which was 56% less than the CHV (1225 ml) obtained with TS_o of 16.90 ± 2 g/l. The highest CHV (1590 ml) was obtained at the highest TS_o concentration.

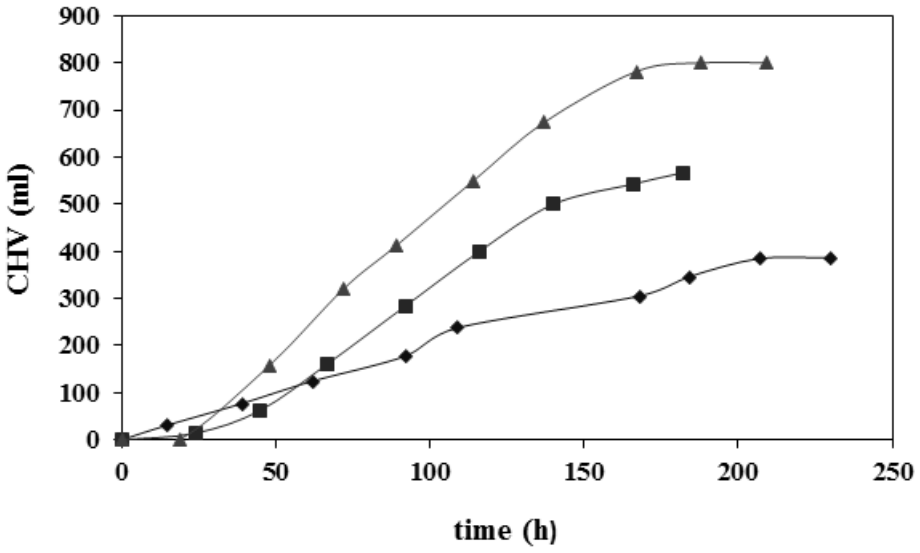


Figure 3.2 Variation of cumulative hydrogen gas volume (CHV) with time for stainless steel scrubber at different initial total sugar concentrations (TS_o). TS_o: (—◆—) 13.17 ± 1.5 g/l, (—■—) 16.90 ± 2 g/l, (—▲—) 26.54 ± 4 g/l.

The hydrogen production results obtained by using stainless steel scrubber particle were summarized in Table 3.2. Y_{H2} was 1.15 mol H_2/mol glucose at TS_o = 13.17 ± 1.5. When TS_o was increased from 13.17 ± 1.5 g/l to 16.90 ± 2 g/l, Y_{H2} increased by 58% and reached its highest value of 1.82 mol H_2/mol glucose for stainless steel scrubber. But it declined to 1.46 mol H_2/mol glucose at TS_o of 26.54 ± 4 g/l. The decrease in Y_{H2} was due to product inhibition because a sharp increase was observed in $[TVFA]_{produced}$ from 4.33 to 10.91 g/l when TS_o increased from 16.90 ± 2 g/l to 26.54 ± 4 g/l. However, HPR demonsrates a gradual increase and maximum HPR of 7.03 ml H_2/h was obtained with TS_o of 26.54 ± 4 g/l. A decline was observed in % of substrate utilization with the increase in TS_o.

Table 3.2 Hydrogen production results obtained by using stainless steel scrubber support particle at different TS_o concentration.

TS_o (g/l)	**CHV (ml)**	**Substrate utilization (%)**	**$[TVFA]_{produced}$ (g/l)**	**Y_{H2} (mol H_2/mol glucose)**	**HPR (ml H_2/h)**
13.17 ± 1.5	386.1	97.6	2.83	1.15	2.31
16.90 ± 2	566.9	72.6	4.33	1.82	5.39
26.54 ± 4	800.3	69.5	10.91	1.46	7.03

([TVFA], TVFA concentration)

3.1.1.3 Volcanic Stone

Figure 3.3 indicates variation of cumulative hydrogen gas volume (CHV) with time for volcanic stone at different initial total sugar concentrations (TS_o). A steady increase in CHV for both TS_o of 13.17 ± 1.5 g/l and 16.90 ± 2 g/l was observed for 40 h of fermentation and the production volume reached up to CHV= 400 ml and CHV= 500 ml, respectively at the end of fermentation period. However, the highest production volume was observed at TS_o = 26.54 ± 4 g/l. The fermentation time extended to 225 h with the hydrogen volume of 914.3 ml at the end of the fermentation.

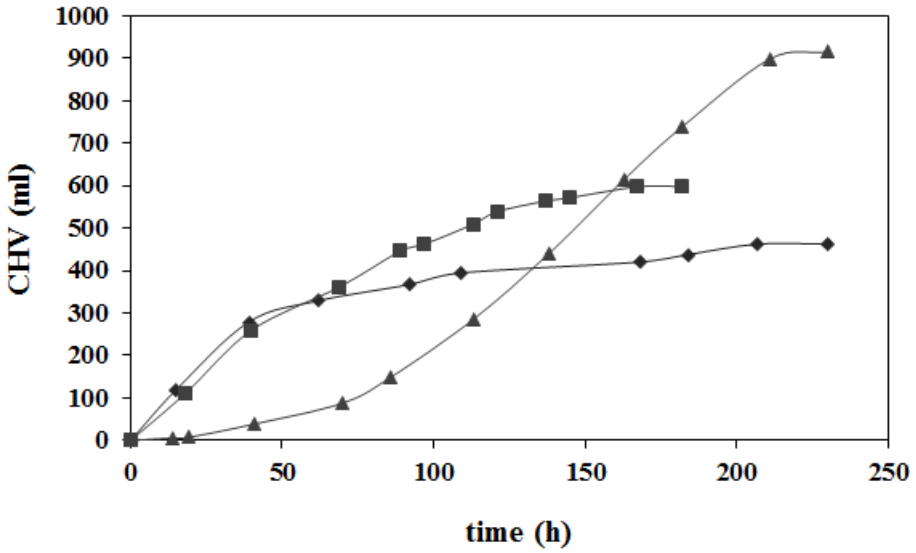


Figure 3.3 Variation of cumulative hydrogen gas volume (CHV) with time for volcanic stone at different initial total sugar concentrations (TS_o). TS_o: (—◆—) 13.17 ± 1.5 g/l, (—■—) 16.90 ± 2 g/l, (—▲—) 26.54 ± 4 g/l.

Table 3.3 summarizes results obtained from batch fermentation experiments by using volcanic stone support particle at different TS_o. Y_{H2}, HPR and % of substrate utilization were almost equal in the range of 1.3-1.5 mol H_2/mol glucose, 5.5-6.5 ml H_2/h and 93-98%, respectively. Besides, daily change of pH values was nearly constant in the range 4.8 and 6.5 for batch experiments conducted at different TS_o (data not shown). These pH values are favorable for best microbial activity for H_2 production. Keskin et al. (2011) used ceramic ring and pumice stone as support material for continuous H_2 production and it was reported that these natural stones showed a good performance of keeping the pH values at 5 and 5.5. That result may arise from the mineralized structure of these kinds of materials. However, $[TVFA]_{produced}$ revealed markedly different trend from Y_{H2} and HPR with the increase in TS_o. $[TVFA]_{produced}$ (11.93 g/l) at TS_o of 26.54 ± 4 g/l was 1.18 times higher than that obtained (TVFA=5.48 g/l) at TS_o of 16.90 ± 2 g/l. Although it seems that there is a contradiction between TVFA and hydrogen production, it is mainly due to the type of organic acid produced during fermentation. The organic acid mixture produced could be mainly non-hydrogen generation ones like lactic acid and propionic acid. Therefore, low hydrogen yield could be obtained.

Table 3.3 Hydrogen production results obtained by using volcanic stone support particle at different TS_o concentration.

TS_o (g/l)	CHV (ml)	Substrate utilization (%)	$[TVFA]_{produced}$ (g/l)	Y_{H2} (mol H_2/mol glucose)	HPR (ml H_2/h)
13.17 ± 1.5	462.5	98.6	2.45	1.44	5.87
16.90 ± 2	598.5	97.7	5.48	1.38	5.51
26.54 ± 4	914.3	93.5	11.93	1.52	6.59

([TVFA], TVFA concentration)

3.1.1.4 Tulle

Variation of cumulative hydrogen gas volume (CHV) with time for tulle at different initial total sugar concentrations (TS_o) is depicted in Figure 3.4. The highest CHV (568.2 ml) was achieved at the lowest TS_o, whereas minimum value of CHV (305.5 ml) was obtained at TS_o of 26.54 ± 4 g/l. CHV for TS_o = 16.90 ± 2 g/l rised rapidly after 10 h of fermentation period and it reached to 475 ml at the end of the fermentation.

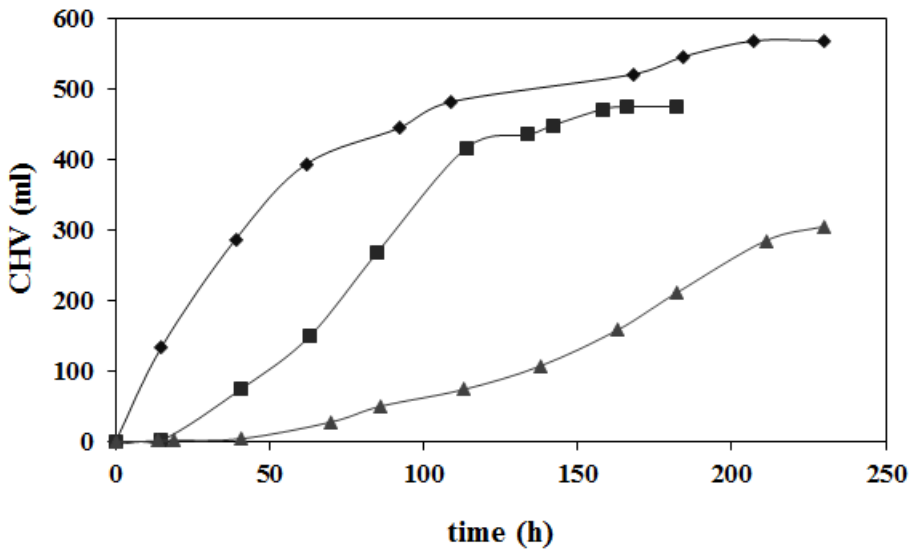


Figure 3.4 Variation of cumulative hydrogen gas volume (CHV) with time for tulle at different initial total sugar concentrations (TS_o). TS_o: (—◆—) 13.17 ± 1.5 g/l, (—■—) 16.90 ± 2 g/l, (—▲—) 26.54 ± 4 g/l.

The highest Y_{H2} and HPR was achieved at TS_o =13.17 ± 1.5 as 1.64 mol H_2/mol glucose and 6.27 ml H_2/h, respectively (Table 3.4). However, considerably lower yield as 0.76 mol H_2/mol glucose and rate as 2.25 ml H_2/h when TS_o = 26.54 ± 4 g/l. Similarly, % of substrate utilization decreased from 93.8% to 68.7% when TS_o was increased from 16.90 ± 2 to 26.54 ± 4 g/l. Lower yield of production and substrate utilization are the indicators of substrate inhibition.

Table 3.4 Hydrogen production results obtained by using tulle support particle at different TS_o concentration

TS_o (g/l)	**CHV (ml)**	**Substrate utilization (%)**	**$[TVFA]_{produced}$ (g/l)**	**Y_{H2} (mol H_2/mol glucose)**	**HPR (ml H_2/h)**
13.17 ± 1.5	568.2	98.8	2.4	1.64	6.27
16.90 ± 2	475	93.8	4.3	1.13	5.53
26.54 ± 4	305.5	68.7	7.9	0.76	2.25

([TVFA], TVFA concentration)

3.1.1.5 Polyester Fiber

Figure 3.5 depicts variation of cumulative hydrogen gas volume (CHV) with time for polyester fiber at different initial total sugar concentrations (TS_o). CHV at TS_o of 13.17 ± 1.5 g/l demonstrated a sudden increase during 110 h of fermentation period, and then remained almost constant with the final CHV=640.5 ml at the end of fermentation. CHVs at TS_o of 16.90 ± 2 g/l showed a similar trend for all fermentation period with the final CHV of 536 ml. The highest volume was obtained at 26.54 ± 4 g/l. The production steadily increased from beginning of fermentation till the end and reached to 907.7 ml.

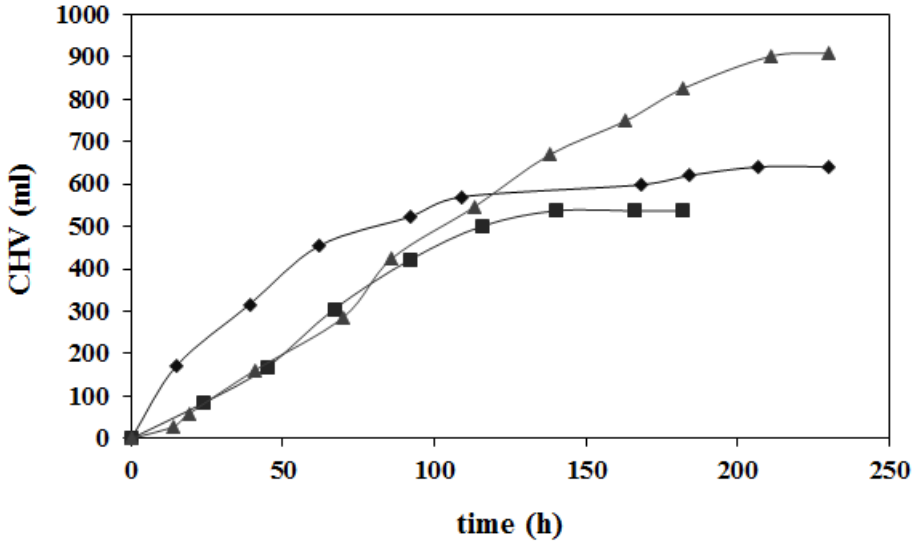


Figure 3.5 Variation of cumulative hydrogen gas volume (CHV) with time for polyester fiber at different initial total sugar concentrations (TS_o). TS_o: (—◆—) 13.17 ± 1.5 g/l, (—■—) 16.90 ± 2 g/l, (—▲—) 26.54 ± 4 g/l.

Yield and rates of production is more comparable data in order to determine the best particle for hydrogen production in immobilized systems. Polyester fiber resulted in a promising rate of production and yield of formation. As seen from Table 3.5, yield varies between 1.96 and 1.55 mol H_2/mol glucose for the sugar concentrations 13.17 ± 1.5 to 26.54 ± 4 g/l, respectively. Rate of production and substrate utilization did not vary substantially for different substrate concentration.

Table 3.5 Hydrogen production results obtained by using polyester fiber support particle at different TS_o concentration

TS_o (g/l)	**CHV (ml)**	**Substrate utilization (%)**	**$[TVFA]_{produced}$ (g/l)**	**Y_{H2} (mol H_2/mol glucose)**	**HPR (ml H_2/h)**
13.17 ± 1.5	640.5	98.7	2.81	1.96	7.39
16.90 ± 2	536.8	97.8	6.35	1.38	6.15
26.54 ± 4	907.7	97.2	8.82	1.55	6.07

([TVFA], TVFA concentration)

3.1.1.6 Loofah Sponge

Figure 3.6 demonstrates variation of cumulative hydrogen gas volume (CHV) with time for loofah sponge at different initial total sugar concentrations (TS_o). There were slight differences between CHVs at different TS_o. The lowest CHV (417.2 ml) was obtained at TS_o of 13.17 $\pm$ 1.5 g/l. CHV increased 1.26 times and reached the highest value of 525.2 ml when TS_o varied from 13.17 $\pm$ 1.5 to 16.90 $\pm$ 2 g/l. Then it declined to 459.5 ml at TS_o of 26.54 $\pm$ 4 g/l.

Table 3.6 summarizes data obtained from batch fermentation experiments of loofah sponge at different TS_o. Same results were obtained for Y_{H2} (1.32 mol H_2/mol glucose) at TS_o of 13.17 $\pm$ 1.5 and 16.90 $\pm$ 2 g/l. But, yield of formation was only Y_{H2} =0.83 mol H_2/mol glucose at TS_o of 26.54 $\pm$ 4 g/l. A slight increase in HPR was observed from 3.10 to 4.23 ml H_2/h for rise in TS_o from 13.17 $\pm$ 1.5 to 16.90 $\pm$ 2 g/l and then rate decreased to 3.98 for the highest total sugar concentration. $[TVFA]_{produced}$ was maximum (9.35 g/l) at the highest TS_o = 26.54 $\pm$ 4 g/l. Low yield of formation, low substrate utilization but high TVFA production indicate both substrate and product inhibitions.

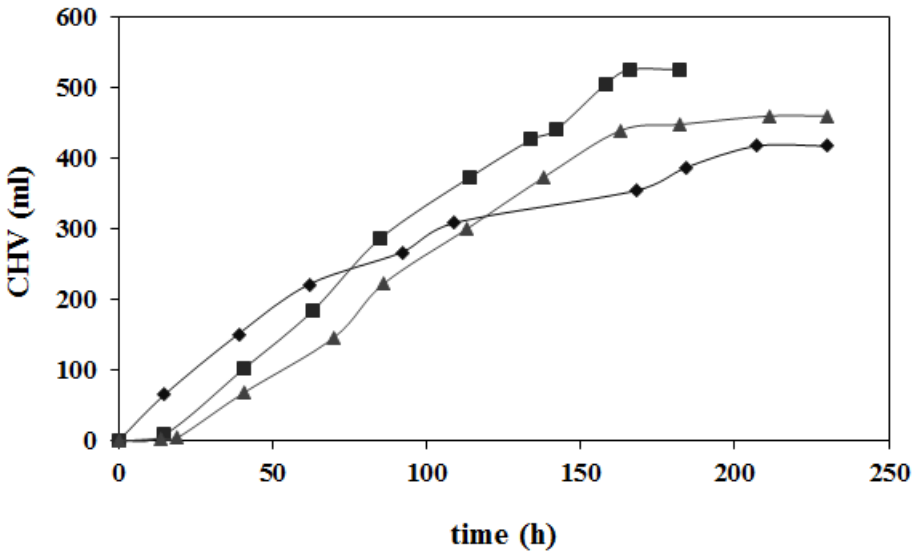


Figure 3.6 Variation of cumulative hydrogen gas volume (CHV) with time for loofah sponge at different initial total sugar concentrations (TS_o). TS_o: (—◆—) 13.17 $\pm$ 1.5 g/l, (—■—) 16.90 $\pm$ 2 g/l, (—▲—) 26.54 $\pm$ 4 g/l.

In summary, loofah sponge does not seem an appropriate support particle for H_2 production with respect to Y_{H2}. Loofah sponge was evaluated according to its biomass retention and hydrogen production capacity by Chang et al (2002) and it was concluded that loofah sponge was not an efficient matrix for hydrogen production as it was obtained in this study.

Table 3.6 Hydrogen production results obtained by using loofah sponge support particle at different TS_o concentration

TS_o (g/l)	**CHV (ml)**	**Substrate utilization (%)**	**$[TVFA]_{produced}$ (g/l)**	**Y_{H2} (mol H_2/mol glucose)**	**HPR (ml H_2/h)**
13.17 ± 1.5	417.2	97.8	1.93	1.32	3.10
16.90 ± 2	525.2	94.6	4.58	1.32	4.23
26.54 ± 4	459.5	79.6	9.35	0.83	3.98

([TVFA], TVFA concentration)

3.1.1.7 Plastic Bath Sponge

Figure 3.7 indicates variation of cumulative hydrogen gas volume (CHV) with time for plastic bath sponge at different initial total sugar concentrations (TS_o). A steady increasing in CHV was observed up to 150 h fermentation period for TS_o =13.17 ± 1.5 g/l and 16.90 ± 4 g/l all initial substrate concentrations. Production at TS_0= 26.54 ± 4 g/l ceased sooner around 100 h of fermentation without no significant increase in the volume for further fermentation period. As a result the highest CHV was obtained as 517.8 ml at TS_o=13.17 ± 1.5 g/l.

The yield of formation and rate of productions were not as good as polyester fiber or volcanic stone. As it was observed in other particle types CHV, Y_{H2} and HPR decreased with increase in TS_o (Table 3.7). The highest Y_{H2} and HPR were 1.53 mol H_2 /mol glucose and 4.46 ml H_2/h, respectively, and they were obtained at the lowest sugar concentration of 13.17 ± 1.5 g/l. Substrate utilization decreased as well with the increase in substrate concentration.

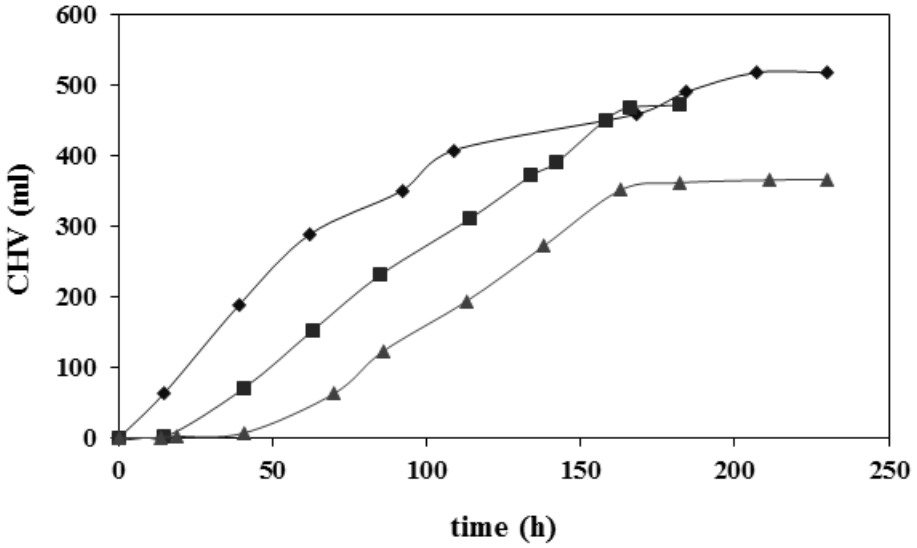


Figure 3.7 Variation of cumulative hydrogen gas volume (CHV) with time for plastic bath sponge at different initial total sugar concentrations (TS_o). TS_o: (—◆—) 13.17 ± 1.5 g/l, (—■—) 16.90 ± 2 g/l, (—▲—) 26.54 ± 4 g/l.

Table 3.7 Hydrogen production results obtained by using plastic bath sponge support particle at different TS_o concentration

TS_o (g/l)	**CHV (ml)**	**Substrate utilization (%)**	**$[TVFA]_{produced}$ (g/l)**	**Y_{H2} (mol H_2/mol glucose)**	**HPR (ml H_2/h)**
13.17 ± 1.5	517.8	98.4	2.59	1.53	4.46
16.90 ± 2	471.5	91.6	4.16	1.18	3.72
26.54 ± 4	366.5	74.6	9.64	0.74	3.66

([TVFA], TVFA concentration)

3.1.1.8 Sea Sponge

Sea sponge is a natural material with high porosity which could enhance the microorganism holding capacity. Figure 3.8 indicates variation of cumulative hydrogen gas volume (CHV) with time for sea sponge at different initial total sugar concentrations (TS_o). There was a moderate increase in CHV at TS_o of 13.17 ± 1.5 g/l and it was 257.6 ml at the end of the fermentation. On the other hand, CHVs at TS_o of 16.90 ± 2 and 26.54 ± 4 g/l increased significantly. CHV reached the highest value of 663.6 ml at TS_o of 16.90 ± 2 g/l, while it was 532.8 ml at TS_o of 26.54 ± 4 g/l.

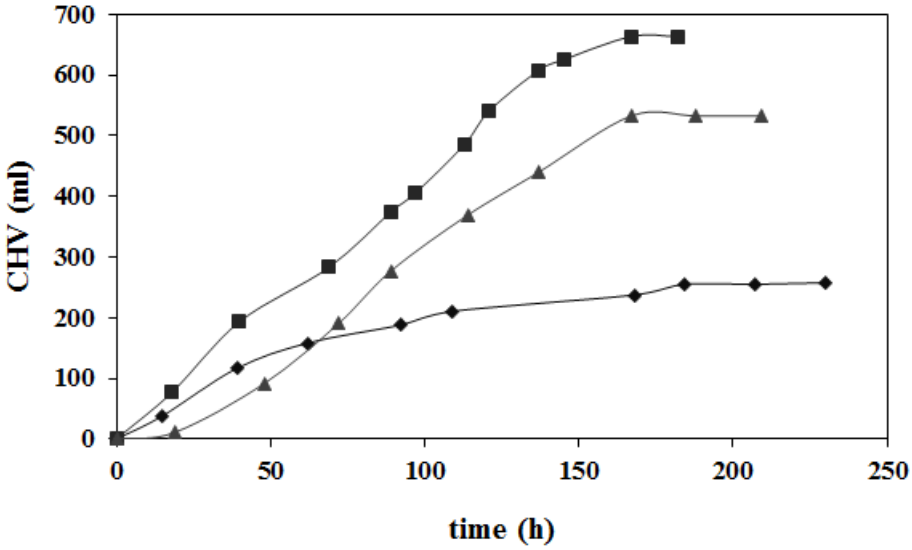


Figure 3.8 Variation of cumulative hydrogen gas volume (CHV) with time for sea sponge at different initial total sugar concentrations (TS_o). TS_o: (—◆—) 13.17 ± 1.5 g/l, (—■—) 16.90 ± 2 g/l, (—▲—) 26.54 ± 4 g/l.

Table 3.8 summarizes hydrogen production results obtained from batch fermentation experiments by using sea sponge at different TS_o. A similar trend was observed for Y_{H2} and HPR. The lowest values for both of them obtained at TS_o of 13.17 ± 1.5 g/l (0.85 mol H_2/mol glucose, 2.49 ml H_2/h, respectively). They increased and reached the highest values at TS_o of 16.90 ± 2 g/l (1.67 mol H_2/mol glucose, 5.01 ml H_2/h, respectively). Then, they fell to 0.97 mol H_2/mol glucose and 4.82 ml H_2/h, respectively, at TS_o of 26.54 ± 4 g/l. $[TVFA]_{produced}$ increased with the increase in TS_o and reached to maximum value of 12.37 g/l at TS_o of 26.54 ± 4 g/l. In contrast, % of substrate utilization decreased with the increase in TS_o.

Table 3.8 Hydrogen production results obtained by using sea sponge support particle at different TS_o concentration

TS_o (g/l)	**CHV (ml)**	**Substrate utilization (%)**	**$[TVFA]_{produced}$ (g/l)**	**Y_{H2} (mol H_2/mol glucose)**	**HPR (ml H_2/h)**
13.17 ± 1.5	257.6	98.8	1.89	0.85	2.49
16.90 ± 2	663.6	94	5.63	1.67	5.01
26.54 ± 4	532.8	78.8	12.37	0.97	4.82

([TVFA], TVFA concentration)

3.1.1.9 Aquarium Biological Sponge

The last particle used in the study was aquarium biological sponge. It has got high porosity which helps biomass holding capacity. CHV steadily increased during fermentation at all initial total sugar concentrations (Figure 3.9). The maximum value was obtained as 890 ml at TS_o of 26.54 $\pm$ 4 g/l at the end of fermentation period. The production volumes were 601.7 and 532.1 ml for substrate concentrations TS_o = 3.17 $\pm$ 1.5 g/l and 16.90 $\pm$ 2 g/l, respectively.

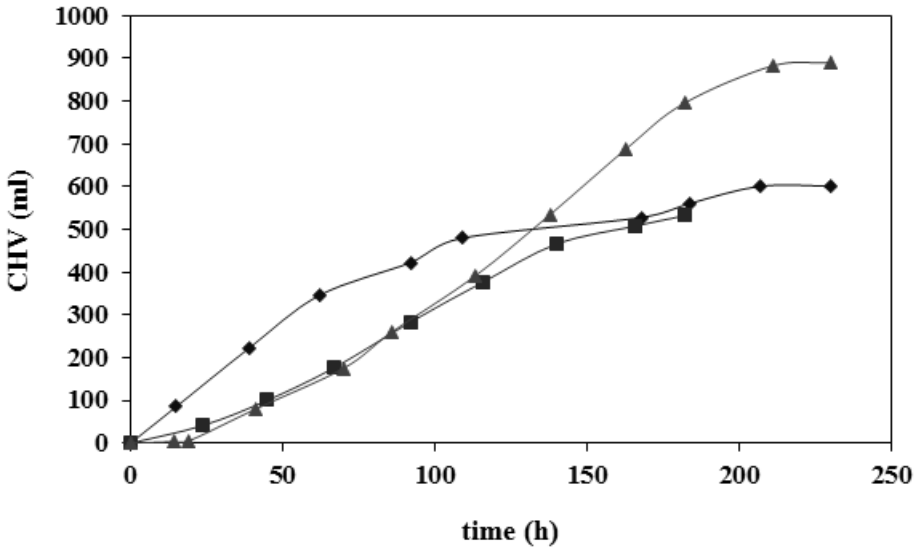


Figure 3.9 Variation of cumulative hydrogen gas volume (CHV) with time for aquarium biological sponge at different initial total sugar concentrations (TS_o). TS_o: (—◆—) 13.17 $\pm$ 1.5 g/l, (—■—) 16.90 $\pm$ 2 g/l, (—▲—) 26.54 $\pm$ 4 g/l.

Table 3.9 summarizes data obtained from batch fermentation experiments of aquarium biological sponge at different TS_o. The highest value of Y_{H2} was obtained at TS_o of 13.17 $\pm$ 1.5 g/l (1.72 mol H_2/mol glucose). It decreased to 1.29 mol H_2/mol glucose at TS_o of 16.90 $\pm$ 2 g/l and almost the same yield (1.31 mol H_2/mol) was obtained at TS_o = 26.54 $\pm$ 4 g/l. There were slight differences in HPR for different TS_o. It was 5.38 ml H_2/h at TS_o of 13.17 $\pm$ 1.5 g/l. A modest decrease was observed when TS_o varied from 13.17 $\pm$ 1.5 to 16.90 $\pm$ 2 g/l (4.32 ml H_2/h). It increased marginally to 6 ml H_2/h at TS_o of 26.54 $\pm$ 4 g/l.

% of substrate utilization decreased slightly from 97.8 % to 94.6 when TS_o increased from 13.17 ± 1.5 to 16.90 ± 2 g/l and it remained almost constant at TS_o of 26.54 ± 4 g/l (93.7%). $[TVFA]_{produced}$ increased sharply from 1.57 g/l to 6.62 g/l when TS_o varied from 13.17 ± 1.5 to 16.90 ± 2 g/l and reached a peak of 10.73 at TS_o of 26.54 ± 4 g/l.

Table 3.9 Hydrogen production results obtained by using aquarium biological sponge support particle at different TS_o concentration

TS_o (g/l)	**CHV (ml)**	**Substrate utilization (%)**	**$[TVFA]_{produced}$ (g/l)**	**Y_{H2} (mol H_2/mol glucose)**	**HPR (ml H_2/h)**
13.17 ± 1.5	601.7	97.8	1.57	1.72	5.38
16.90 ± 2	532.1	94.6	6.62	1.29	4.32
26.54 ± 4	890	93.7	10.73	1.31	6.00

([TVFA], TVFA concentration)

3.1.1.10 Comparison

Figure 3.10 demonstrates hydrogen yield (mol H_2/mol glucose) for different support material types and initial total sugar concentrations. Hydrogen yield is the most important parameter which shows the effectiveness of the fermentation. As mentioned in part *1.2.1,* theoretically, maximum 4 mol H_2 can be obtained per mol glucose if the only end product is acetic acid. If it is butyric acid, hydrogen yield declines 2 mol H_2/mol glucose. The mixture of acetic acid and butyric acid results in 2.5 mol H_2/mol glucose. But, low hydrogen yield is associated with the formation of end-products, like ethanol, propionic acid and lactic acid. In the light of this fact, the highest Y_{H2} was 1.96 mol H_2/mol glucose which was obtained with polyester fiber at TS_o of 13.17 ± 1.5 g/l that is comparable with theoretical yield. The second highest Y_{H2} was obtained with stainless steel scrubber at TS_o of 16.90 ± 2 g/l (1.82 mol H_2/mol glucose) and the third was obtained with aquarium biological sponge at TS_o of 13.17 ± 1.5 g/l (1.72 mol H_2/mol glucose). Y_{H2} obtained with suspended culture at different initial total sugar concentrations were lower than those obtained with immobilized cultures which shows immobilization improves product yield.

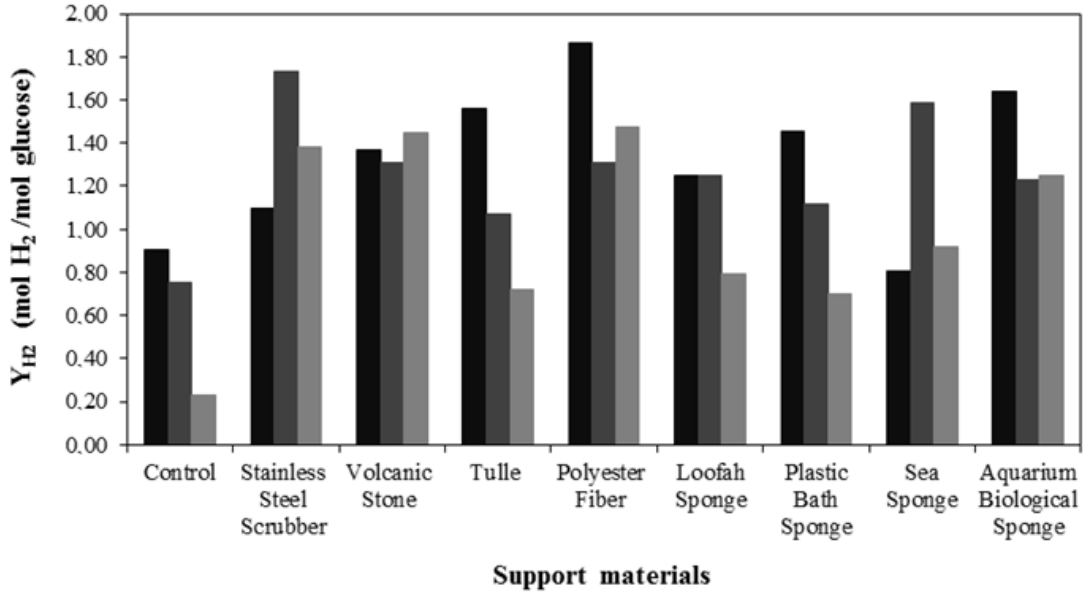


Figure 3.10 Hydrogen yield (Y_{H2}) for varied support materials with different initial total sugar concentrations (TS_o). TS_o: (■) 13.17 ± 1.5 g/l, (■) 16.90 ± 2 g/l, (■) 26.54 ± 4 g/l.

CHV data were correlated with the Gompertz equation (Equation 2.8) to determine the constants by regression analysis. Table 3.10 summarizes the Gompertz equation constants for varied support materials at different initial total sugar concentrations. Hydrogen production potential increased with increase in initial total sugar concentration for stainless steel scrubber, volcanic stone and aquarium biological sponge. There was no as steady increase in volume for the other particle with increasing substrate concentration. The highest hydrogen production potential was 1212 ml which was obtained with volcanic stone at TS_o of 26.54 ± 4 g/l. On the other hand, the maximum hydrogen production rate (HPR, R_m) was obtained with polyester fiber at TS_o of 13.17 ± 1.5 g/l (7.39 ml H_2/h) which was in parallel with Y_{H2}. The lag phases for support materials at TS_o of 13.17 ± 1.5 g/l were relatively short. However, the longest lag phases for almost all support materials were obtained at TS_o of 26.54 ± 4 g/l due to the high substrate concentration.

Table 3.11, Table 3.12 and Table 3.13 indicate variation of substrate utilization and TVFA formation for different support materials and substrate concentrations. Sugar is converted to H_2, TVFAs, CO_2 and biomass during dark fermentation. Final TVFA concentrations are related to hydrogen gas production since H_2 gas is a co-

product of TVFA formation. Theoretically, percent conversion of sugars to TVFA is 67%, when acetic acid is the sole TVFA produced from per mole glucose. As indicated in Table 3.11, $[TVFA]_f$ were in the range of 3.5 and 4.2 g/l at TS_o of 13.17 ± 1.5, in general. Also, the lowest value of percent conversion of sugars to TVFA was 11.3% which was obtained with aquarium biological sponge and the highest value was 23.8% which was obtained with control. These results were rather smaller than others which were obtained at TS_o of 16.90 $\pm$ 2 and 26.54 $\pm$ 4 g/l. Besides, percent substrate utilization was nearly constant in the range 95-98%. However, Table 3.12 demonstrates that percent substrate utilization decreased when TS_o varied from 13.17 ± 1.5 to 16.90 $\pm$ 2 g/l. In contrast, $[TVFA]_f$ and percent conversion of sugars to TVFA increased. Table 3.13 shows that sharp decrease were observed in percent substrate utilization when TS_o varied from 16.90 $\pm$ 2 to 26.54 $\pm$ 4 g/l. The highest value for $[TVFA]_f$ and percent conversion of sugars to TVFA were obtained at TS_o of 26.54 $\pm$ 4 g/l.

The particles selected after comparison and evaluation of the results was polyester fiber which resulted in the highest yield of formation at minimum and maximum substrate concentrations. The substrate inhibition effects at high concentrations were lower compared to that of other particles. There was relatively lower lag phase at high substrate concentrations which indicates high biomass holding capacity.

Table 3.10 Gompertz equation constants for varied support materials at different initial total sugar concentrations

Support Materials	Initial total sugar concentration, TS_o, (g/l)	P (ml)	R_m (ml/h)	λ (h)	R^2
Control	14.74	377.22	2.10	6.37	0.995
	19.03	385.80	2.45	38.92	0.996
	29.16	179.46	0.56	38.32	0.993
Stainless Steel Scrubber	13.29	432.95	2.31	11.18	0.996
	16.58	625.77	5.39	38.01	0.996
	30.64	858.92	7.03	28.84	0.970
Volcanic Stone	12.60	435.80	5.87	0	0.985
	17.20	616.95	5.51	0	0.947
	24.91	1212.46	6.59	69.10	0.982
Tulle	13.56	546.62	6.27	0	0.950
	17.38	499.81	5.53	33.51	0.983
	22.83	683.87	2.25	90.27	0.996
Polyester Fiber	12.80	622.88	7.39	0	0.950
	15.42	559.52	6.15	15.73	0.984
	23.36	989.29	6.07	20.71	0.979
Loofah Sponge	12.55	413.91	3.10	0	0.973
	16.35	597.02	4.23	20.58	0.976
	26.94	485.58	3.98	31.51	0.992
Plastic Bath Sponge	13.31	509.45	4.46	1.29	0.971
	16.96	564.04	3.72	25.59	0.981
	25.84	390.29	3.66	54.82	0.991
Sea Sponge	11.89	253.03	2.49	0	0.991
	16.37	795.57	5.01	10.43	0.923
	27.09	574.38	4.82	32.11	0.988
Aquarium Biological Sponge	13.83	585.15	5.38	0.86	0.960
	16.84	613.37	4.32	25.27	0.995
	28.06	1082.86	6.00	44.86	0.976

Table 3.11 Variation of substrate utilization and TVFA formation for different support materials at $TS_o = 13.17 \pm 1.5$ g/l

Support Materials	Initial total sugar concentration TS_0, (g/l)	Final total sugar concentration TS_f, (g/l)	Substrate utilization (%)	Initial TVFA concentration $[TVFA]_0$, (g/l)	Final TVFA concentration $[TVFA]_f$, (g/l)	Substrate conversion to TVFA (%)
Control	14.74	0.65	95.6	0.70	4.05	23.8
Stainless Steel Scrubber	13.29	0.32	97.6	1.38	4.21	21.8
Volcanic Stone	12.60	0.18	98.6	1.14	3.59	19.7
Tulle	13.56	0.16	98.8	1.18	3.58	17.9
Polyester Fiber	12.80	0.16	98.7	1.29	4.10	22.2
Loofah Sponge	12.55	0.28	97.8	1.69	3.62	15.8
Plastic Bath Sponge	13.31	0.21	98.4	1.04	3.63	19.8
Sea Sponge	11.89	0.15	98.8	1.63	3.52	16.1
Aquarium Biological Sponge	13.83	0.31	97.8	1.92	3.46	11.3

Table 3.12 Variation of substrate utilization and TVFA formation for different support materials at $TS_o = 16.90 \pm 2$ g/l

Support Materials	Initial total sugar concentration TS_0, (g/l)	Final total sugar concentration TS_f, (g/l)	Substrate utilization (%)	Initial TVFA concentration $[TVFA]_0$, (g/l)	Final TVFA concentration $[TVFA]_f$, (g/l)	Substrate conversion to TVFA (%)
Control	19.03	4.77	74.9	1.89	5.24	23.5
Stainless Steel Scrubber	16.58	4.54	72.6	2.54	6.87	35.9
Volcanic Stone	17.20	0.39	97.7	1.53	7.01	32.6
Tulle	17.38	1.07	93.8	1.72	6.02	26.3
Polyester Fiber	15.42	0.34	97.8	3.65	10.00	42.1
Loofah Sponge	16.35	0.88	94.6	1.56	6.14	29.6
Plastic Bath Sponge	16.96	1.42	91.6	2.14	6.30	26.8
Sea Sponge	16.37	0.98	94.0	1.58	7.21	36.6
Aquarium Biological Sponge	16.84	0.90	94.6	2.87	9.49	41.5

Table 3.13 Variation of substrate utilization and TVFA formation for different support materials at $TS_o = 26.54 \pm 4$ g/l

Support Materials	Initial total sugar concentration TS_0, (g/l)	Final total sugar concentration TS_f, (g/l)	Substrate utilization (%)	Initial TVFA concentration $[TVFA]_0$, (g/l)	Final TVFA concentration $[TVFA]_f$, (g/l)	Substrate conversion to TVFA (%)
Control	29.16	12.45	57.3	2.28	13.01	64.2
Stainless Steel Scrubber	30.64	9.33	69.5	2.72	13.63	51.2
Volcanic Stone	24.91	1.63	93.5	2.67	14.60	51.2
Tulle	22.83	7.16	68.7	2.56	10.49	50.6
Polyester Fiber	23.36	0.64	97.2	3.26	12.08	38.8
Loofah Sponge	26.94	5.51	79.6	2.79	12.14	43.6
Plastic Bath Sponge	25.84	6.56	74.6	2.63	12.27	50.0
Sea Sponge	27.09	5.74	78.8	3.85	16.22	57.9
Aquarium Biological Sponge	28.06	1.77	93.7	2.34	13.07	40.8

3.2 The Effect of Support Material Size

Particle size is a significant factor in immobilized systems. An optimal particle size should be used to reach maximum surface area which will help to obtain the maximum biomass concentration, to eliminate substrate diffusion limitation and to get optimal void fraction which provide homogenous environment in the reactor systems. Therefore, particle with diameter as 0.5cm, 1 cm, 2 cm, 3 cm were used. Surface area of particles contained within bottles kept constant at almost 45 cm^2. Total particle numbers in the bottles were as follows; R = 0.5 cm, N_1= 241; R = 1 cm, N_2= 60; R = 2 cm, N_3= 15; R = 3 cm, N_4= 7. Initial total sugar concentration was kept constant at 14.83 ± 0.5g/l AHWS.

Figure 3.11 shows variation of cumulative hydrogen gas volume (CHV) with time at different polyester fiber sizes. The highest CHV was obtained with the particles which were 0.5 cm in diameter (566.8 ml). CHV decreased to 476.3 ml when particle size was 1 cm in diameter. There was a slight increase in CHV obtained with

particles 2 cm in diameter (499.2 ml). However, it decreased sharply to 250.4 ml when particles with 3 cm in diameter were used.

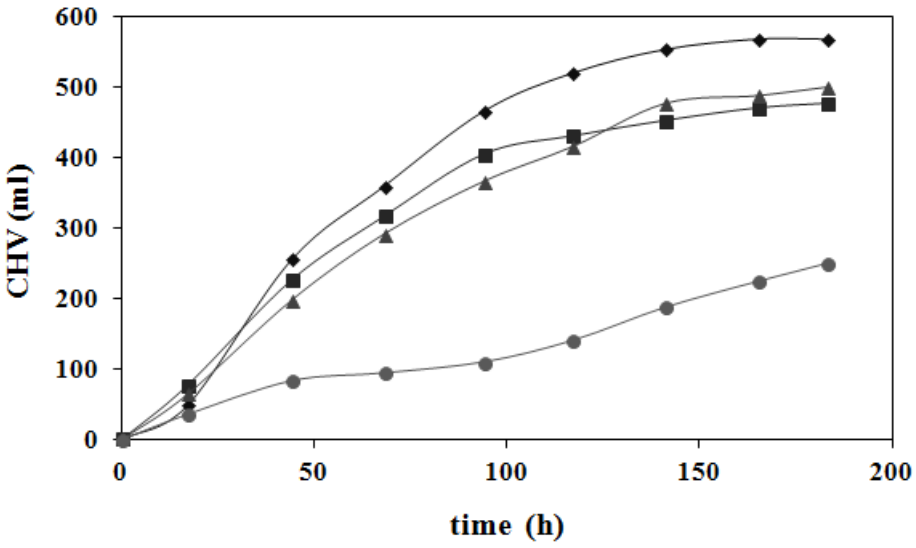


Figure 3.11 Variation of cumulative hydrogen gas volume (CHV) with time for polyester fiber with various sizes. The diameter of the particles: (◆) 0.5cm, (■) 1 cm, (▲) 2 cm, (●) 3 cm.

Table 3.14 summarizes the Gompertz equation constants for polyester fiber with various sizes. Hydrogen production potentials were in the range of 473.82 and 571.77 ml which were in parallel with the experimental results. Maximum hydrogen production rate (HPR=6.72 ml H_2/h) was obtained for particles with 0.5 cm in diameter similar. It decreased slightly from 5.50 and 4.67 ml H_2/h when particle size was increased from 1 cm to 2 cm in diameter, respectively. The lowest rate was HRP=1.48 ml H_2/h when particles with 3 cm in diameter were used.

Table 3.14 Gompertz equation constants for polyester fiber with various sizes.

Support Material Size	P (ml)	R_m (ml/h)	λ (h)	R^2
R=0.5 cm	571.77	6.72	10.32	0.998
R=1 cm	473.82	5.50	5.14	0.998
R=2 cm	511.59	4.67	5.49	0.997
R=3 cm	517.47	1.48	14.79	0.987

Table 3.15 indicates variation of substrate utilization and TVFA formation for polyester fiber for different particle sizes. % substrate utilization was in the range of 94.2% and 96.1%. The highest values of $[TVFA]_f$ and percent conversion of sugars to TVFA were obtained with particles 1 cm in diameter (6.90 g/l, 37.1%, respectively). The lowest value of percent conversion of sugars to TVFA was 27.6% which was obtained with particles 2 cm in diameter. However, $[TVFA]_f$ obtained with both particles 2 cm and 3 cm in diameter were nearly the same (5.08 g/l, 5.92 g/l, respectively).

Table 3.15 Variation of substrate utilization and TVFA formation for polyester fiber with various sizes.

Support Materials	Initial total sugar concentration TS_0, (g/l)	Final total sugar concentration TS_f, (g/l)	Substrate utilization (%)	Initial TVFA concentration $[TVFA]_0$, (g/l)	Final TVFA concentration $[TVFA]_f$, (g/l)	Substrate conversion to TVFA (%)
R=0.5	15.20	0.64	95.8	1.50	4.51	34.2
R=1	15.16	0.59	96.1	1.06	6.90	37.1
R=2	14.64	0.85	94.2	1.26	5.08	27.6
R=3	14.07	0.64	95.5	1.42	5.92	33.8

Figure 3.12 demonstrates hydrogen yield (mol H_2/mol glucose) for polyester fiber with various sizes. The highest Y_{H2} was 1.51 mol H_2/mol glucose obtained using 0.5 cm particles and it was 1.1 times higher than the lowest value of 0.72 mol H_2/mol glucose obtained by using 3 cm particles. It was assumed that decrease in Y_{H2} was due to the availability of the substrate and the exchange of products. Thus, particles 3 cm in diameter were not found suitable for use in hydrogen production. The second highest Y_{H2} was 1.40 mol H_2/mol glucose obtained using 2 cm particles. A slight difference was observed in Y_{H2} obtained using 1 cm particles (1.27 mol H_2/mol glucose).

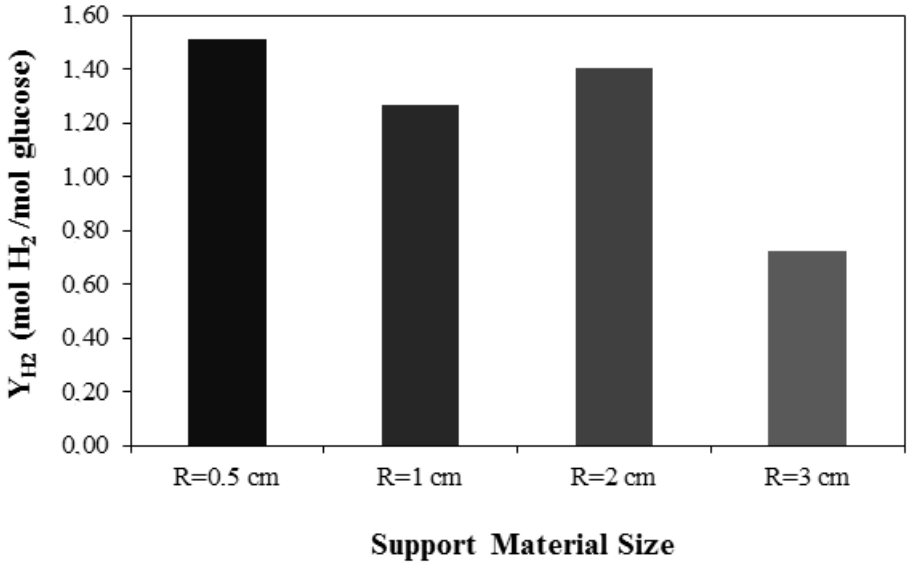


Figure 3.12 Hydrogen yield (Y_{H2}) for polyester fiber with various sizes.

The results indicated that the highest values of Y_{H2} and HPR were obtained with particles size of 0.5 cm in diameter. This particle size was optimal among the investigated sizes in terms of no mass transfer limitation and the highest microbial attachment surface area. Therefore, the most suitable appropriate size for H_2 production was determined to be 0.5 cm and further studies were carried out with these particles size.

3.3 Box-Wilson Statistical Experiment Design

Variations of hydrogen yield and hydrogen production rate with particle number, initial substrate concentration and temperature were investigated by using a Box-Wilson statistical experiment design approach. The responses were yield of formation and rate of production. An optimization of these independent variables for the highest yield of formation and rate of production was conducted. The actual and coded experimental points of the Box- Wilson statistical design are presented in Table 2.2. A response equation was developed and linear, quadratic coefficients of response equation were determined. The results were evaluated by plotting contour and three dimensional surface plots for different dependent responses as yield and rate.

3.3.1 The Effect of Independent Variables on Hydrogen Yield

The coefficients of the response functions were determined by regression analysis are summarized in Table 3.16. These coefficients were used to predict the response at both experimental points and any point within the range of the factors. The experimental results of the Box-Wilson design experiments are presented in Table 3.17 along with the predicted values from the response functions.

Hydrogen yield predictions were in good agreement with the experimental results (R^2=0.89) as shown in Table 3.17. As indicated in Table 3.18, model term was significant. Also, variance analysis demonstrates that temperature was the main factor than affect Y_{H2} significantly. In addition, the interaction between particle number and initial substrate concentration and quadratic effect of particle number were significant.

Table 3.16 Coefficients of the response functions for Y_{H2}

Coefficients	**Values**
b_0	-11.1
b_1	-0.0883
b_2	0.154
b_3	0.821
b_{12}	-0.000656
b_{13}	-0.000206
b_{23}	-0.000413
b_{11}	0.000310
b_{22}	-0.000391
b_{33}	-0.00831

Table 3.17 Experimental and predicted values of $Y_{H2,}$ (R^2 = 0.89)

Experimental point	Yield(exp) (mol H_2/mol glucose)	Yield(pred) (mol H_2/mol glucose)
A_1	2.18	2.11
A_2	2.01	2.04
A_3	1.50	1.69
A_4	1.90	1.68
A_5	1.48	1.57
A_6	1.35	1.23
F_1	1.90	1.74
F_2	1.39	1.50
F_3	2.44	2.59
F_4	2.25	2.18
F_5	2.59	2.66
F_6	2.07	1.93
F_7	2.04	1.93
F_8	0.87	1.03
C_1	1.91	1.70
C_2	1.42	1.70
C_3	1.68	1.70

Table 3.18 Variance analysis for Y_{H2} (ANOVA, α=0.05).

Source	Sum of Squares	df	Mean Square	F Value	p-value Prob > F	Evaluation
Model	2.80	9	0.311	5.96	0.0140	significant
A- Particle number	0.0299	1	0.0299	0.572	0.474	insignificant
B- Initial substrate concentration	0.00139	1	0.00139	0.0266	0.875	insignificant
C- Temperature	0.699	1	0.699	13.4	0.00808	significant
AB	1.24	1	1.24	23.8	0.00180	significant
AC	0.123	1	0.123	2.35	0.169	insignificant
BC	0.0136	1	0.0136	0.261	0.625	insignificant
A^2	0.446	1	0.446	8.55	0.0222	significant
B^2	0.000576	1	0.000576	0.0110	0.919	insignificant
C^2	0.260	1	0.260	4.98	0.0608	insignificant
Pure Error	0.120	2	0.0601			
Cor Total	3.17	16				

Figure 3.13 and 3.14 demonstrate contour and surface plots of the variation of hydrogen yield (Y_{H2}, mol H_2/mol glucose) with particle number and initial substrate concentration at constant fermentation temperature, T=35 ºC. Y_{H2} reached a peak value over 1.8 mol H_2/mol glucose at 35 ºC when particle number was between 230-240 and TS_0 was between 10-20 g/l. Particle number had more substantial effect on the yield at this temperature rather than initial substrate concentration. Figure 3.15 and Figure 3.16 show the effect of the same factors on the yield at temperature, T=45 ºC. Y_{H2} increased significantly at 45 ºC. Response function resulted in that there is a high possibility to obtain 2.95 mol H_2/mol glucose yield at this temperature at high TS_0 (>20 g/l) or at the particle numbers around over 230. The yield was quite high at low particle number and high total sugar concentration. It seems that at low particle number, biomass is more active and can produce more hydrogen probably due to no mass transfer limitation. Similarly, at high particle numbers, the biomass can tolerate low susbtrate concentrations which is effectively converted to end products rather than biomass synthesis as it was the case at high susbtrate concentrations. The metabolic activity of microorganisms could be higher at high fermentation temperatures. In addition, the spore forming bacteria selection is conducted at high temperatures which means selection of thermophilic bacteria is possible. Therefore, yield of production at 55 ºC was estimated. Figure 3.17 and Figure 3.18 indicate the variation of hydrogen yield (Y_{H2}, mol H_2/mol glucose) with particle number and initial substrate concentration at temperature, T=55 ºC. The maximum yields obtained at this temperature was lower than the one at 45 ºC but higher than the yields obatined at 35 ºC. This result indicates that the process operates efficiently at thermophilic range rather than mesophilic conditions. T=45 ^{o}C is sufficient to get high yield of formation for the sake of process economy.

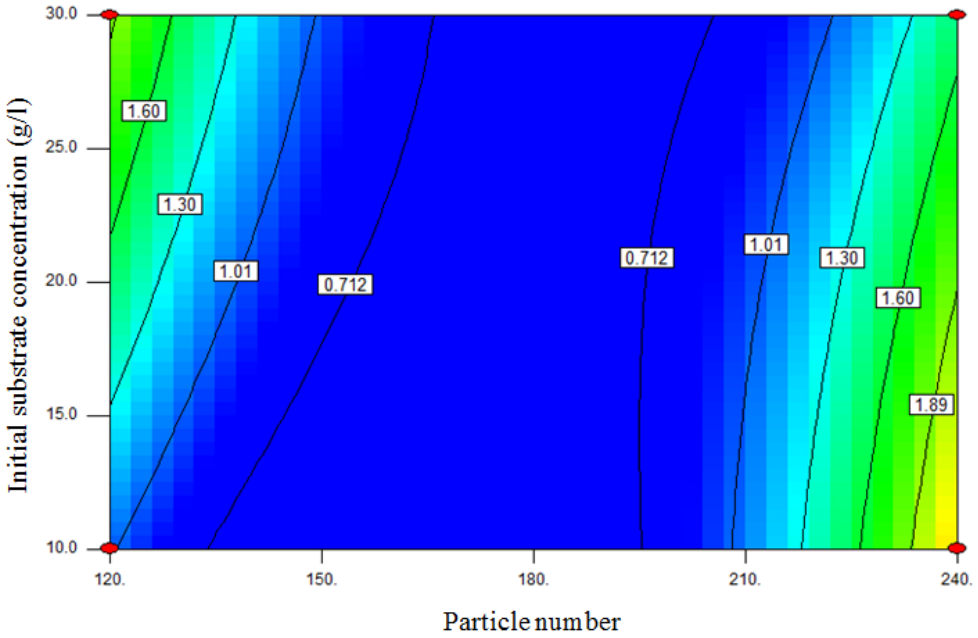


Figure 3.13 The contour plot of response surface showing the variation of hydrogen yield (Y_{H2}, mol H_2/mol glucose) with particle number and initial substrate concentration at temperature, T= 35 ºC.

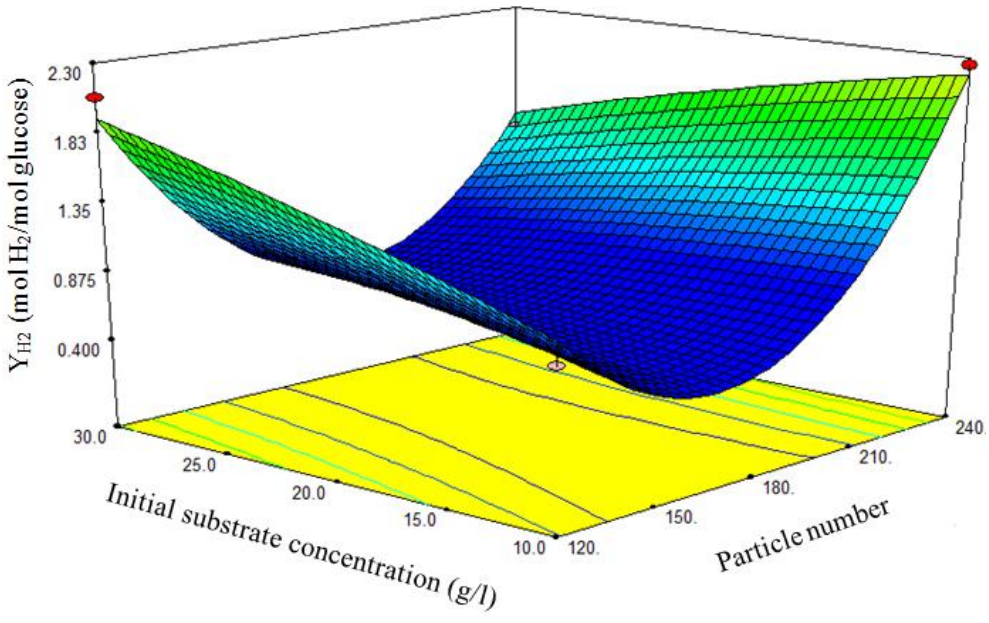


Figure 3.14 The three-dimensional response surface showing the variation of hydrogen yield (Y_{H2}, mol H_2/mol glucose) with particle number and initial substrate concentration at temperature, T=35 ºC.

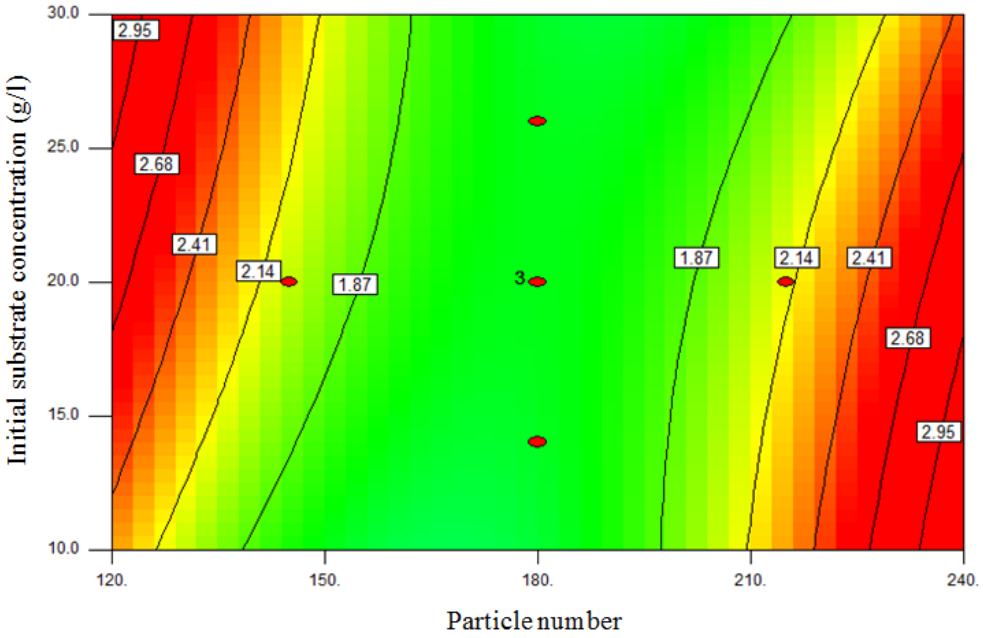


Figure 3.15 The contour plot of response surface showing the variation of hydrogen yield (Y_{H2}, mol H_2/mol glucose) with particle number and initial substrate concentration at temperature, T= 45 ºC.

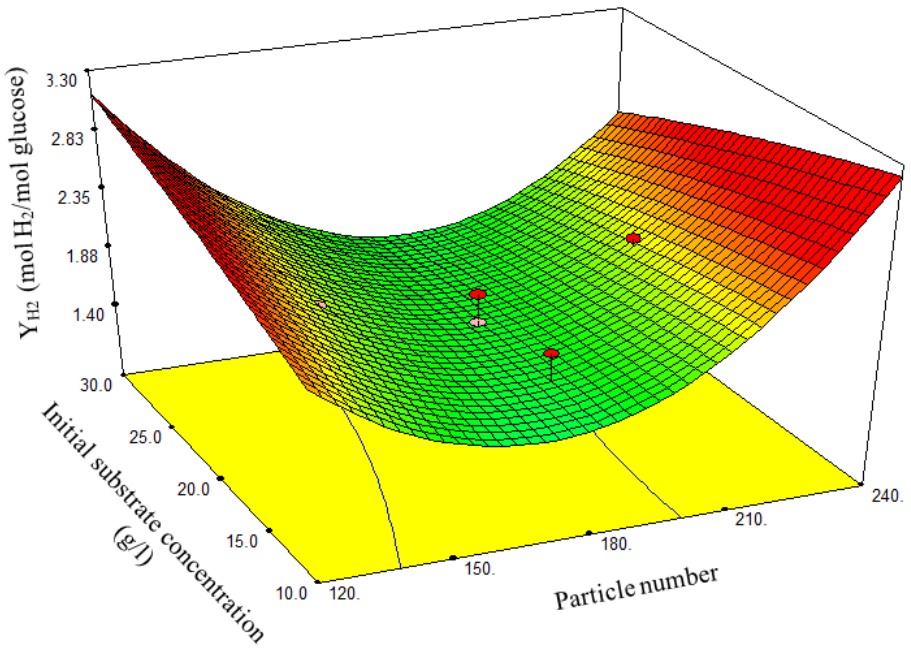


Figure 3.16 The three-dimensional response surface showing the variation of hydrogen yield (Y_{H2}, mol H_2/mol glucose) with particle number and initial substrate concentration at temperature, T= 45 ºC.

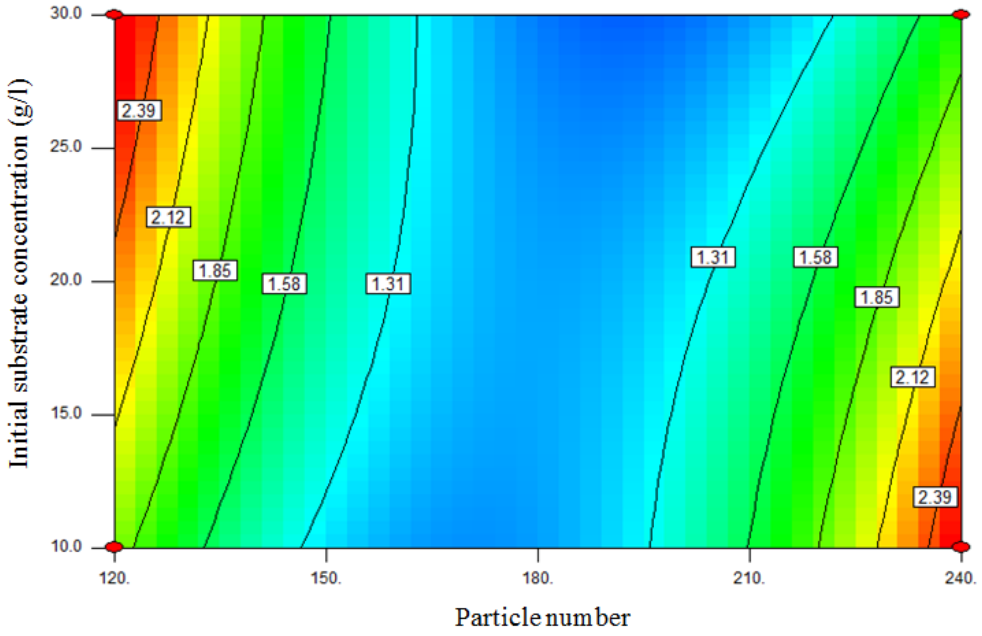


Figure 3.17 The contour plot of response surface showing the variation of hydrogen yield (Y_{H2}, mol H_2/mol glucose) with particle number and initial substrate concentration at temperature, T= 55 ºC.

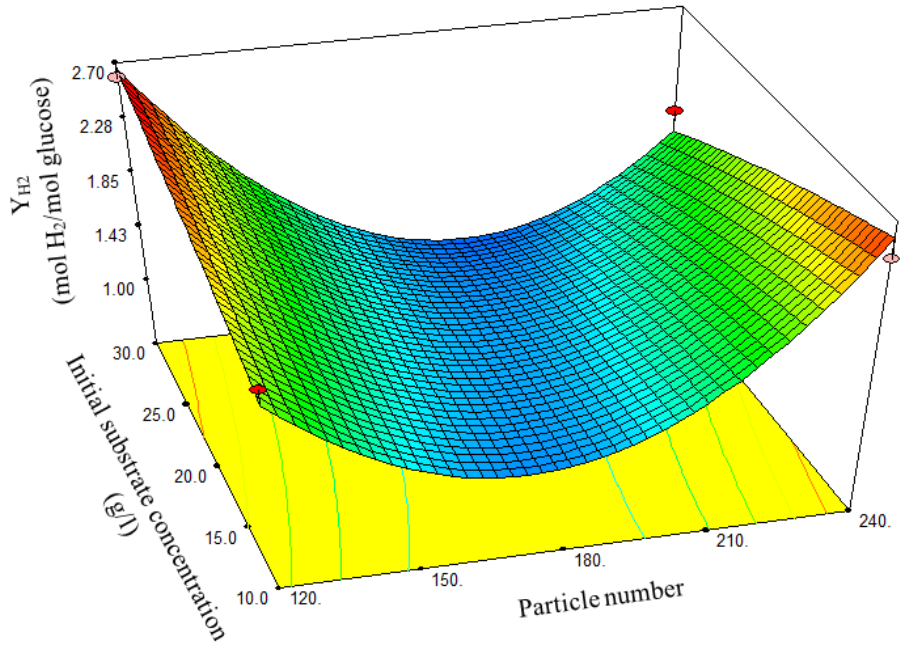


Figure 3.18 The three-dimensional response surface showing the variation of hydrogen yield (Y_{H2}, mol H_2/mol glucose) with particle number and initial substrate concentration at temperature, T= 55 ºC.

The effect of substrate concentration was also evaluated in order to determine the process performance at low, medium and high substrate concentrations. Figure 3.19 and Figure 3.20 show the variation of hydrogen yield (Y_{H2}, mol H_2/mol glucose) with temperature and particle number at initial substrate concentration, TS_0= 10 g/l. Y_{H2} increased with the increase in particle number and the highest values obtained as 2.58 mol H_2/mol glucose when particle number was between 230-240 and temperature was 45-50 ºC. No substantial difference in the yield was observed when initial substrate concentration was 20 g/l (Figure 3.21 and Figure 3.22). The highest Y_{H2} was obtained as 2.38 mol H_2/mol glucose at extreme particle numbers (low and high) and at 45-50 ºC. Finally, the yield of formation was evaluated when TS_o= 30 g/L (Figure 3.23 and Figure 3.24). The maximum yield can be obtained as 2.53 mol H_2/mol glucose, if the particle number is 120 and fermentation temperature is between 45-50 ºC. The final results can be evaluated that, 20 g/L initial substrate concentration is the optimal sugar concentration, process should be operated at thermophilic conditions, particle number could be adjusted to low or high values.

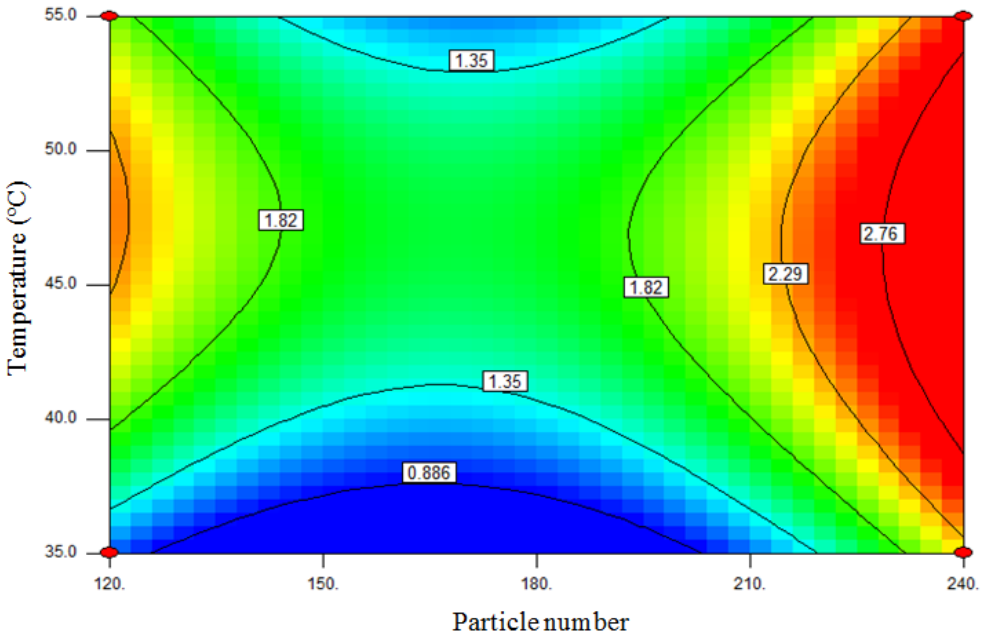


Figure 3.19 The contour plot of response surface showing the variation of hydrogen yield (Y_{H2}, mol H_2/mol glucose) with temperature and particle number at initial substrate concentration, TS_0 = 10 g/l.

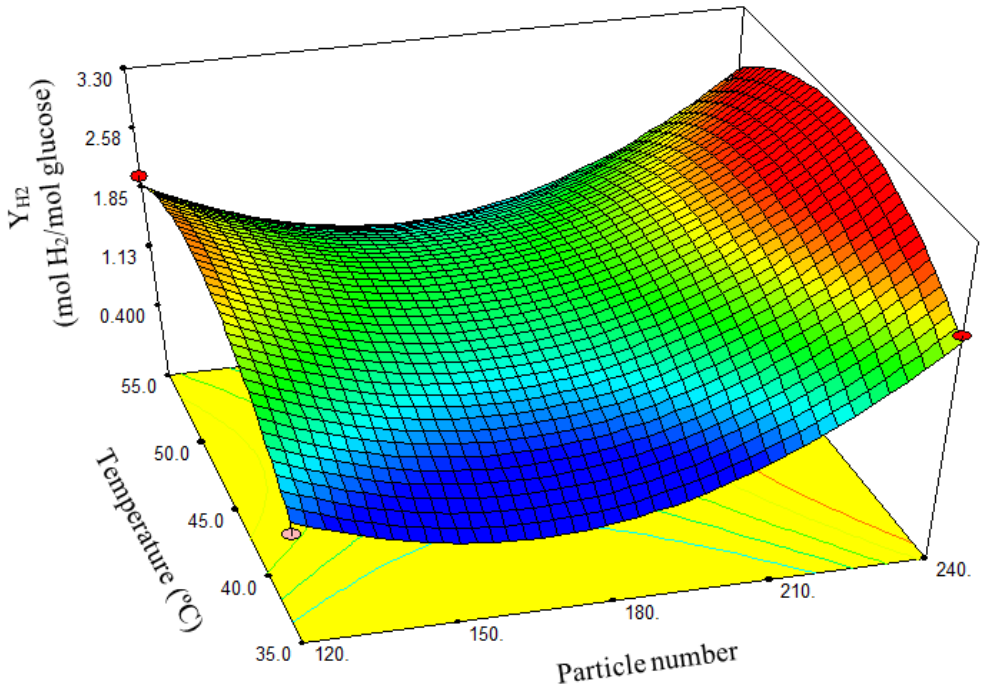


Figure 3.20 The three-dimensional response surface showing the variation of hydrogen yield (Y_{H2}, mol H_2/mol glucose) with temperature and particle number at initial substrate concentration, TS_0 = 10 g/l.

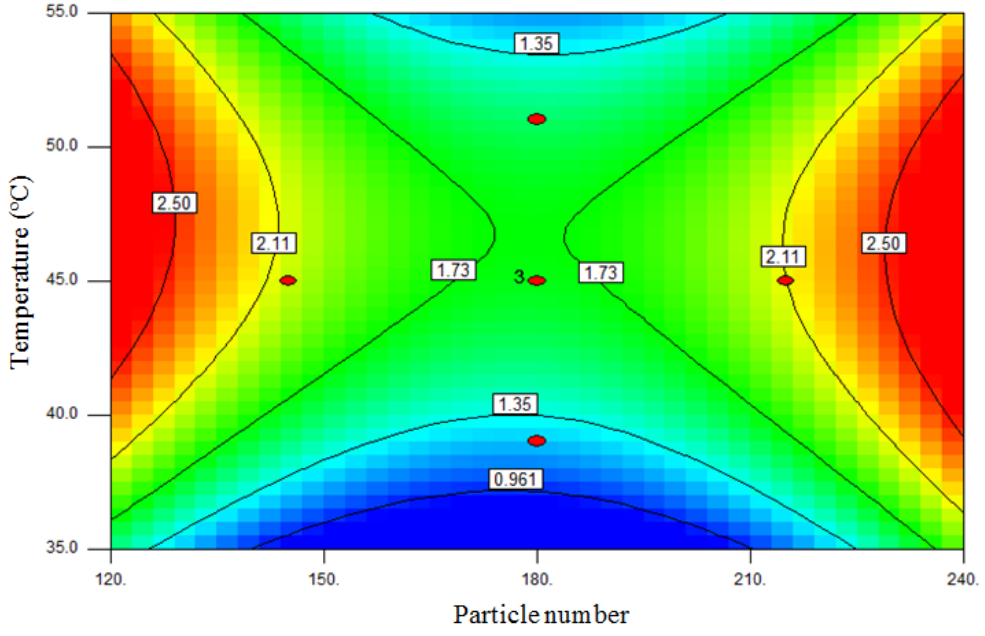


Figure 3.21 The contour plot of response surface showing the variation of hydrogen yield (Y_{H2}, mol H_2/mol glucose) with temperature and particle number at initial substrate concentration, TS_0 = 20 g/l

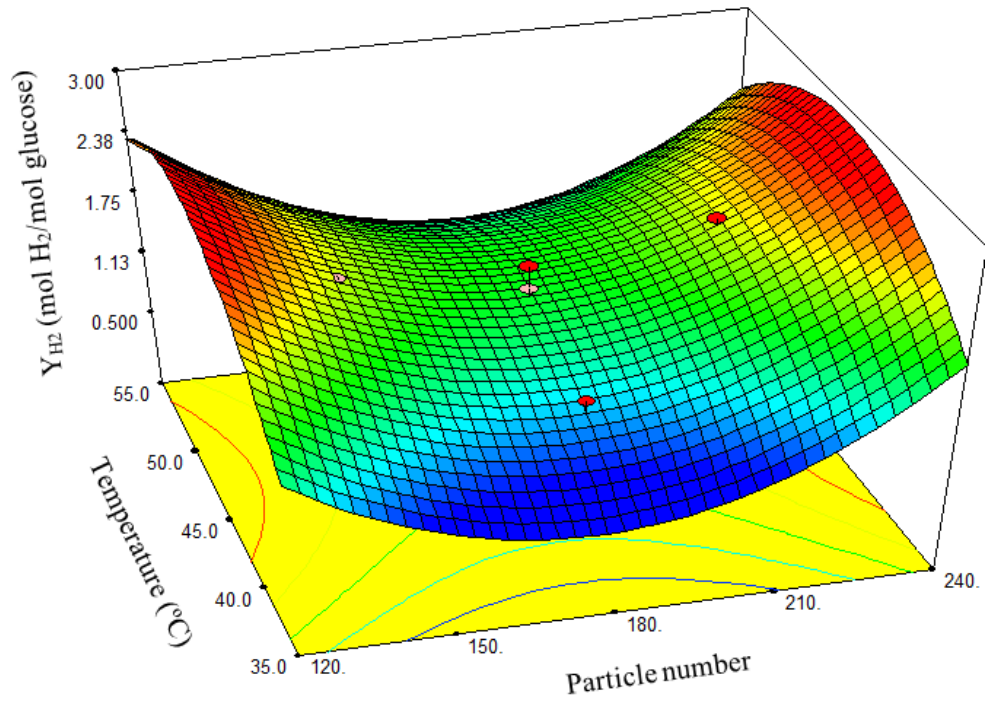


Figure 3.22 The three-dimensional response surface showing the variation of hydrogen yield (Y_{H2}, mol H_2/mol glucose) with temperature and particle number at initial substrate concentration, TS_0 = 20 g/l.

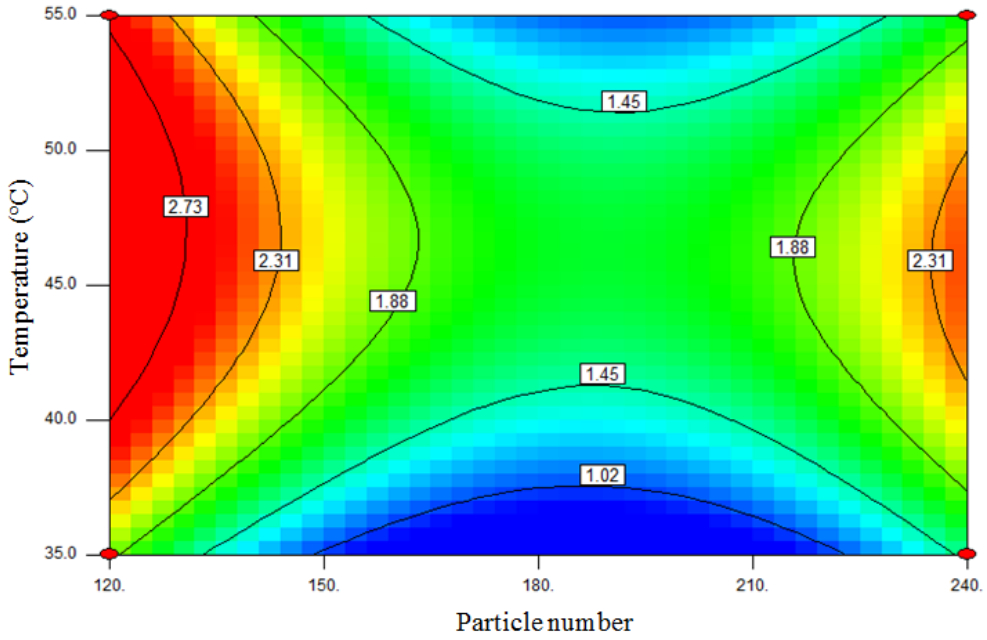


Figure 3.23 The contour plot of response surface showing the variation of hydrogen yield (Y_{H2}, mol H_2/mol glucose) with temperature and particle number at initial substrate concentration, TS_0 = 30 g/l

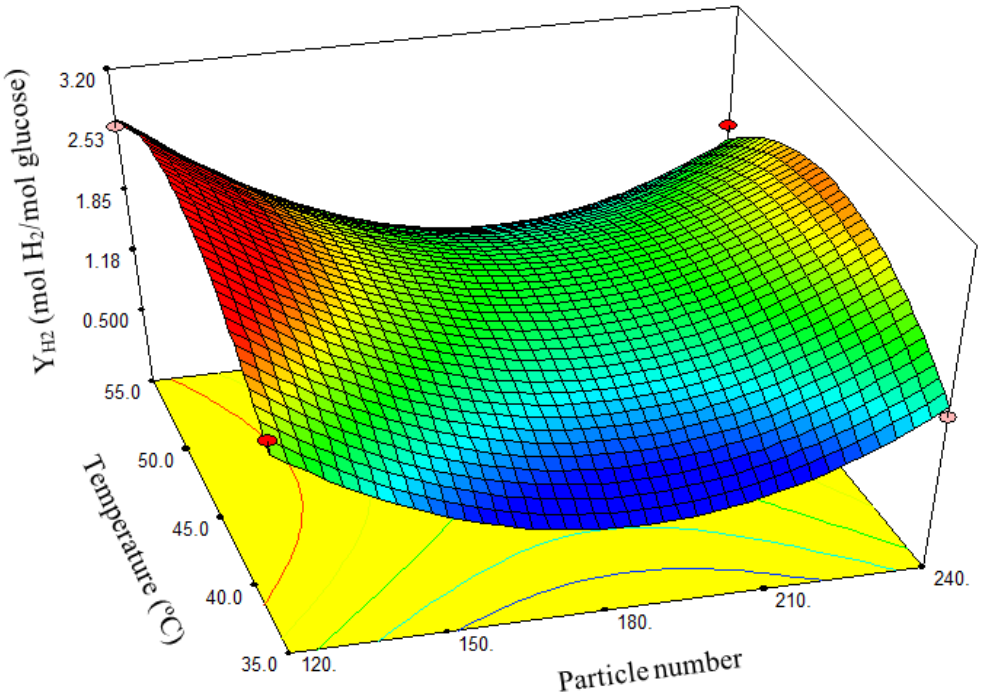


Figure 3.24 The three-dimensional response surface showing the variation of hydrogen yield (Y_{H2}, mol H_2/mol glucose) with temperature and particle number at initial substrate concentration, TS_0 = 30 g/l.

It seems that particle number could be high or low depending on the operating conditions as temperature and initial substrate concentration. Therefore, yield of formation was evaluated for different particle numbers as low, medium and high. Initially, yield of formation at particle number, PN= 120 was evaluated at different temperatures and initial substrate concentrations (Figure 3.25 and Figure 3.26). The highest yield reached up to 3.2 mol H_2/mol glucose for the conditions as T= 45 ºC and TS_0 = 30 g/l at 120 particle number. Similarly, when particle number was increased to PN=180 (Figure 3.27 and Figure 3.28), there was a sharp decrease to around 1.52 mol/ mol glucose in the yield. Finally at high particle number of PN=240 (Figure 3.29 and Figure 3.30) the yield was only around 2.8 mol H_2/mol glucose which was obtained at low substrate concentration of 10 g/L and temperature of 45 ^{o}C.

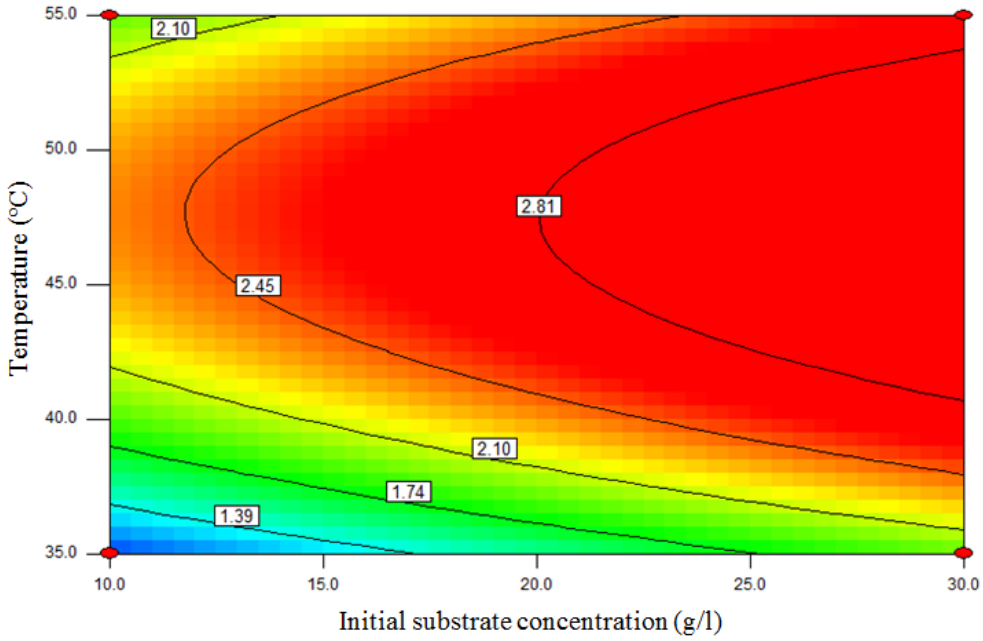


Figure 3.25 The contour plot of response surface showing the variation of hydrogen yield (Y_{H2}, mol H_2/mol glucose) with temperature and initial substrate concentration at particle number, PN= 120.

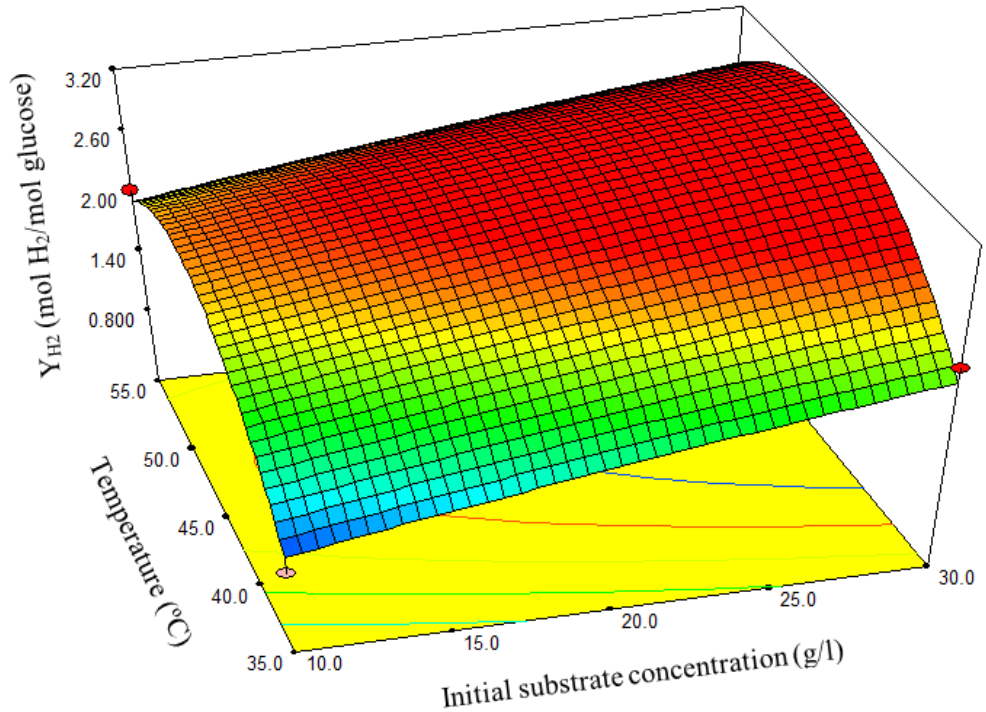


Figure 3.26 The three-dimensional response surface showing the variation of hydrogen yield (Y_{H2}, mol H_2/mol glucose) with temperature and initial substrate concentration at particle number, PN = 120.

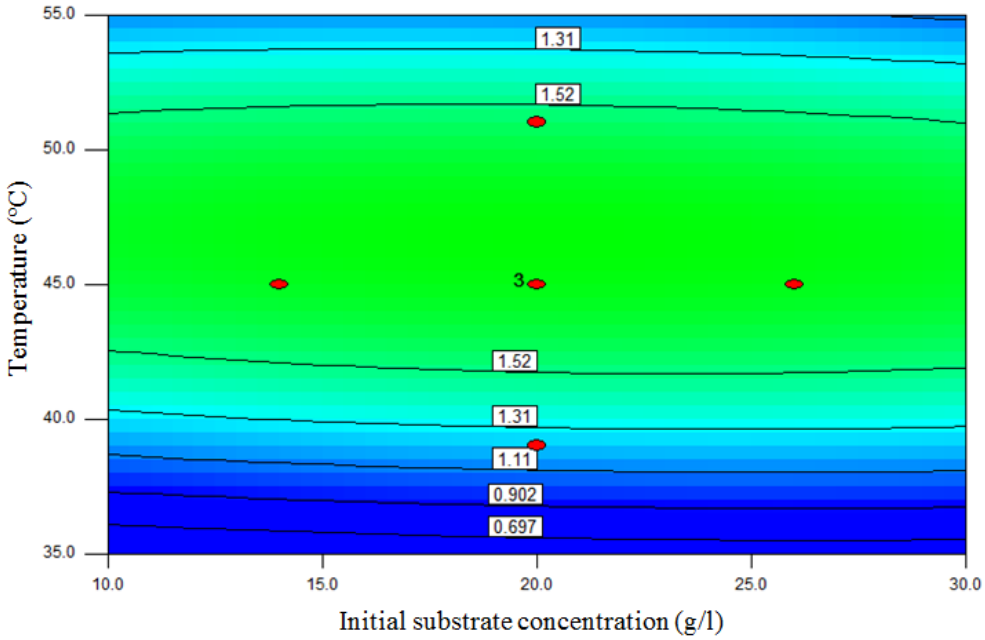


Figure 3.27 The contour plot of response surface showing the variation of hydrogen yield (Y_{H2}, mol H_2/mol glucose) with temperature and initial substrate concentration at particle number, PN = 180.

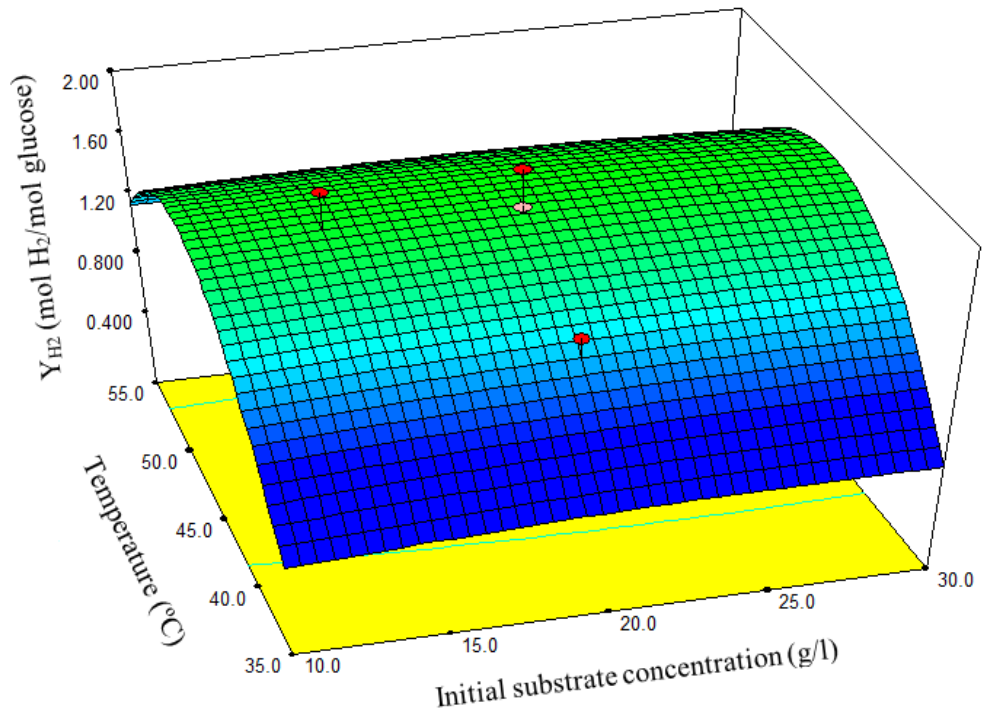


Figure 3.28 The three-dimensional response surface showing the variation of hydrogen yield (Y_{H2}, mol H_2/mol glucose) with temperature and initial substrate concentration at particle number, PN = 180.

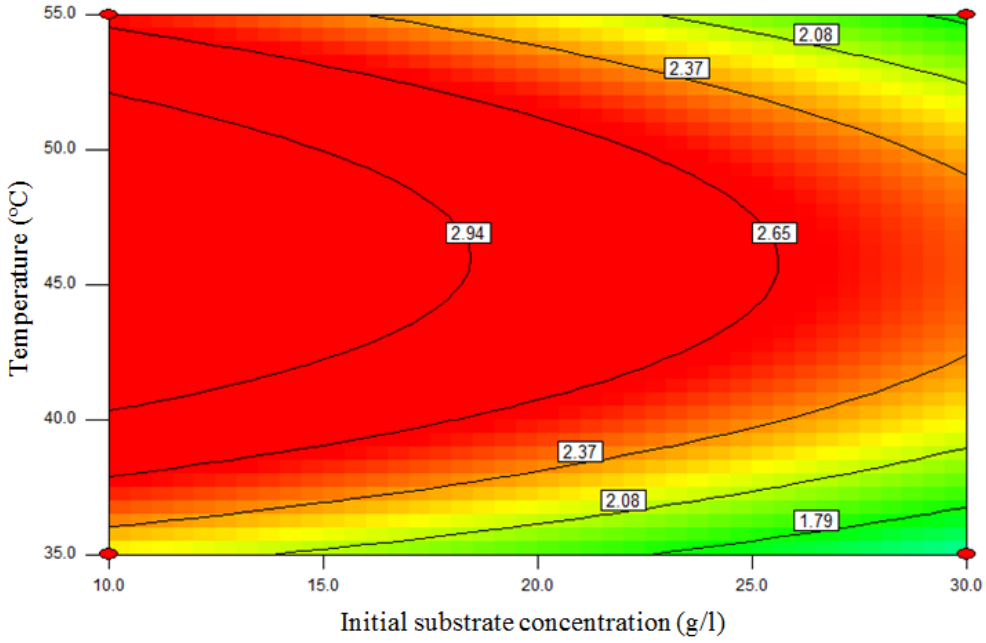


Figure 3.29 The contour plot of response surface showing the variation of hydrogen yield (Y_{H2}, mol H_2/mol glucose) with temperature and initial substrate concentration at particle number, PN = 240.

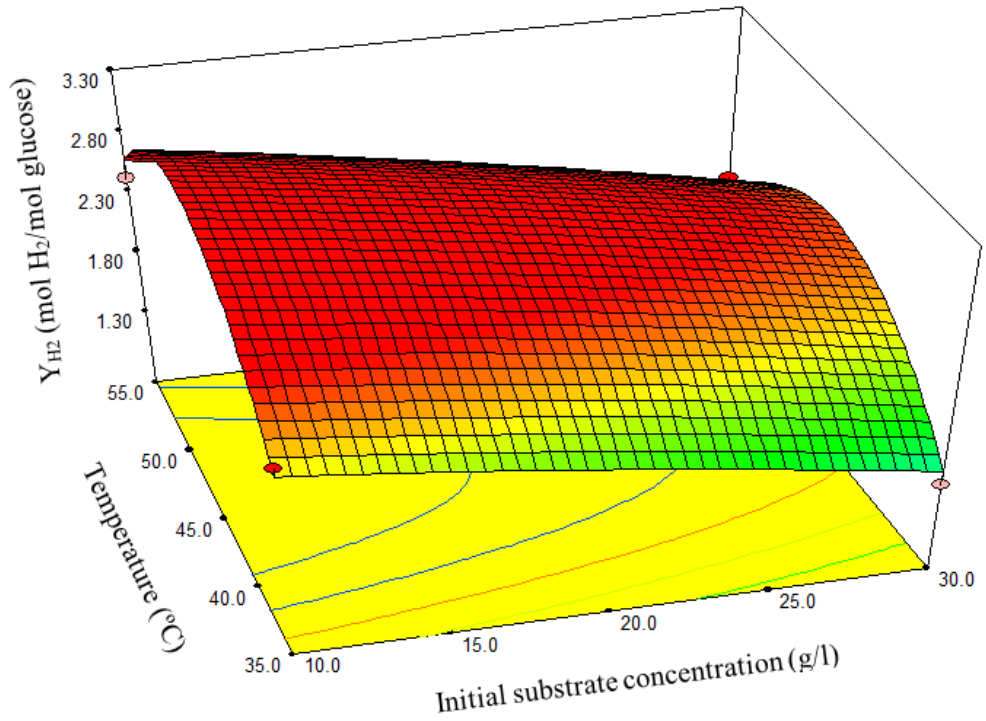


Figure 3.30 The three-dimensional response surface showing the variation of hydrogen yield (Y_{H2}, mol H_2/mol glucose) with temperature and initial substrate concentration at particle number, PN = 240.

3.3.2 The Effect of Independent Variables on Hydrogen Production Rate

A response equation was also developed for the hydrogen production rate as dependent variable for the same independent variables as particle number, fermentation temperature and initial sugar concentration. The coefficients of the quadratic equation for HPR as a function of these independent variables were calculated by regression analysis and given in Table 3.19. The experimental values were compared with the predicted values in Table 3.20. HPR predictions were in good agreement with the experimental results (R^2=0.94) as shown in Table 3.20. The analysis of variance (ANOVA) is presented in Table 3.21. The ANOVA test indicated that the model for HPR was statistically significant ($p < 0.05$). However, the main effects of factors are not significant. HPR is affected by the interaction between particle number and initial substrate concentration, significantly. In addition, quadratic effect of TS_0 and temperature were significant.

Table 3.19 Coefficients of the response functions for HPR

Coefficients	**Values**
b_0	-663
b_1	-0.734
b_2	-9.30
b_3	37.1
b_{12}	-0.0120
b_{13}	-0.000192
b_{23}	0.0307
b_{11}	0.00296
b_{22}	0.249
b_{33}	-0.415

Table 3.20 Experimental and predicted values of HPR (R^2=0.94)

Experimental point	**HPR(exp) (ml H_2/h)**	**HPR(pred) (ml H_2/h)**
A_1	33.97	30.83
A_2	24.21	25.01
A_3	29.99	32.55
A_4	38.75	33.98
A_5	10.5	10.9
A_6	10.39	7.78
F_1	22.39	20.47
F_2	7.76	9.36
F_3	28.92	31.16
F_4	32.69	32.32
F_5	24.61	25.18
F_6	15.65	13.61
F_7	8.36	6.96
F_8	5.54	7.66
C_1	25.19	24.29
C_2	22.39	24.29
C_3	19.32	24.29

Table 3.21 Variance analysis for HPR (ANOVA, α=0.05).

Source	**Sum of Squares**	**df**	**Mean Square**	**F Value**	**p-value Prob > F**	**Evaluation**
Model	1537.5	9	171	12.2	0.00168	significant
A- Particle number	216	1	216	15.4	0.00575	insignificant
B- Initial substrate concentration	12.3	1	12.3	0.875	0.381	insignificant
C- Temperature	59.1	1	59.1	4.21	0.0794	insignificant
AB	418	1	418	29.7	0.000952	significant
AC	0.106	1	0.106	0.00753	0.933	insignificant
BC	75.3	1	75.3	5.36	0.0538	insignificant
A^2	40.7	1	40.7	2.90	0.133	insignificant
B^2	234	1	234	16.7	0.00469	significant
C^2	650	1	650	46.3	0.000253	significant
Pure Error	17.2	2	8.62			
Cor Total	1635.8	16				

Hydrogen production rate shows differences according to operation temperature. Therefore, the variation of hydrogen production rate (HPR, ml H_2/h) with particle number and initial substrate concentration under mesophilic condition which is at T=38 ºC was evaluated (Figure 3.31 and Figure 3.32). The highest HPR was obtained as 54 ml/ h at PN= 240 and TS_0= 10 g/l. Particle number had substantial effect on the rate rather than substrate concentration at the mesophilic condition. Increasing fermentation temperature to T= 45 ºC provided a substantial improvement in HPR (Figure 3.33 and Figure 3.34). It rised to HPR= 74 ml/ h at PN= 240 and TS_0= 10 g/l. The effect of tempertaure on HPR was evaluated for T=52 ºC (Figure 3.35 and Figure 3.36), too. HPR showed a similar trend at T=52 ºC as it was at T=38 ºC and T=45 ºC. However, the maximum HPR obtained at this fermentation tempereture was 44.6 ml H_2/h at TS_0 of ~ 10-12 g/l when particle number was around 240. Although maximum HPRs were obtained at the same conditions like PN= 240 and TS_0= 10 g/l, the rate of production decreases with increasing fermentation temperature. The best fermentation temperature can be selected as T=45 ºC.

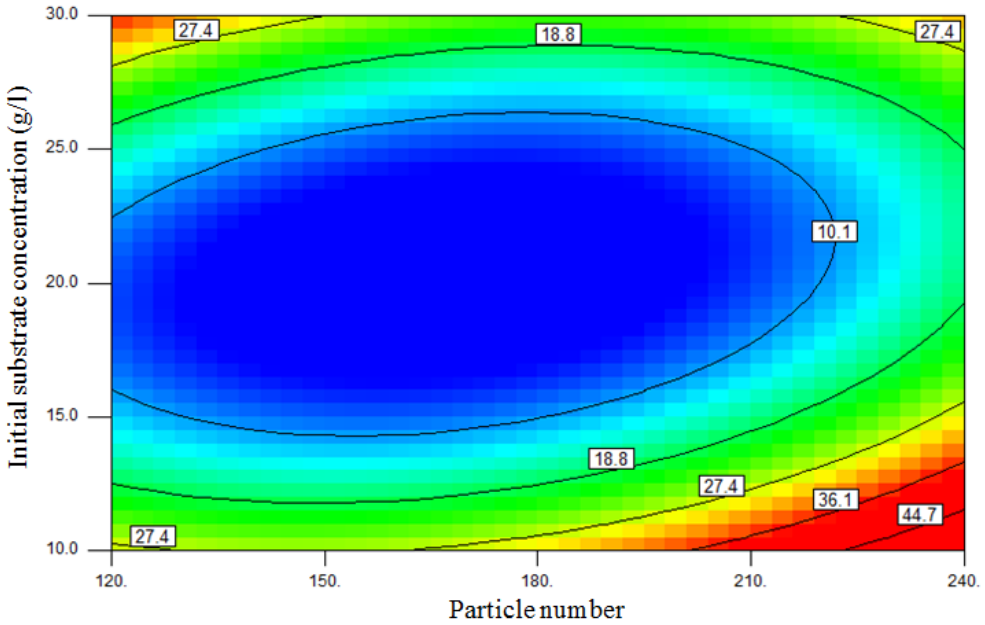


Figure 3.31 The contour plot of response surface showing the variation of hydrogen production rate (HPR, ml H_2/h) with particle number and initial substrate concentration at temperature, T = 38 ºC.

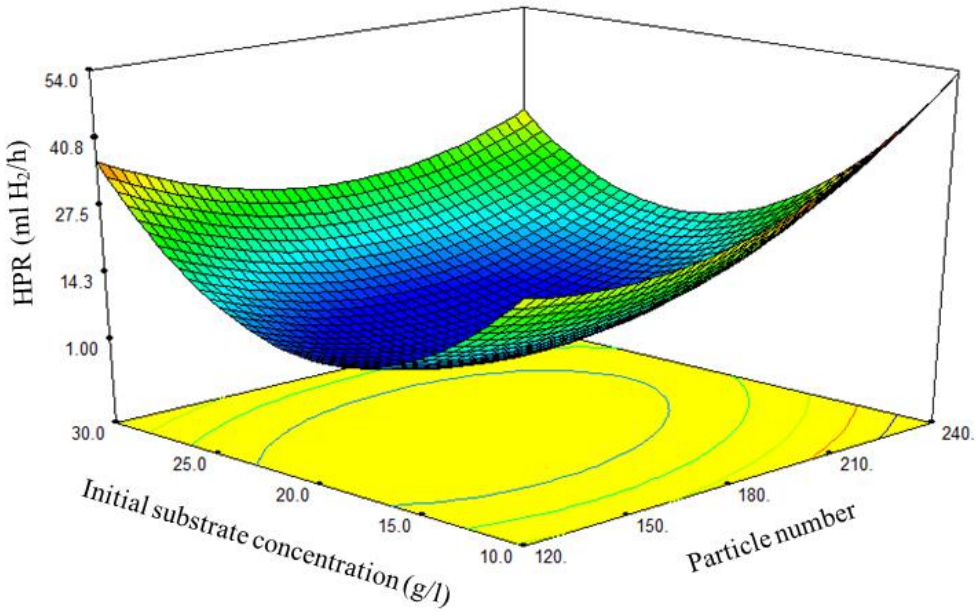


Figure 3.32 The three-dimensional response surface showing the variation of hydrogen production rate (HPR, ml H_2/h) with particle number and initial substrate concentration at temperature, T = 38 ºC.

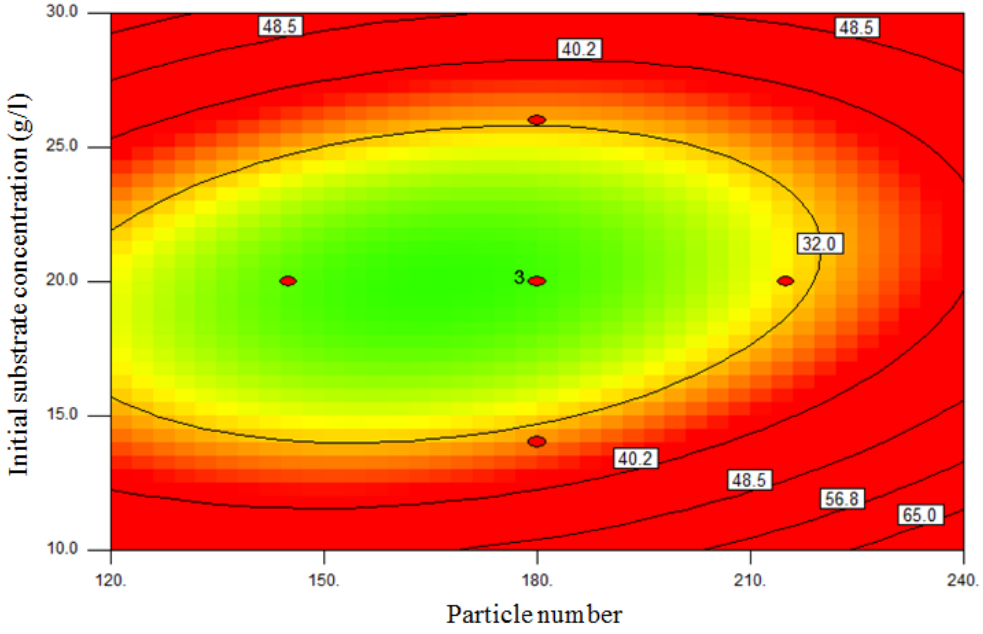


Figure 3.33 The contour plot of response surface showing the variation of hydrogen production rate (HPR, ml H_2/h) with particle number and initial substrate concentration at temperature, T= 45 ºC.

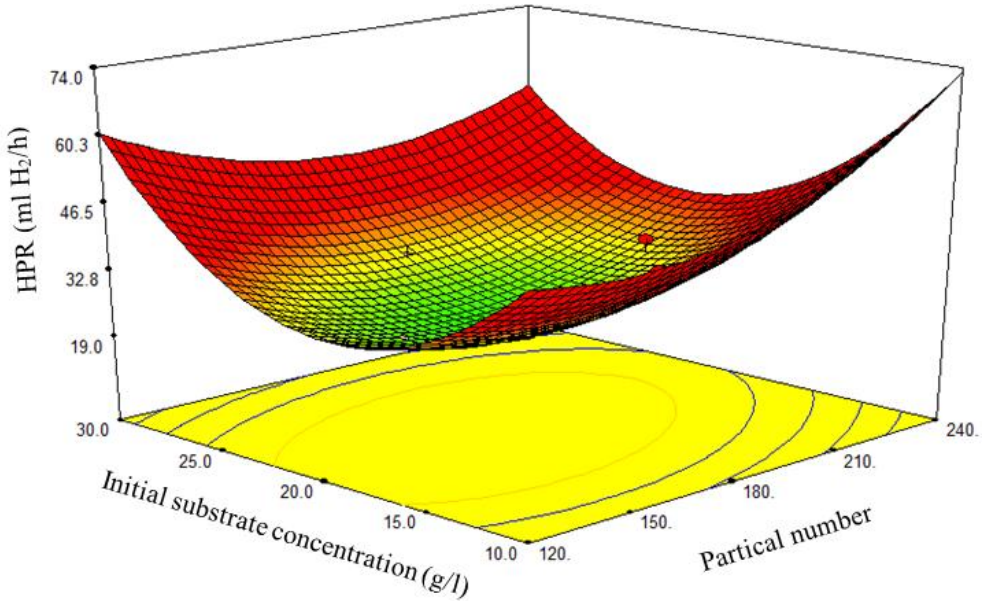


Figure 3.34 The three-dimensional response surface showing the variation of hydrogen production rate (HPR, ml H_2/h) with particle number and initial substrate concentration at temperature, T= 45 ºC.

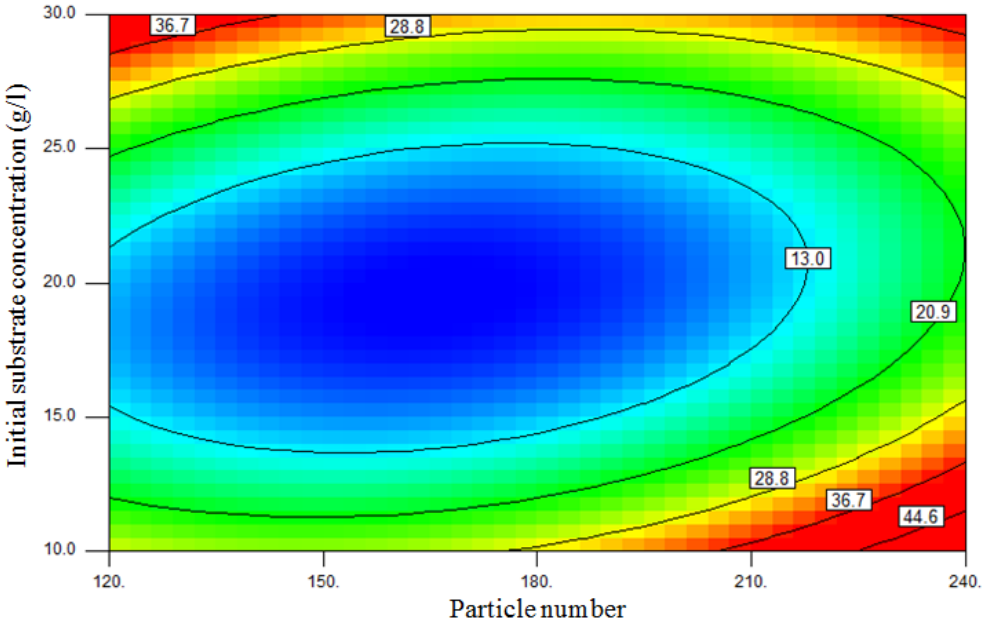


Figure 3.35 The contour plot of response surface showing the variation of hydrogen production rate (HPR, ml H_2/h) with particle number and initial substrate concentration at temperature, T= 52 ºC.

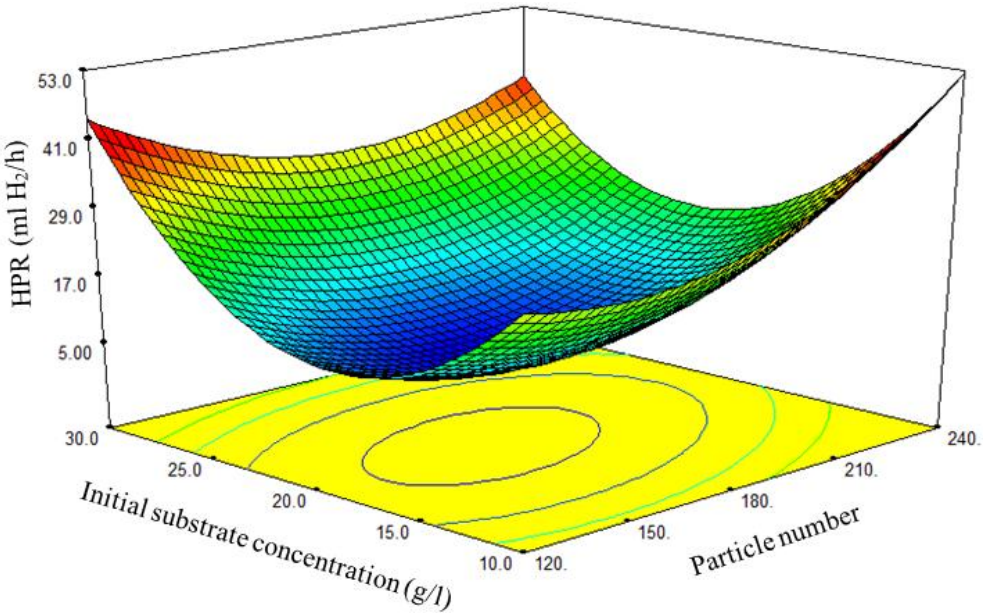


Figure 3.36 The three-dimensional response surface showing the variation of hydrogen production rate (HPR, ml H_2/h) with particle number and initial substrate concentration at temperature, T = 52 ºC.

Figure 3.37 and Figure 3.38 indicate the variation of hydrogen production rate (HPR, ml H_2/h) with temperature and particle numbere at initial substrate concentration TS_0 = 10 g/l. The highest HPR values were obtained at 40-50 ºC when particle number was over PN= 180. Figure 3.39 and Figure 3.40 demonstrate the variation of hydrogen production rate (HPR, ml H_2/h) with temperature and particle number at initial substrate concentration TS_0 = 30 g/l. HPR decreased gradually at TS_0 of 30 g/l when temperature was either < 40 ºC or > 50 ºC. Particle number did not subtnatially affect the rate of production. The most significant factor was the tempertaıre at high substrate concentration.

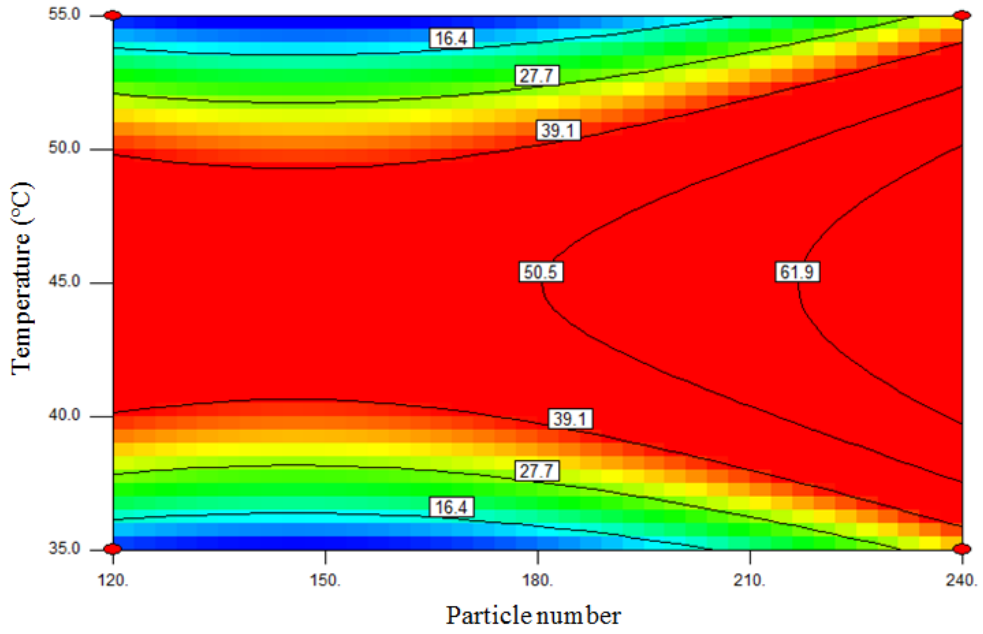


Figure 3.37 The contour plot of response surface showing the variation of of hydrogen production rate (HPR, ml H_2/h) with temperature and particle number at initial substrate concentration, TS_0= 10 g/l.

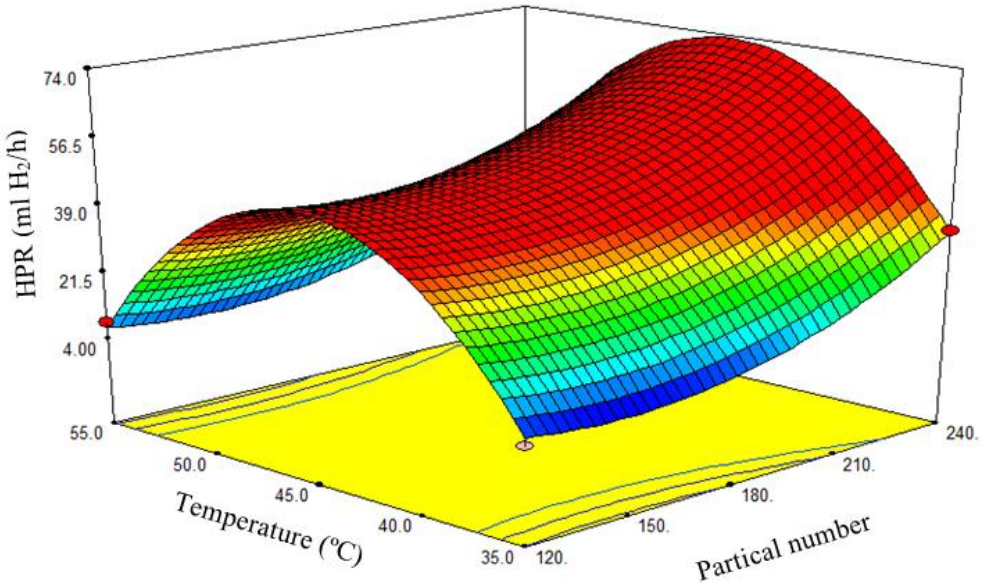


Figure 3.38 The three-dimensional response surface showing the variation of hydrogen production rate (HPR, ml H_2/h) with temperature and particle number at initial substrate concentration, TS_0= 10 g/l.

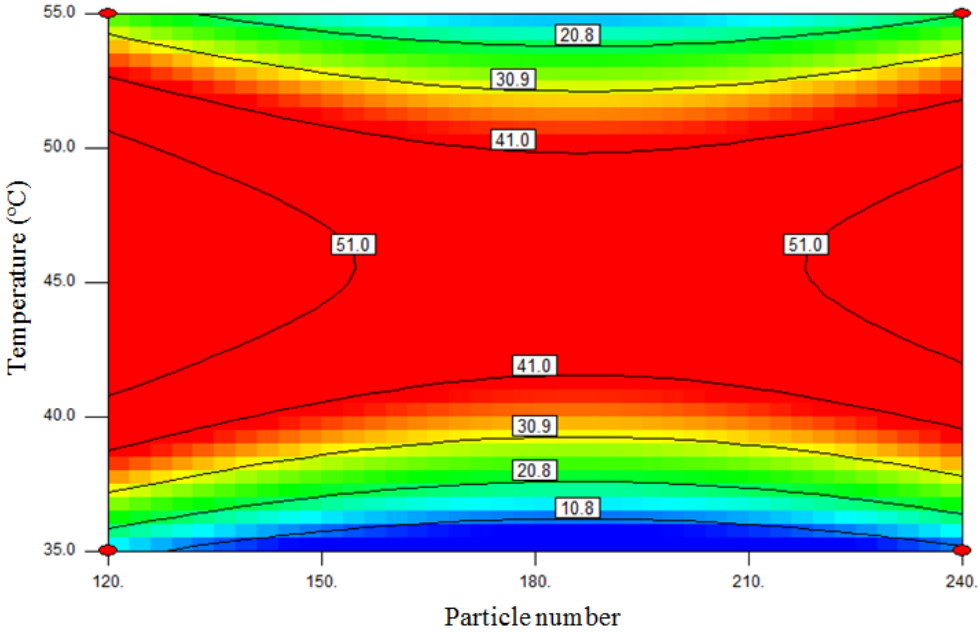


Figure 3.39 The contour plot of response surface showing the variation of of hydrogen production rate (HPR, ml H_2/h) with temperature and particle number at initial substrate concentration, TS_0= 30 g/l.

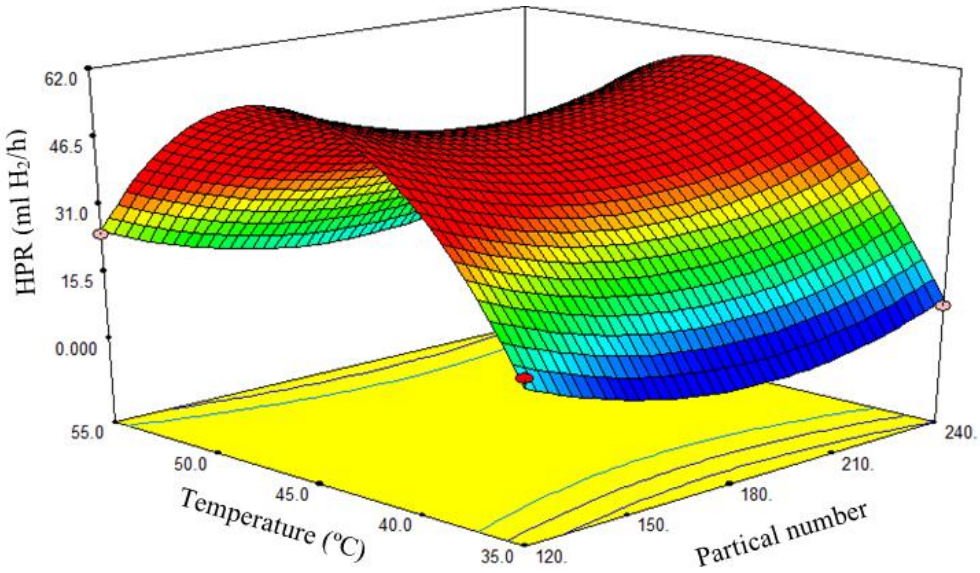


Figure 3.40 The three-dimensional response surface showing the variation of hydrogen production rate (HPR, ml H_2/h) with temperature and particle number at initial substrate concentration, TS_0= 30 g/l.

3.3.3 Optimization of Dark Fermentation Operating Conditions for Hydrogen Yield and Hydrogen Production Rate

The optimum operating conditions of dark fermentation were determined by using Design Expert 7.0 statistical program. By using response function coefficients, within the range of factors in Box-Wilson experimental design, values of independent variables that maximize Y_{H2} and HPR were determined. As it is seen from contour and surface plots given in previous sections, the highest value of Y_{H2} and HPR could be obtained at high particle numbers, low substrate concentrations and temperature around T=45 ºC. Running an optimization program for maximization of yield and rate resulted in the almost the same condtions. It was found that hydrogen yield of Y_{H2} = 3.15 mol H_2/mol glucose and hydrogen production rate of HPR= 69 ml H_2/h could be obtained when particle number was PN = 240; initial substrate concentration was TS_0 = 10.6 g/l and temperature was T = 43.6 ºC (Figure 3.41).

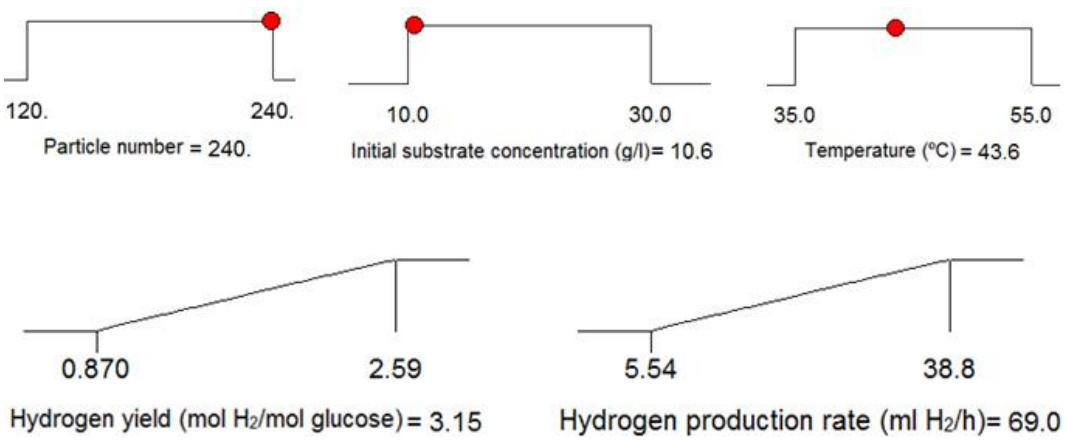


Figure 3.41 Optimum operating conditions yielding the maximum hydrogen yield (Y_{H2}) and production rate (HPR).

CHAPTER FOUR
CONCLUSIONS AND RECOMMENDATIONS

World energy demand is supplied from fossil fuels. It is obvious that energy demand is increasing day by day. However, fossil fuels reserves are diminishing. Besides, burning fossil fuels generates CO_2 which is the primary cause of global warming. Thus, to meet the needs of energy and prevent global warming, it is necessary to develop clean alternative energy sources. So, H_2 seems a promising energy carrier to this problem.

H_2 is the simplest element in the universe. But, H_2 does not occur naturally as a gas on the Earth, it is just found in many organic compounds. Release of H_2 from these compounds requires high energy input which makes them expensive and not environmentally-friendly. Fortunately, H_2 is produced biologically using algae and bacteria under mild conditions. The limitation in biohydrogen production is the rate and yield of production. The process need improvement to be able to compete with the other conventional, high rate hydrogen production methods.

Previous studies showed that H_2 production by immobilized culture has several advantages over suspended culture. The rate and yield of production could be improved by the immobilized systems. The most important factor affecting H_2 yield in immobilized system is type of particle. So, in the first part of the thesis, effect of particle type on biohydrogen production was investigated by conducting batch fermentation experiments with eight different support particles at different initial sugar concentration and 55 ºC. When particles were compared in terms of Y_{H2} and HPR obtained, polyester fiber was superior over the other particles used in the study. The highest Y_{H2} and HPR were obtained with polyester fiber at TS_o of 13.17 ± 1.5 g/l (1.96 mol H_2/mol glucose, 7.39 ml H_2/h, respectively). In general the highest yields were obtained at low sugar concentrations around 13.17 ± 1.5 g/l and a decreasing trend in the yield was observed when substrate concentration was increased. One of the reasons could be substrate inhibition at high substrate concentrations. The other reason is the product inhibition effect. The main product

that causes inhibition was the volatile fatty acids generated during dark fermentation. Final TVFA concentration increased in parallel to the increase in total sugar concentration from 13.17 $\pm$ 1.5 g/l to 26.54 $\pm$ 4 g/l. This problem can be overcome only if the product is removed from the fermentation media if the processes desired to be operated at high substrate concentrations. Continuous operation can result in high yield and rate of formations even at high initial substrate concentrations.

Batch fermentation experiments were conducted with suspended culture (control experiments) under same conditions to compare suspended culture with immobilized culture. The results showed that immobilized systems are superior over suspended ones. The highest Y_{H2} obtained with control was 0.96 mol H_2/mol glucose which was lower than one obtained from most of the support particles.

Support particle size is another important factor in immobilized system. In the light of literature, decreasing particle size results in higher product yield. Because lower particle sizes increases the surface area of immobilization. Also, substrate or product transfer problems are eliminated. Thus, effect of particle size on biohydrogen production was investigated in the second part of the study. Polyester fiber particles were prepared at different sizes (0.5, 1, 2, 3 cm in diameter). Batch fermentation experiments were conducted with these particles at TS_o of 14.83 $\pm$ 0.5g/l and 55 ºC. Similar to literature, the highest CHV, Y_{H2} and HPR obtained with particles 0.5 cm in diameter (566.8 ml, 1.51 mol H_2/mol glucose, 6.72 ml H_2/h, respectively).

Operating conditions of batch fermentation medium affect Y_{H2} highly. Particle number, initial substrate concentration and temperature are other important parameters for immobilized system. Box–Wilson statistical experiment design was used by considering these factors as the independent variables while Y_{H2} and HPR were the objective functions to be optimized. Particle number was varied between 120 and 240, initial substrate concentration between 10 and 30 g/l and temperature between 35 and 55 ºC. The predictions for Y_{H2} (R^2 = 0.885) and HPR (R^2 = 0.94) were in good agreement with the experimental results. Also, ANOVA showed that temperature, the interaction between particle number and initial substrate

concentration, quadratic effect of particle number were significant for Y_{H2}. Besides, the interaction between particle number and initial substrate concentration, quadratic effect of TS_0 and temperature affected HPR significantly. The optimum conditions resulting in the maximum hydrogen yield (Y_{H2} = 3.15 mol H_2/mol glucose) and production rate (HPR= 69 ml H_2/h) were particle number, PN= 240, TS_0 = 10.6 g/l and T = 43.6 ºC

In the first part of thesis, polyester fiber particles were preapered approximately 1.5 cm in diameter and particle number was PN= 15. The highest Y_{H2} of 1.96 mol H_2/mol glucose and HPR of 7.39 ml H_2/h were obtained when batch dark fermentation experiment conditions were TS_0 of 13.17 $\pm$ 1.5 g/l and temperature of 55 ºC. But, in optimization studies which were carried out under almost the same operating conditions (TS_0= 10 g/l and T= 55 ºC), significant increase was observed in Y_{H2} and HPR. Just particle size and number were different (0.5 cm in diameter, PN= 240, respectively). Y_{H2} increased 1.2 times to 2.44 mol H_2/mol glucose and HPR increased 3.9 times to 28.92 ml H_2/h by the improvement in particle size, particle number. Also, when first results were compared to one obtained from optimization studies which optimum conditions were satisfied (PN= 240, TS_0 = 10.6 g/l and T = 43.6 ºC), Y_{H2} increased from 1.96 to 3.15 mol H_2/mol glucose and HPR increased from 7.39 to 69 ml H_2/h. This shows that improving operation conditions leads to obtain higher hydrogen yield and production rate.

A number of batch dark fermentation studies were reported in literature for bio-hydrogen production by immobilized system from different support materials, substrates and culture types. The results of this study are compared with other batch dark fermentation studies in Table 4.1. The highest hydrogen yield obtained in this study (3.15 mol H_2/mol glucose) is higher than some of the reported studies.

In summary, maximizing hydrogen production by a biological process is a major challenge. As indicated in the results, immobilization provided considerable benefit in obtaining higher hydrogen yield. Particle type and size, operating conditions such as particle number, initial substrate concentration and temperature are important

parameters affected hydrogen yield and production rate. However, process still need further improvements.

Table 4.1 Comparison of hydrogen yields of immobilized systems obtained from batch dark fermentation studies

Culture	**Substrate Type**	**Conc. of Substrate**	**Support particle Type**	**Temperature**	**H_2 production yield**	**Ref.**
Acid pretreated anaerobic sludge	Sucrose-based synthetic wastewater	20 g COD/l	Polymethyl methacrylate (PMMA)	35 ºC	2.25 mol H_2 / mol sucrose.	Wu.&.Chang (2007)
Acid pretreated anaerobic sludge	Sucrose	20 g COD/l	Ethylene-vinyl acetate copolymer (EVA)	40 ºC	1.41 mol H_2/mol sucrose	Wu et al. (2005)
Clostridium butyricum TISTR 1032	Sugarcane juice	25 g COD/l	Sugarcane bagasse (SCB)	37 ºC	1.34 mol H_2/ mol hexose	Plangklang et al. (2012)
A novel isolated Safen strain associated to the genus *Thermoanaerobacterium*	Glucose	ca. 5 g/l	Calcium alginate (CA)	60 ºC	1.9 mol H_2/mol glucose	Basile et al. (2010)
Acid pretreated anaerobic sludge	Sucrose	20 g COD/l	Polyethylene –octene– elastomer (POE)	35 ºC	1.7 mol H_2/ mol sucrose	Wu, Lo, Chen & Chang (2007)
Clostridium butyricum CGS2	Sucrose	20 g COD/l	Monoliths (square-structured ceramic fittings)	37 ºC	0.82 mol H_2/ mol hexose	Fritsch et al. (2008)
Heat and acid pretreated anaerobic sludge	Acid hydrolysed wheat starch	13.17 ± 1.5 g/l	Polyester fiber (1.5 cm in diameter)	55 ºC	1.96 mol H_2/mol glucose	This study
Heat and acid pretreated anaerobic sludge	Acid hydrolysed wheat starch	30 g/l	Polyester fiber (0.5 cm in diameter)	55 ºC	2.59 mol H_2/mol glucose	This study
Heat and acid pretreated anaerobic sludge	Acid hydrolysed wheat starch	10.6 g/l	Polyester fiber (0.5 cm in diameter)	43.6 ºC	3.15 mol H_2/mol glucose	This study (Result of optimization)

Conc.: Concentration

Some of the recommendations for future studies are listed below:

- Continuous fermentation experiments should be conducted with polyester fiber particles to compare batch system to continuous system. The optimum operating conditions can be determined and the hydrogen production with this particle can be compared with the other expensive support particles or some other natural particles in the literature.
- Kinetic coefficients of hydrogen production in continuous dark fermentation can be determined.
- The other support particles such as stainless steel scrubber and aquarium biological sponge, by which relatively high hydrogen production rates and yield were obtained, can be further investigated to improve production if the conditions are optimization.
- Second generation and third generation substrate can be used as feed instead of waste wheat.
- Hydrogen gas production in an immobilized sequential dark and photo-fermentation can be studied.
- Hydrogen production in an immobilized single stage dark and photo-fermentation process can be studied.

REFERENCES

Argun, H., Kargi, F., Kapdan, I.K., & Oztekin, R. (2008). Biohydrogen production by dark fermentation of wheat powder solution: Effects of C/N and C/P ratio on hydrogen yield and formation rate. *International Journal of Hydrogen Energy, 33*, 1813 – 1819.

Argun, H., Kargi, F., & Kapdan, I.K. (2009a). Hydrogen production by combined dark and light fermentation of ground wheat solution. *International Journal of Hydrogen Energy, 34*, 4305 – 4311.

Argun, H., Kargi, F., & Kapdan, I.K. (2009b). Microbial culture selection for bio-hydrogen production from waste ground wheat by dark fermentation. *International Journal of Hydrogen Energy, 34*, 2195 – 2200.

Argun, H., & Kargi, F. (2011). Bio-hydrogen production by different operational modes of dark and photo-fermentation: An overview. *International Journal of Hydrogen Energy, 36*, 7443-7459.

Asada, Y., & Miyake, J. (1999). Photobiological hydrogen production. *Journal of Bioscience and Bioengineering, 88* (1), 1-6.

Azbar, N., & Kapdan, I.K. (2012). Use of immobilized cell systems in biohydrogen production. In D.B. Levin, & N. Azbar (Eds.). *State of the art and progress in production of biohydrogen* (227-249). Bentham Science Publishers.

Azwar, M.Y., Hussain, M.A., & Abdul-Wahab, A.K. (2014). Development of biohydrogen production by photobiological, fermentation and electrochemical processes: A review. *Renewable and Sustainable Energy Reviews, 31*, 158–173.

Basile, M.A., Dipasquale, L., Gambacorta, A., Vella, M.F., Calarco, A., Cerruti, P. et al. (2010). The effect of the surface charge of hydrogel supports on thermophilic biohydrogen production. *Bioresource Technology, 101,* 4386–4394.

Cai, M., Liu, J., & Wei, Y. (2004). Enhanced biohydrogen production from sewage sludge with alkaline pretreatment. *Environmental Science Technology, 38* (11), 3195–3202.

Carere, C., & Levin, D.B. (2012). Role of metabolic engineering in enhancing hydrogen yields. In D.B. Levin, & N. Azbar (Eds.). *State of the art and progress in production of biohydrogen* (188-203). Bentham Science Publishers.

Chang, J.S., Lee K.S., & Lin, P.J. (2002), Biohydrogen production with fixed-bed bioreactors. *International Journal of Hydrogen Energy, 27,* 1167 – 1174.

Das, D., & Veziroglu, T. N. (2001). Hydrogen production by biological processes: A survey of literature. *International Journal of Hydrogen Energy, 26,* 13-28.

Dubois, M., Gilles, K., Hamilton, J., Rebers, P., & Smith, F. (1956). Colorimetric method for determination of sugars and related substances. *Analytical Chemistry, 28* (3), 350–356.

Fritsch, M., Hartmeier, W., & Chang, J.S. (2008). Enhancing hydrogen production of *Clostridium butyricum* using a column reactor with square-structured ceramic fittings. *International Journal of Hydrogen Energy, 33,* 6549 – 6557.

Gupta, S.K., Kumari, S., Reddy, K., & Bux, F. (2013). Trends in biohydrogen production: Major challenges and state-of-the-art developments. *Environmental Technology, 34* (13–14), 1653–1670.

Hallenbeck, P.C. (2005). Fundamentals of the fermentative production of hydrogen. *Water Science and Technology, 52,* 21–29.

Hallenbeck, P.C. (2012). Fundamentals of dark hydrogen fermentations: Multiple pathways and enzymes. In D.B. Levin, & N. Azbar (Eds.). *State of the art and progress in production of biohydrogen* (94-111). Bentham Science Publishers.

Hallenbeck, P.C., & Ghosh, D. (2012). Improvements in fermentative biological hydrogen production through metabolic engineering. *Journal of Environmental Management, 95*, 360-364.

Hallenbeck, P.C., Abo-Hashesh, M., & Ghosh, D. (2012). Strategies for improving biological hydrogen production. *Bioresource Technology*, *110*, 1–9.

Han, S.K., & Shin, H.S. (2004) Bio-hydrogen production by anaerobic fermentation of food waste. *International Journal of Hydrogen Energy*, *29*, 569-577.

Hay, J.X.W., Wu, T.Y., Juan, J.C., & Jahim, J.M. (2013). Biohydrogen production through photo fermentation or dark fermentation using waste as a substrate: Overview, economics, and future prospects of hydrogen usage. *Biofuels, Bioproducts and Biorefining, 7*, 334–352.

Heinekey, D.M. (2009). Hydrogenase enzymes: Recent structural studies and active site models. *Journal of Organometallic Chemistry, 694*, 2671-2680.

International Energy Agency: Hydrogen production and storage: R&D priorities and gaps. (2006). Retrieved December 18, 2013, from http://www.iea.org/publications/freepublications/publication/hydrogen.pdf.

Inui, M., Vertes, A.A., & Yukawa, H. (2010). Advanced Fermentation Technologies. In A.A. Vertes, N. Qureshi, H.P. Blaschek, & H. Yukawa (Eds.). *Biomass to biofuels: Strategies for global industries* (311-330). UK: John Wiley & Sons Ltd.

Ishikawa, M.,Yamamura, S., Takamura, Y., Sode, K., Tamiya, E., & Tomiyama, M. (2006). Development of a compact high-density microbial hydrogen reactor for portable bio-fuel cell system. *International Journal of Hydrogen Energy, 31*, 1484–1489.

Kapdan, I.K., & Kargi, F. (2006). Bio-hydrogen production from waste materials. *Enzyme and Microbial Technology, 38*, 569–582.

Karadag, D. (2011). Anaerobic H_2 production at elevated temperature (60 °C) by enriched mixed consortia from mesophilic sources. *International Journal of Hydrogen Energy, 36* (1), 458-465.

Keskin, T., Aksoyek, E., & Azbar, N. (2011). Comparative analysis of thermophilic immobilized biohydrogen production using packed materials of ceramic ring and pumice stone. *International Journal of Hydrogen Energy, 36*, 15160-15167.

Keskin, T., Giusti, L., & Azbar, N. (2012). Continuous biohydrogen production in immobilized biofilm system versus suspended cell culture. *International Journal of Hydrogen Energy, 37*, 1418-1424.

Kim, D.H., & Kim, M.S. (2011). Hydrogenases for biological hydrogen production. *Bioresource Technology, 102*, 8423–8431.

Krishna, R.H. (2013). Review of research on production methods of hydrogen: Future fuel. *European Journal of Biotechnology and Bioscience, 1* (2), 84-93.

Levin, D.B., & Azbar, N. (Eds.). (2012). *State of the art and progress in production of biohydrogen.* Bentham Science Publishers.

Li, C.L., & Fang, H.H.P. (2007). Fermentative hydrogen production from wastewater and solid wastes by mixed cultures. *Environmental Science Technology, 37*, 1–39.

Margaritis, A., & Kilonzo, P.M. (2005). Production of ethanol using immobilised cell bioreactor systems. In V. Nedovic, & R. Willaert (Eds.). *Applications of cell immobilisation biotechnology* (375-405). Netherlands: Springer.

Mathews, J., & Wang, G. (2009). Metabolic pathway engineering for enhanced biohydrogen production. *International Journal of Hydrogen Energy, 34,* 7404-7416.

Melis, A. (2002). Green alga hydrogen production: Progress, challenges and prospects. *International Journal of Hydrogen Energy, 27,* 1217-1228.

Mohan, S.V., Mohanakrishna, G., Reddy, S.S., Raju, B.D., Rao, K.S.R., & Sarma, P.N. (2008). Self-immobilization of acidogenic mixed consortia on mesoporous material (SBA-15) and activated carbon to enhance fermentative hydrogen production. *International Journal of Hydrogen Energy, 33,* 6133 – 6142.

Nedovic, V., Willaert, R., Cukalovic, I.L., Obradovic, B., & Bugarski, B. (2005). Beer production using immobilised cells. In V. Nedovic, & R. Willaert (Eds.). *Applications of cell immobilisation biotechnology* (259-273). Netherlands: Springer.

Oh, Y.K., Raj, S.M., Jung, G.Y., & Park, S. (2011). Current status of the metabolic engineering of microorganisms for biohydrogen production. *Bioresource Technology, 102,* 8357–8367.

Ozmihci, S., Kargi, F., & Cakir, A. (2011). Thermophilic dark fermentation of acid hydrolyzed waste ground wheat for hydrogen gas production. *International Journal of Hydrogen Energy, 36,* 2111-2117.

Oztekin, R., Kargi, F., Kapdan, I.K., & Argun, H. (2008). Optimization of media composition for hydrogen gas production from hydrolyzed wheat starch by dark fermentation. *International Journal of Hydrogen Energy, 33,* 4083 – 4090.

Pilkington, P.H., Margaritis, A., Mensour, N.A., & Russell, I. (1998). Fundamentals of immobilised yeast cells for continuous beer fermentation: A review. *Journal of the Institute of Brewing, 104,* 19-31.

Plangklang, P., Reungsang, A., & Pattra, S. (2012). Enhanced bio-hydrogen production from sugarcane juice by immobilized *Clostridium butyricum* on sugarcane bagasse. *International Journal of Hydrogen Energy, 37,* 15525-15532.

Sabaratnam, V., & Hassan, M.A. (2012). Biohydrogen production via fermentation of biowastes by microorganisms. In D.B. Levin, & N. Azbar (Eds.). *State of the art and progress in production of biohydrogen* (112-126). Bentham Science Publishers.

Seol, E., Manimaran, A., Jang, Y., Kim, S., Oh, Y.K., & Park, S. (2011). Sustained hydrogen production from formate using immobilized recombinant *Escherichia coli* SH5. *International Journal of Hydrogen Energy, 36,* 8681-8686.

Shuler, M.L., & Kargi, F. (2002) *Bioprocess engineering: Basic concepts* (2nd ed.). New Jersey: Pearson Education.

Tampion, J., & Tampion, M.D. (1987). *Immobilized cells: Principles and applications.* Cambridge: Cambridge University Press.

Tsygankov, A.A., & Tekucheva, D.N. (2012). Integration of biological H_2 producing processes. In D.B. Levin, & N. Azbar (Eds.). *State of the art and progress in production of biohydrogen* (78-93). Bentham Science Publishers.

Uemoto, H. (2005). Wastewater treatment by immobilised cell systems. In V. Nedovic, & R. Willaert (Eds.). *Applications of cell immobilisation biotechnology* (481-506). Netherlands: Springer.

Vardar-Schara, G., Maeda, T., & Wood, T.K. (2008). Metabolically engineered bacteria for producing hydrogen via fermentation. *Microbial Biotechnology, 1 (2),* 107–125.

Verbelen, P.J., De Schutter D.P., Delvaux, F., Verstrepen, K.J., & Delvaux, F.R. (2006). Immobilized yeast cell systems for continuous fermentation applications. *Biotechnology Letters, 28,* 1515–1525.

Veziroglu, T.N., & Sahin, S. (2008). 21st Century's energy: Hydrogen energy system. *Energy Conversion and Management, 49,* 1820–1831.

Wang, J., & Wan, W. (2008). Comparison of different pretreatment methods for enriching hydrogen-producing cultures from digested sludge. *International Journal of Hydrogen Energy, 33,* 2934–2941.

Wang, J., & Wan, W. (2009). Factors influencing fermentative hydrogen production: A review. *International Journal of Hydrogen Energy, 34,* 799–811.

Winter, C.J. (2009). Hydrogen energy -Abundant, efficient, clean: A debate over the energy-system-of-change. *International Journal of Hydrogen Energy, 34,* 1-52.

Wu, K.J., & Chang, J.S. (2007). Batch and continuous fermentative production of hydrogen with anaerobic sludge entrapped in a composite polymeric matrix. *Process Biochemistry, 42,* 279–284.

Wu, K.J., Lo, Y.C., Chen, S.D., & Chang, J.S. (2007). Fermentative production of biofuels with entrapped anaerobic sludge using sequential HRT shifting operation in continuous cultures. *Journal of the Chinese Institute of Chemical Engineer, 38,* 205–213.

Wu, S.Y., Lin, C.N., Chang, J.S., & Chang, J.S. (2005). Biohydrogen production with anaerobic sludge immobilized by ethylene-vinyl acetate copolymer. *International Journal of Hydrogen Energy, 30*, 1375 – 1381.

Zhao, L., Cao, G., Wang, A., Guo, W., Liu, B., Ren, H., et al. (2012). Enhanced bio-hydrogen production by immobilized *Clostridium sp*. T2 on a new biological carrier. *International Journal of Hydrogen Energy, 37*, 162-166.

APPENDICES

A.1 Raw Data for Batch Dark Fermentation Experiments

Nomenclature used in the tables of raw experimental data are listed below:

$V_{G,\ i}$; the head space volume of the bottle for the i^{th} measurement, mL

$V_{W,\ i}$; total gas volume measured by the water displacement method for the i^{th} measurement, mL

$\sum V_{W,\ i}$; cumulative total gas volume calculated for the i^{th} measurement, mL

$^{1}C_{H2,\ i}$; the concentration of H_2 gas in the total gas for the i^{th} measurement, %

$^{2}C_{H2,\ i}$; the concentration of H_2 gas in the head space of the bottle after argon gas was passed through for the i^{th} measurement, %

$^{total}V_{H2,i}$; Total volume of of H_2 gas calculated for the i^{th} measurement, mL/day

$V_{H2,\ i}$; Cumulative H_2 volume calculated for the i^{th} measurement, mL

$n_{H2,\ i}$; the moles of CHV calculated for the i^{th} measurement, mmol

TS_o ; Initial total sugar concentration, g/L

TS_f ; Final total sugar concentration, g/L

A.1.1 Selection of Support Material

A.1.1.1 Control

Table A.1 Raw data for control at TS_0=13.17 ± 1.5 g/l

Time (h)	**V_G, i (ml)**	**V_W, i (ml)**	**$\sum V_W$, i (ml)**	**$^1C_{H2}$, i (%)**	**$^2C_{H2}$, i (%)**	**$^{total}V_{H2}$,i (ml/day)**	**V_{H2},i (ml)**	**n_{H2},i (mmol)**	**pH**	**ORP**	**TS_o (g/l)**	**TS_f (g/l)**
0	420	0	0	0	0	0	0	0	5.47		14.74	
15	420	130	130	9.323	4.6615	31.6982	31.6982	1.297193	5.34	-194		
39	422	150	280	14.085	7.0425	50.84685	82.54505	3.37801	5.67	-176		
62	424	150	430	10.8	5.4	39.096	121.6411	4.977944	5.19	-156		
92	428	120	550	15.193	7.5965	50.74462	172.3857	7.054578	6.03	-150		
109	432	130	680	15.174	7.587	52.50204	224.8877	9.203131	5.76	-175		
168	436	130	810	14.452	7.226	50.29296	275.1807	11.26128	5.4	-114		
184	438	40	850	13.39	6.695	34.6801	309.8608	12.6805	5.42	-87		
207	440	90	940	11.636	11.636	36.0716	345.9324	14.15667	5.47	-77		
230	442	11	951	14.169	14.169	1.55859	347.491	14.22045				0.65

Table A 2 Raw data for control at TS_0= 16.90 ± 2 g/l

Time (h)	V_G, i (ml)	V_W, i (ml)	$\sum V_W$, i (ml)	$^1C_{H2}$, i (%)	$^2C_{H2}$, i (%)	$^{total}V_{H2,}$i (ml/day)	$V_{H2,}$i (ml)	n_{H2},i (mmol)	pH	ORP	TS_o (g/l)	TS_f (g/l)
0	420	0	0	0		0	0	0	5.61		19.03	
15	420	30	30	3.697	3	4.0365	4.0365	0.165187	5.69	88		
41	422	110	140	8.02	4.01	25.7442	29.7807	1.218722	5.4	8		
63	424	110	250	12.627	6.313	40.65894	70.43964	2.882617	6.98	-153		
85	426	75	325	15.203	7.601	43.78464	114.2243	4.674426	6.08	-191		
114	428	80	405	15.419	7.709	45.33186	159.5561	6.529552	5.7	-109		
134	430	510	915	10.883	5.441	78.90175	238.4579	9.758467	6.6	-139		
142	430	70	985	10.883	5.441	7.6181	246.076	10.07022	6.0	-113		
158	432	110	1095	11.747	5.873	38.29522	284.3712	11.63739	5.15	-61		
166	432	60	1155	11.747	11.74	7.0482	291.4194	11.92582				4.77

Table A 3 Raw data for control at TS_0= 26.54 ± 4 g/l

Time (h)	V_G, i (ml)	V_W, i (ml)	$\sum V_W$, i (ml)	$^1C_{H2}$, i (%)	$^2C_{H2}$, i (%)	$^{total}V_{H2,}$i (ml/day)	$V_{H2,}$i (ml)	n_{H2},i (mmol)	pH	ORP	TS_o (g/l)	TS_f (g/l)
0	420	0	0	0	3	0	0	0	5.35		29.16	
14	420	10	10	3.51	3	2.493	2.493	0.102022	5.52	43		
19	422	30	40	3.51	3	1.053	3.546	0.145114	5.6	30		
41	422	0	40	4.805	3	7.6171	111631	0.45683	6.25	-35,2		
70	424	40	80	6.311	3	16.56304	27.72614	1.134643	6.07	-40		
86	426	10	90	4.796	3	8.13056	35.8567	1.467372	6.32	-80		
113	428	30	120	4.673	3	8.56234	44.41904	1.817771	5.86	-74		
138	430	20	140	4.694	3	8.223	52.64204	2.154282	6.29	-105		
163	432	30	170	5.099	3	10.59738	63.23942	2.587961	5.75	-63		
182	434	30	200	5.958	3	14.62512	77.86454	3.186468	5.77	-67		
211	436	50	250	8.46	4.2	22.6728	100.5373	4.114312	5.97	-120		
230	438	30	280	12.239	12.239	3.6717	104.209	4.26457				12.45

A.1.1.2 Stainless Steel Scrubber

Table A.4 Raw data for stainless steel scrubber at TS_0=13.17 ± 1.5 g/l

Time (h)	V_G, i (ml)	V_W, i (ml)	$\sum V_W$, i (ml)	$^1C_{H2}$, i (%)	$^2C_{H2}$, i (%)	$^{total}V_{H2}$,i (ml/day)	V_{H2},i (ml)	n_{H2},i (mmol)	pH	ORP	TS_o (g/l)	TS_f (g/l)
0	390	0	0	0	0	0	0	0	5.55		13.29	
15	390	90	90	11.058	5.529	31.5153	31.5153	1.289708	5.57	-217		
39	392	80	170	16.486	8.243	45.50136	77.01666	3.15177	5.39	-239		
62	394	0	170	24.157	12.0785	47.58929	124.606	5.099278	5.19	-243		
92	398	50	220	21.304	10.652	53.04696	177.6529	7.270131	5.22	-193		
109	400	80	300	21.478	10.739	60.1384	237.7913	9.731188	5.57	-191		
168	404	130	430	20.327	10.1635	67.48564	305.277	12.49292	5.76	-214		
184	406	10	440	19.163	9.5815	40.81719	346.0941	14.16329	5.91	-197		
207	408	90	530	13.232	13.232	38.90208	384.9962	15.75529	6.07	-150		
230	410	7	537	15.271	15.271	1.06897	386.0652	15.79903				0.32

Table A.5 Raw data for stainless steel scrubber at TS_0=16.90 ± 2 g/l

Time (h)	V_G, i (ml)	V_W, i (ml)	$\sum V_W$, i (ml)	$^1C_{H2}$, i (%)	$^2C_{H2}$, i (%)	$^{total}V_{H2}$,i (ml/day)	V_{H2},i (ml)	n_{H2},i (mmol)	pH	ORP	TS_o (g/l)	TS_f (g/l)
0	390	0	0	0		0	0	0	5.96		16.58	
24	390	40	40	6.078	3.039	14.2833	14.2833	0.584519	5.73	-88		
45	392	110	150	15.708	7.854	48.06648	62.34978	2.551554	6.55	-100		
67	394	195	345	25.45	12.725	99.764	162.1138	6.634219	5.75	-136		
92	396	250	595	27.134	13.567	121.5603	283.6741	11.60886	5.72	-58		
116	398	230	825	26.999	13.4995	115.8257	399.4998	16.34882	5.75	-56		
140	400	180	1005	26.413	13.2065	100.3694	499.8692	20.45626	5.77	-47		
166	402	140	1145	30.816	30.816	43.1424	543.0116	22.22179	5.47	-65		
182	404	80	1225	29.919	29.919	23.9352	566.9468	23.20129				4.54

Table A.6 Raw data for stainless steel scrubber at TS_0=26.54 ± 4 g/l

Time (h)	V_G, i (ml)	V_W, i (ml)	$\sum V_W$, i (ml)	$^1C_{H2}$, i (%)	$^2C_{H2}$, i (%)	$^{total}V_{H2}$,i (ml/day)	V_{H2},i (ml)	n_{H2},i (mmol)	pH	ORP	TS_o (g/l)	TS_f (g/l)
0	390	0	0	0	0	0	0	0	5.74		30.64	
19	390	20	20	3.737	3.527	1.5664	1.5664	0.064102	5.7	4		
48	392	340	360	28.062	12.5	156.4138	157.9802	6.465061	5.73	-45		
72	394	280	640	33.091	15.415	162.2982	320.2785	13.10683	5.73	-56		
89	396	140	780	27.429	14.047	91.39332	411.6718	16.84694	5.64	-139		
114	398	280	1060	29.715	16.123	137.2982	548.97	22.46562	5.75	-75		
137	400	230	1290	30.163	16.415	124.3669	673.3369	27.55512	5.78	-118		
167	402	200	1490	28.447	15.582	108.6113	781.9482	31.99984	5.87	-139		
188	404	100	1590	18.307	18.307	18.307	800.2552	32.74902	5.61	-53		9.33
209	406		1590		0	0	800.2552	32.74902				

A.1.1.3 Volcanic Stone

Table A.7 Raw data for volcanic stone at TS_0=13.17 ± 1.5 g/l

Time (h)	V_G, i (ml)	V_W, i (ml)	$\sum V_W$, i (ml)	$^1C_{H2}$, i (%)	$^2C_{H2}$, i (%)	$^{total}V_{H2}$,i (ml/day)	V_{H2},i (ml)	n_{H2},i (mmol)	pH	ORP	TS_o (g/l)	TS_f (g/l)
0	320	0	0	0	0	0	0	0	5.53		12.60	
15	320	560	560	16.527	8.2635	118.9944	118.9944	4.869635	5.86	-295		
39	322	570	1130	21.886	10.943	159.9867	278.9811	11.41681	5.96	-284		
62	324	130	1260	17.125	8.5625	50.005	328.9861	13.46317	5.72	-195		
92	328	100	1360	14.401	7.2005	38.01864	367.0047	15.01902	6.24	-360		
109	330	90	1450	10.742	5.371	27.3921	394.3968	16.13999	5.16	-152		
168	334	90	1540	10.056	5.028	25.84392	420.2407	17.19761	6.32	-300		
184	336	10	1550	9.822	4.911	17.48316	437.7239	17.91307	6.41	-291		
207	338	75	1625	10.147	5.0735	24.75868	462.4826	18.92628	6.51	-297		
230	340	0	1625	7.018	7.018	0	462.4826	18.92628				0.18

Table A.8 Raw data for volcanic stone at TS_0=16.90 ± 2 g/l

Time (h)	V_G, i (ml)	V_W, i (ml)	$\sum V_W$, i (ml)	$^1C_{H2}$, i (%)	$^2C_{H2}$, i (%)	$^{total}V_{H2}$,i (ml/day)	V_{H2},i (ml)	n_{H2},i (mmol)	pH	ORP	TS_o (g/l)	TS_f (g/l)
0	320	0	0	0	0	0	0	0	5.6		17.20	
18	320	310	310	23.455	11.7275	110.2385	110.2385	4.511315	5.31	-192		
40	322	320	630	31.124	15.562	149.7064	259.9449	10.63779	5.33	-277		
69	324	265	895	23.83	11.915	101.7541	361.699	14.80189	5.48	-172		
89	326	300	1195	18.182	9.091	84.18266	445.8817	18.24692	5.34	-176		
97	326	90	1285	18.182	9.091	16.3638	462.2455	18.91658	5.3			
113	328	80	1365	19.172	9.586	46.77968	509.0252	20.83095	5.38	-130		
121	328	80	1445	12.177	6.0885	29.71188	538.7371	22.04686	5.4			
137	330	30	1475	12.826	6.413	25.0107	563.7478	23.07038	5.5	-105		
145	330	60	1535	12.826	6.413	7.6956	571.4434	23.38531	5.52			
167	332	0	1535	15.458	15.458	25.66028	597.1036	24.43541	5.57	-117		
182	334	10	1545	14.3	14.3	1.43	598.5336	24.49393				0.39

Table A.9 Raw data for volcanic stone at TS_0=26.54 ± 4 g/l

Time (h)	V_G, i (ml)	V_W, i (ml)	$\sum V_W$, i (ml)	$^1C_{H2}$, i (%)	$^2C_{H2}$, i (%)	$^{total}V_{H2}$,i (ml/day)	V_{H2},i (ml)	n_{H2},i (mmol)	pH	ORP	TS_o (g/l)	TS_f (g/l)
0	320	0	0	0	0	0	0	0	5.57		24.91	
14	320	15	15	4.603	3	5.82005	5.82005	0.238175	5.96	-91		
19	322	30	45	4.603	4.603	1.3809	7.20095	0.294686	5.9	-100		
41	322	100	145	12.161	6.0805	31.74021	38.94116	1.593598	5.76	-121		
70	324	120	265	17.362	8.681	48.96084	87.902	3.597234	5.97	-191		
86	326	100	365	23.407	11.7035	61.56041	149.4624	6.116484	5.85	-183		
113	328	230	595	34.22	17.11	134.8268	284.2892	11.63403	5.62	-188		
138	330	230	825	39.281	19.6405	155.16	439.4492	17.98368	5.6	-188		
163	332	260	1085	41.249	20.6245	175.7207	615.1699	25.17474	5.55	-223		
182	334	170	1255	36.466	18.233	122.8904	738.0603	30.20381	5.62	-225		
211	336	230	1485	40.273	20.1365	160.2865	898.3469	36.76325	5.55	-211		
230	338	50	1535	31.985	31.985	15.9925	914.3394	37.41772				1.63

A.1.1.4 Tulle

Table A.10 Raw data for tulle at TS_0=13.17 ± 1.5 g/l

Time (h)	V_G, i (ml)	V_W, i (ml)	$\sum V_W$, i (ml)	$^1C_{H2}$, i (%)	$^2C_{H2}$, i (%)	$^{total}V_{H2}$,i (ml/day)	V_{H2},i (ml)	n_{H2},i (mmol)	pH	ORP	TS_o (g/l)	TS_f (g/l)
0	370	0	0	0	0	0	0	0	5.44		13.56	
15	370	450	450	21.208	10.604	134.6708	134.6708	5.511164	5.17	-230		
39	372	390	840	26.459	13.2295	152.4038	287.0746	11.74802	5.51	-248		
62	374	190	1030	28.333	14.1665	106.8154	393.8901	16.11925	5.5	-213		
92	376	80	1110	18.947	9.4735	50.77796	444.668	18.19725	5.64	-230		
109	378	90	1200	13.331	6.6655	37.19349	481.8615	19.71933	5.64	-175		
168	380	60	1260	15.571	7.7855	38.9275	520.789	21.31237	5.68	-155		
184	382	25	1285	11.358	5.679	24.53328	545.3223	22.31635	5.71	-148		
207	384	75	1360	8.55	4.275	22.8285	568.1508	23.25056	5.74	-164		
230	386	0	1360	7.74	7.74	0	568.1508	23.25056				0.16

Table A.11 Raw data for tulle at TS_0=16.90 ± 2 g/l

Time (h)	V_G, i (ml)	V_W, i (ml)	$\sum V_W$, i (ml)	$^1C_{H2}$, i (%)	$^2C_{H2}$, i (%)	$^{total}V_{H2}$,i (ml/day)	V_{H2},i (ml)	n_{H2},i (mmol)	pH	ORP	TS_o (g/l)	TS_f (g/l)
0	370	0	0	0	0	0	0	0	5.5		17.38	
15	370	30	30	3.485	3	2.84	2.84	0.116222	5.58	-161		
41	372	210	240	18.469	9.2345	73.13724	75.97724	3.109234	5.3	-250		
63	374	180	420	20.103	10.0515	73.77801	149.7553	6.128468	5.61	-130		
85	376	270	690	25.944	12.972	118.8235	268.5788	10.99111	5.47	-175		
114	378	310	1000	29.691	14.8455	148.1581	416.7369	17.05422	5.85	-180		
134	380	0	1000	9.763	4.8815	18.5497	435.2866	17.81333	5.45	-298		
142	380	90	1090	5.264	3	13.3408	448.6274	18.35928	5.3	-112		
158	382	80	1170	7.384	3	22.65408	471.2814	19.28636	5.39	-68		
166	382	50	1220	7.384	7.384	3.692	474.9734	19.43745	5.4	-53		
182	384	0	1220	10.536	10.536	0	474.9734	19.43745				1.07

Table A.12 Raw data for tulle at TS_0=26.54 ± 4 g/l

Time (h)	V_G, i (ml)	V_W, i (ml)	$\sum V_W$, i (ml)	$^1C_{H2}$, i (%)	$^2C_{H2}$, i (%)	$^{total}V_{H2}$,i (ml/day)	V_{H2},i (ml)	n_{H2},i (mmol)	pH	ORP	TS_o (g/l)	TS_f (g/l)
0	370	0	0	0	0	0	0	0	5.46		24.91	
14	370	10	10	3.419	3	1.8922	1.8922	0.077435	5.54	21,3		
19	372	20	30	3.419	3	0.6838	2.576	0.105418	5.5	10.6		
41	372	0	30	3.652	3	2.42544	5.00144	0.204675	5.52	-8,6		
70	374	60	90	7.999	3	23.49566	28.4971	1.166193	6.3	-134		
86	376	40	130	9.819	4.9095	22.38732	50.88442	2.082355	5.91	-99		
113	378	30	160	10.831	5.4155	23.71989	74.60431	3.053049	5.52	-52		
138	380	50	210	13.937	6.9685	33.4488	108.0531	4.421882	6.31	-131		
163	382	90	300	18.125	9.0625	50.93125	158.9844	6.506153	5.66	-94		
182	384	70	370	19.926	9.963	52.20612	211.1905	8.642596	5.94	-95		
211	386	120	490	23.637	11.8185	73.98381	285.1743	11.67025	5.64	-80		
230	388	75	565	27.085	27.085	20.31375	305.488	12.50156				1.63

A.1.1.5 Polyester Fiber

Table A.13 Raw data for polyester fiber at TS_0=13.17 ± 1.5 g/l

Time (h)	V_G, i (ml)	V_W, i (ml)	$\sum V_W$, i (ml)	$^1C_{H2}$, i (%)	$^2C_{H2}$, i (%)	$^{total}V_{H2}$,i (ml/day)	V_{H2},i (ml)	n_{H2},i (mmol)	pH	ORP	TS_o (g/l)	TS_f (g/l)
0	350	0	0	0	0	0	0	0	5.49		12.80	
15	350	510	510	25.116	12.558	172.0446	172.0446	7.04062	5.27	-200		
39	352	390	900	25.421	12.7105	143.8829	315.9275	12.92877	5.44	-230		
62	354	330	1230	27.291	13.6455	138.3654	454.2928	18.59113	5.3	-162		
92	358	160	1390	20.282	10.141	68.75598	523.0488	21.40485	6.07	-209		
109	360	90	1480	17.237	8.6185	46.5399	569.5887	23.30941	6.2	-168		
168	364	60	1540	11.804	5.902	28.56568	598.1544	24.47841	6.39	-194		
184	366	30	1570	10.202	5.101	21.73026	619.8847	25.36768	6.59	-203		
207	368	60	1630	8.447	4.2235	20.61068	640.4953	26.21114	6.74	-217		
230	370	0	1630	7.497	7.497	0	640.4953	26.21114				0.16

Table A.14 Raw data for polyester fiber at TS_0=16.90 ± 2 g/l

Time (h)	V_G, i (ml)	V_W, i (ml)	$\sum V_W$, i (ml)	$^1C_{H2}$, i (%)	$^2C_{H2}$, i (%)	$^{total}V_{H2}$,i (ml/day)	V_{H2},i (ml)	n_{H2},i (mmol)	pH	ORP	TS_o (g/l)	TS_f (g/l)
0	390	0	0	0		0	0	0	6.01		15.42	
24	390	90	90	29.706	14.853	84.6621	84.6621	3.464646	5.49	-300		
45	392	170	260	23.144	11.572	84.70704	169.3691	6.931132	5.63	-320		
67	394	240	500	31.112	15.556	135.9594	305.3286	12.49503	5.57	-449		
92	396	190	690	29.95	14.975	116.206	421.5346	17.25056	5.73	-390		
116	398	160	850	22.15	11.075	79.5185	501.0531	20.50471	5.65	-350		
140	400	80	930	12.752	6.376	35.7056	536.7587	21.9659	5.7	-400		
166	402	0	930	13.398	13.398	0	536.7587	21.9659	5.71	-224		
182	402	0	930	14.655	14.655	0	536.7587	21.9659				0.34

Table A.15 Raw data for polyester fiber at TS_0=26.54 ± 4 g/l

Time (h)	V_G, i (ml)	V_W, i (ml)	$\sum V_W$, i (ml)	$^1C_{H2}$, i (%)	$^2C_{H2}$, i (%)	$^{total}V_{H2}$,i (ml/day)	V_{H2},i (ml)	n_{H2},i (mmol)	pH	ORP	TS_o (g/l)	TS_f (g/l)
0	350	0	0	0	0	0	0	0	5.63		23.36	
14	350	15	15	14.881	7.4405	28.2739	28.2739	1.157059	5.76	-173		
19	352	200	215	14.881	14.881	29.762	58.0359	2.375016	5.7	-160		
41	352	110	325	36.237	18.1185	103.6378	161.6737	6.616211	5.23	-156		
70	354	100	425	44.91	22.455	124.4007	286.0744	11.70709	5.76	-330		
86	356	135	560	44.217	22.1085	138.3992	424.4736	17.37083	5.78	-311		
113	358	100	660	43.233	21.6165	120.6201	545.0937	22.30699	5.7	-300		
138	360	90	750	45.807	22.9035	123.6789	668.7726	27.36833	5.55	-319		
163	362	60	810	33.018	16.509	79.57338	748.346	30.62473	5.55	-263		
182	364	50	860	32.845	16.4225	76.2004	824.5464	33.7431	5.58	-400		
211	366	70	930	30.215	15.1075	76.44395	900.9903	36.87143	5.66	-400		
230	368	20	950	33.651	33.651	6.7302	907.7205	37.14685				0.64

A.1.1.6 Loofah Sponge

Table A.16 Raw data for loofah sponge at TS_0=13.17 ± 1.5 g/l

Time (h)	V_G, i (ml)	V_W, i (ml)	$\sum V_W$, i (ml)	$^1C_{H2}$, i (%)	$^2C_{H2}$, i (%)	$^{total}V_{H2}$,i (ml/day)	V_{H2},i (ml)	n_{H2},i (mmol)	pH	ORP	TS_o (g/l)	TS_f (g/l)
0	360	0	0	0	0	0	0	0	5.46		12.55	
15	360	110	110	22.609	11.3045	65,5661	65.5661	2.683176	5.27	-207		
39	362	90	200	31.693	15.8465	85,88803	151.4541	6.197992	5.85	-249		
62	364	70	270	27.91	13.955	70,3332	221.7873	9.076253	5.32	-132		
92	366	0	270	24.763	12.3815	45,31629	267.1036	10.93074	5.64	-160		
109	368	0	270	22.476	11.238	41,35584	308.4595	12.62316	5.73	-138		
168	370	50	320	19.466	9.733	45,7451	354.2046	14.49519	5.92	-168		
184	372	11	331	16.44	8.22	32,3868	386.5914	15.82057	5.99	-208		
207	374	0	331	16.35	16.35	30,5745	417.1659	17.07177	6.08	-207		
230	376	0	331	20.402	20.402	0	417.1659	17.07177				0.28

Table A.17 Raw data for loofah sponge at TS_0=16.90 ± 2 g/l

Time (h)	V_G, i (ml)	V_W, i (ml)	$\sum V_W$, i (ml)	$^1C_{H2}$, i (%)	$^2C_{H2}$, i (%)	$^{total}V_{H2}$,i (ml/day)	V_{H2},i (ml)	n_{H2},i (mmol)	pH	ORP	TS_o (g/l)	TS_f (g/l)
0	360	0	0	0	0	0	0	0	5.47		16.35	
15	360	0	0	5.59	3	9.324	9.324	0.381568	6.06	-132		
41	362	70	70	37.441	18.7205	93.97691	103.3009	4.227407	5.14	-165		
63	364	50	120	34.737	17.3685	80.58984	183.8908	7.525403	5.36	-189		
85	366	70	190	40.466	20.233	102.379	286.2697	11.71508	5.27	-188		
114	368	30	220	40.46	20.23	86.5844	372.8541	15.25839	5.19	-129		
134	370	10	230	27.358	13.679	53.3481	426.2022	17.44157	5.4	-167		
142	370	50	280	27.358	27.358	13.679	439.8812	18.00136	5.45	-160		
158	372	30	310	29.832	14.916	64.43712	504.3184	20.63833	5.57	-139		
166	372	70	380	29.832	29.832	20.8824	525.2008	21.49291	5.75	-120		
182	374	0	380	32.582	32.582	0	525.2008	21.49291				0.88

Table A.18 Raw data for loofah sponge at TS_0=26.54 ± 4 g/l

Time (h)	V_G, i (ml)	V_W, i (ml)	$\sum V_W$, i (ml)	$^1C_{H2}$, i (%)	$^2C_{H2}$, i (%)	$^{total}V_{H2}$,i (ml/day)	V_{H2},i (ml)	n_{H2},i (mmol)	pH	ORP	TS_o (g/l)	TS_f (g/l)
0	360	0	0	0		0	0	0	5.42		26.94	
14	360	0	0	3.984	3	3.5424	3.5424	0.144966	5.71	-34		
19	362	20	20	3.984	3	0.7968	4.3392	0.177574	5.7	-30		
41	362	0	20	35.753	17.8765	64.71293	69.05213	2.825836	5.58	-126		
70	364	0	20	42.557	21.2785	77.45374	146.5059	5.995493	5.72	-151		
86	366	0	20	41.357	20.6785	75.68331	222.1892	9.092698	5.48	-115		
113	368	0	20	42.163	21.0815	77.57992	299.7691	12.26752	5.71	-140		
138	370	0	20	39.58	19.79	73.223	372.9921	15.26404	5.55	-113		
163	372	0	20	35.608	17.804	66.23088	439.223	17.97442	6.06	-340		
182	72	0	20	23.587	11.7935	8.49132	447.7143	18.32191	5.83	-92		
211	74	0	20	31.958	31.958	11.82446	459.5388	18.80581	5.51	-80		
230	76	0	20	30.369	30.369	0	459.5388	18.80581				5.51

A.1.1.7 Plastic Bath Sponge

Table A.19 Raw data for plastic bath sponge at TS_0=13.17 ± 1.5 g/l

Time (h)	V_G, i (ml)	V_W, i (ml)	$\sum V_W$, i (ml)	$^1C_{H2}$, i (%)	$^2C_{H2}$, i (%)	$^{total}V_{H2}$,i (ml/day)	V_{H2},i (ml)	n_{H2},i (mmol)	pH	ORP	TS_o (g/l)	TS_f (g/l)
0	370	0	0	0	0	0	0	0	5.54		13.31	
15	370	70	70	25.37	12.685	64.6935	64.6935	2.647467	5.33	-260		
39	372	175	245	34.141	17.0705	123.249	187.9425	7.691214	5.67	-270		
62	374	170	415	28.133	14.0665	100.4348	288.3773	11.80133	5.54	-190		
92	376	90	505	22.392	11.196	62.24976	350.6271	14.34879	5.73	-169		
109	378	110	615	19.132	9.566	57.20468	407.8318	16.68979	5.78	-199		
168	380	110	725	16.986	8.493	50.958	458.7898	18.77516	6.19	-174		
184	382	30	755	14.03	7.015	31.0063	489.7961	20.04404	6.22	-226		
207	384	40	795	12.063	12.063	27.98616	517.7822	21.18932	6.28	-198		
230	386	0	795	12.69	12.69	0	517.7822	21.18932				0.21

Table A.20 Raw data for plastic bath sponge at TS_0=16.90 ± 2 g/l

Time (h)	V_G, i (ml)	V_W, i (ml)	$\sum V_W$, i (ml)	$^1C_{H2}$, i (%)	$^2C_{H2}$, i (%)	$^{total}V_{H2}$,i (ml/day)	V_{H2},i (ml)	n_{H2},i (mmol)	pH	ORP	TS_o (g/l)	TS_f (g/l)
0	370	0	0	0		0	0	0	5.5		16.96	
15	370	10	10	3.487	3	2.1506	2.1506	0.088009	5.81	-77		
41	372	70	80	27.255	13.6275	69.7728	71.9234	2.943338	5.49	-158		
63	374	45	125	34.761	17.3805	80.64552	152.5689	6.243613	5.4	-184		
85	376	50	175	33.088	16.544	78.74944	231.3184	9.466294	5.69	-221		
114	378	55	230	32.5	16.25	79.3	310.6184	12.71151	5.53	-131		
134	380	50	280	25.547	12.7735	61.3128	371.9312	15.22062	5.26	-140		
142	380	70	350	25.547	25.547	17.8829	389.8141	15.95245	5.2	-130		
158	382	50	400	25.179	12.5895	60.68139	450.4955	18.43573	5.11	-85		
166	382	70	470	25.179	25.179	17.6253	468.1208	19.15701	5.1	-80		
182	384	10	480	33.458	33.458	3.3458	471.4666	19.29393				1.42

Table A.21 Raw data for plastic bath sponge at TS_0=26.54 ± 4 g/l

Time (h)	V_G, i (ml)	V_W, i (ml)	$\sum V_W$, i (ml)	$^1C_{H2}$, i (%)	$^2C_{H2}$, i (%)	$^{total}V_{H2}$,i (ml/day)	V_{H2},i (ml)	n_{H2},i (mmol)	pH	ORP	TS_o (g/l)	TS_f (g/l)
0	370	0	0	0	0	0	0	0	5.48		25.84	
14	370	10	10	3.355	3	1.649	1.649	0.067482	5.49	15		
19	372	40	50	3.355	3	1.342	2.991	0.122401	5.53	-10		
41	372	0	50	4.331	3	4.95132	7.94232	0.325025	5.48	-21		
70	374	0	50	29.752	14.876	55.63624	63.57856	2.60184	6.17	-153		
86	376	5	55	31.114	15.557	60.05002	123.6286	5.059281	5.34	-133		
113	378	0	55	37.364	18.682	70.61796	194.2465	7.949195	5.92	-153		
138	380	0	55	41	20.5	77.9	272.1465	11.13711	5.77	-121		
163	382	0	55	41.574	20.787	79.40634	351.5529	14.38668	5.63	-332		
182	82	30	85	14.473	7.2365	10.27583	361.8287	14.8072	5.67	-96		
211	84	0	85	8.996	8.996	3.77832	365.607	14.96182	5.45	-64		
230	86	6	91	15.236	15.236	0.91416	366.5212	14.99923				6.56

A.1.1.8 Sea Sponge

Table A.22 Raw data for sea sponge at TS_0=13.17 ± 1.5 g/l

Time (h)	V_G, i (ml)	V_W, i (ml)	$\sum V_W$, i (ml)	$^1C_{H2}$, i (%)	$^2C_{H2}$, i (%)	$^{total}V_{H2}$,i (ml/day)	V_{H2},i (ml)	n_{H2},i (mmol)	pH	ORP	TS_o (g/l)	TS_f (g/l)
0	340	0	0	0	0	0	0	0	5.54		11.89	
15	340	130	130	12.78	6.39	38.34	38.34	1.568997	5.15	-243		
39	342	170	300	22.881	11.4405	78.02421	116.3642	4.761999	5.9	-244		
62	344	80	380	16.593	8.2965	41.81436	158.1786	6.473178	6.06	-185		
92	346	10	390	16.235	8.1175	29.71005	187.8886	7.689009	5.55	-260		
109	350	0	390	12.925	6.4625	22.61875	210.5074	8.614641	5.71	-291		
168	352	80	470	10.565	5.2825	27.0464	237.5538	9.721467	5.81	-322		
184	354	40	510	8.122	4.061	1762474	255.1785	10.44273	5.85	-321		
207	356	0	510	0	0	0	255.1785	10.44273	5.8	-320		
230	358	70	580	3.483	3.483	2.4381	257.6166	10.5425				0.15

Table A.23 Raw data for sea sponge at TS_0=16.90 ± 2 g/l

Time (h)	V_G, i (ml)	V_W, i (ml)	$\sum V_W$, i (ml)	$^1C_{H2}$, i (%)	$^2C_{H2}$, i (%)	$^{total}V_{H2}$,i (ml/day)	V_{H2},i (ml)	n_{H2},i (mmol)	pH	ORP	TS_o (g/l)	TS_f (g/l)
0	340	0	0	0	0	0	0	0	5.75		16.37	
18	340	90	90	29.56	14.78	76.856	76.856	3.145196	5.19	-199		
40	342	140	230	37.543	18.7715	116.7587	193.6147	7.92334	5.52	-181		
69	344	90	320	34.148	17.074	89.46776	283.0825	11.58465	5.45	-214		
89	346	90	410	34.668	17.334	91.17684	374.2593	15.3159	5.43	-117		
97	346	90	500	34.668	34.668	31.2012	405.4605	16.59275	5.4	-132		
113	348	95	595	30.08	15.04	80.9152	486.3757	19.90406	5.53	-140		
121	348	100	695	20.054	10.027	54.94796	541.3237	22.15271	5.5	-135		
137	350	90	785	25.073	12.5365	66.44345	607.7671	24.87179	5.6	-125		
145	350	70	855	25.073	25.073	17.5511	625.3182	25.59004	5.83	-110		
167	352	25	880	19.04	19.04	38.2704	663.5886	27.15619	5.72	-123		
182	354	0	880	31.08	31.08	0	663.5886	27.15619				0.98

Table A.24 Raw data for sea sponge at TS_0=26.54 ± 4 g/l

Time (h)	V_G, i (ml)	V_W, i (ml)	$\sum V_W$, i (ml)	$^1C_{H2}$, i (%)	$^2C_{H2}$, i (%)	$^{total}V_{H2}$,i (ml/day)	V_{H2},i (ml)	n_{H2},i (mmol)	pH	ORP	TS_o (g/l)	TS_f (g/l)
0	390	0	0	0	0	0	0	0	5.62		27.09	
19	390	0	0	6.737	3.896	11.0799	11.0799	0.453425	5.53	25		
48	392	0	0	36.771	16.194	80.66184	91.74174	3.754368	5.86	-72		
72	394	3	3	33.823	9.07	98.54151	190.2833	7.787005	5.71	-132		
89	396	0	3	21.862	6.131	86.57352	276.8568	11.32987	5.72	-132		
114	398	1	4	23.17	8.805	92.4483	369.3051	15.11316	5.54	-126		
137	400	0	4	17.652	9.948	70.608	439.9131	18.00266	6.11	-112		
167	402	0	4	23.1	14.184	92.862	532.7751	21.80288	5.76	-131		
188	404	0	4	16.131	16.131	0	532.7751	21.80288	5.38	-45		
209	406		4		0	0	532.7751	21.80288	5.62			5.74

A.1.1.9 Aquarium Biological Sponge

Table A.25 Raw data for aquarium biological sponge at TS_0=13.17 ± 1.5 g/l

Time (h)	V_G, i (ml)	V_W, i (ml)	$\sum V_W$, i (ml)	$^1C_{H2}$, i (%)	$^2C_{H2}$, i (%)	$^{total}V_{H2}$,i (ml/day)	V_{H2},i (ml)	n_{H2},i (mmol)	pH	ORP	TS_o (g/l)	TS_f (g/l)
0	390	0	0	0	0	0	0	0	5.49		13.83	
15	390	300	300	17.245	8.6225	85.36275	85.36275	3.493319	5.23	-230		
39	392	300	600	27.636	13.818	137.0746	222.4373	9.102853	5.57	-250		
62	394	320	920	23.814	11.907	123.1184	345.5557	14.14125	5.1	-185		
92	396	130	1050	23.502	11.751	77.08656	422.6423	17.29589	5.33	-206		
109	398	80	1130	20.456	10.228	57.07224	479.7145	19.63147	5.38	-210		
168	400	130	1260	14.673	7.3365	48.4209	528.1354	21.613	5.79	-322		
184	402	40	1300	13.706	6.853	33.03146	561.1669	22.96476	5.86	-212		
207	404	90	1390	13.76	13.76	40.1792	601.3461	24.60902	5.95	-171		
230	406	3	1393	11.7	11.7	0.351	601.6971	24.62339				0.31

Table A.26 Raw data for aquarium biological sponge at TS_0=16.90 ± 2 g/l

Time (h)	V_G, i (ml)	V_W, i (ml)	$\sum V_W$, i (ml)	$^1C_{H2}$, i (%)	$^2C_{H2}$, i (%)	$^{total}V_{H2}$,i (ml/day)	V_{H2},i (ml)	n_{H2},i (mmol)	pH	ORP	TS_o (g/l)	TS_f (g/l)
0	390	0	0	0	0	0	0	0	5.83		16.84	
24	390	0	0	21.508	10.754	41.9406	41.9406	1.716345	6	-268		
45	392	150	150	16.929	8.4645	58.57434	100.5149	4.113396	6.06	-52		
67	394	150	300	21.935	10.9675	76.11445	176.6294	7.228245	5.96	-89		
92	396	205	505	26.478	13.239	106.7063	283.3357	11.59501	6.15	-111		
116	398	225	730	22.181	11.0905	94.04744	377.3832	15.44374	6.03	-86		
140	400	180	910	23.298	11.649	88.5324	465.9156	19.06677	5.91	-73		
166	402	130	1040	32.446	32.446	42.1798	508.0954	20.7929	5.56	-79		
182	402	70	1110	34.343	34.343	24.0401	532.1355	21.7767				0.90

Table A.27 Raw data for aquarium biological sponge at TS_0=26.54 ± 4 g/l

Time (h)	V_G, i (ml)	V_W, i (ml)	$\sum V_W$, i (ml)	$^1C_{H2}$, i (%)	$^2C_{H2}$, i (%)	$^{total}V_{H2}$,i (ml/day)	V_{H2},i (ml)	n_{H2},i (mmol)	pH	ORP	TS_o (g/l)	TS_f (g/l)
0	390	0	0	0	0	0	0	0	5.47		28.06	
14	390	20	20	3.701	3	3.4741	3.4741	0.142171	5.48	44		
19	392	40	60	3.701	3	1.4804	4.9545	0.202754	5.55	-23		
41	392	170	230	20.4	10.2	74.664	79.6185	3.258246	5.74	-146		
70	394	150	380	27.504	13.752	95.43888	175.0574	7.163913	6.32	-171		
86	396	115	495	27.27	13.635	85.3551	260.4125	10.65692	5.78	-146		
113	398	145	640	37.6	18.8	129.344	389.7565	15.95009	5.81	-123		
138	400	150	790	41.584	20.792	145.544	535.3005	21.90622	6.29	-166		
163	402	130	920	46.459	23.2295	153.7793	689.0798	28.19937	5.5	-144		
182	404	95	1015	35.744	17.872	106.1597	795.2395	32.54377	5.68	-125		
211	406	90	1105	29.81	29.81	87.3433	882.5828	36.11814	5.48	-97		
230	408	20	1125	37.2	37.2	7.44	890.0228	36.4226				1.77

A.1.2 The Effect of Support Material Size

Table A.28 Raw data for polyester fiber, R= 0.5 cm in diameter

Time (h)	V_G, i (ml)	V_W, i (ml)	$\sum V_W$, i (ml)	$^1C_{H2}$, i (%)	$^2C_{H2}$, i (%)	$^{total}V_{H2}$,i (ml/day)	V_{H2},i (ml)	n_{H2},i (mmol)	pH	ORP	TS_o (g/l)	TS_f (g/l)
0	320	0	0	0	0	0	0	0	6.25		15.20	
17	320	70	70	12.284	4.247	47.9076	47.9076	1.960534	5.93	-87		
44	322	80	150	54.728	16.386	206.3312	254.2388	10.40427	5.81	-245		
68	326	80	230	38.804	23.472	104.1259	358.3647	14.66544	5.48	-194		
94	328	160	390	37.649	19.221	106.739	465.1037	19.03354	5.64	-180		
117	330	95	485	27.564	15.153	53.7177	518.8214	21.23184	5.75	-149		
141	332	60	545	21.382	13.326	33.50948	552.3308	22.60316	5.94	-203		
165	334	30	575	16.205	16.205	14.47736	566.8082	23.19562	6.04	-166		
183	336	0	575	15.956	15.956	0	566.8082	23.19562	6.13	-252		0.64

Table A.29 Raw data for polyester fiber, R= 1 cm in diameter

Time (h)	V_G, i (ml)	V_W, i (ml)	$\sum V_W$, i (ml)	$^1C_{H2}$, i (%)	$^2C_{H2}$, i (%)	$^{total}V_{H2}$,i (ml/day)	V_{H2},i (ml)	n_{H2},i (mmol)	pH	ORP	TS_o (g/l)	TS_f (g/l)
0	350	0	0	0	0	0	0	0	6.06		15.16	
17	350	90	90	30.088	14.16	76.6392	76.6392	3.136323	6	-119		
44	352	80	170	46.047	15.564	149.0798	225.719	9.237152	5.64	-265		
68	354	100	270	32.012	14.575	90.23792	315.957	12.92998	6.03	-324		
94	356	100	370	30.787	11.498	88.50172	404.4587	16.55175	6.12	-320		
117	358	65	435	15.782	6.26	25.59502	430.0537	17.59919	5.69	-153		
141	360	40	475	11.111	7.019	21.908	451.9617	18.49573	5.75	-202		
165	362	25	500	11.139	11.139	17.69915	469.6609	19.22004	5.8	-119		
183	364	0	500	12.957	12.957	6.61752	476.2784	19.49085	5.86	-209		0.59

Table A.30 Raw data for polyester fiber, R= 2 cm in diameter

Time (h)	V_G, i (ml)	V_W, i (ml)	$\sum V_W$, i (ml)	$^1C_{H2}$, i (%)	$^2C_{H2}$, i (%)	$^{total}V_{H2}$,i (ml/day)	V_{H2},i (ml)	n_{H2},i (mmol)	pH	ORP	TS_o (g/l)	TS_f (g/l)
0	360	0	0	0	0	0	0	0	5.66		14.64	
17	360	105	105	13.741	9.79	63.89565	63.89565	2.614816	6.56	-161		
44	362	130	235	34.301	13.2	133.3211	197.2168	8.070747	5.85	-139		
68	364	160	395	27.077	14.219	93.83548	291.0523	11.9108	6.31	-268		
94	366	130	525	25.625	14.742	75.05846	366.1107	14.98243	5.83	-188		
117	368	100	625	22.042	14.754	48.906	415.0167	16.98382	5.55	-120		
141	370	100	725	24.617	13.6	61.1101	476.1268	19.48465	5.53	-179		
165	372	95	820	11.721	11.721	11.13495	487.2618	19.94032	5.57	-140		
183	374	15	835	14.339	14.339	11.94217	499.2039	20.42904	5.64	-125		0.85

Table A.31 Raw data for polyester fiber, R= 3 cm in diameter

Time (h)	V_G, i (ml)	V_W, i (ml)	$\sum V_W$, i (ml)	$^1C_{H2}$, i (%)	$^2C_{H2}$, i (%)	$^{total}V_{H2}$,i (ml/day)	V_{H2},i (ml)	n_{H2},i (mmol)	pH	ORP	TS_o (g/l)	TS_f (g/l)
0	360	0	0	0	0	0	0	0	5.67		14.07	
17	360	60	60	8.519	6.11	35.7798	35.7798	1.464225	5.95	-73		
44	362	80	140	15.836	5.184	47.87692	83.65672	3.423503	6.07	-160		
68	364	30	170	7.63	5.655	11.19244	94.84916	3.881534	6.34	-228		
94	366	30	200	9.166	6.323	15.60006	110.4492	4.519939	5.88	-198		
117	368	60	260	12.578	7.526	30.5652	141.0144	5.770765	5.7	-93		
141	370	80	340	16.676	11.4	47.1958	188.2102	7.70217	5.81	-126		
165	372	100	440	16.737	16.737	36.59064	224.8009	9.199577	5.55	-140		
183	374	60	500	20.325	20.325	25.61412	250.415	10.24779	5.53	-115		0.64

A.1.3 Box-Wilson Statistical Experiment Design

Table A.32 Raw data for experimental point of A_1; PN= 215, TS_o = 20 g/l, T=45 ºC

Time (h)	V_G, i (ml)	V_W, i (ml)	$\sum V_W$, i (ml)	$^1C_{H2}$, i (%)	$^2C_{H2}$, i (%)	$^{total}V_{H2}$,i (ml/day)	V_{H2},i (ml)	n_{H2},i (mmol)	pH	ORP	TS_o (g/l)	TS_f (g/l)
0	330	0	0	0	0	0	0	0	5.83		19.93	
14	330	700	700	33.733	4	347.4499	347.4499	13.75712	5.54	-276		
43	332	1260	1960	49.335	20.677	772.1332	1119.583	44.32939	5.57	-86		
65	334	470	2430	45.161	25.668	294.0333	1413.616	55.97151	5.91	-144		
94	336	30	2460	24.845	24.845	7.4535	1421.07	56.26662	6.08	-127		1.4

Table A.33 Raw data for experimental point of A_2; PN= 145, TS_o = 20 g/l, T=45 ºC

Time (h)	V_G, i (ml)	V_W, i (ml)	$\sum V_W$, i (ml)	$^1C_{H2}$, i (%)	$^2C_{H2}$, i (%)	$^{total}V_{H2}$,i (ml/day)	V_{H2},i (ml)	n_{H2},i (mmol)	pH	ORP	TS_o (g/l)	TS_f (g/l)
0	360	0	0	0	0	0	0	0	5.99		19.67	
14	360	90	90	22.78	9	102.51	102.51	4.058838	5.46	-240		
43	362	440	530	37.087	15.613	264.8577	367.3677	14.54576	5.79	-135		
65	364	490	1020	43.318	28.109	313.1044	680.4721	26.94299	6.08	-229		
94	366	160	1180	30.406	30.406	57.05662	737.5288	29.20212	5.87	-153		
112	368	35	1215	31.509	31.509	15.08719	752.616	29.79949	6	-130		
137	370	0	1215	30.485	30.485	0	752.616	29.79949				0.46

Table A.34 Raw data for experimental point of A_3; PN= 180, TS_o = 26 g/l, T=45 ºC

Time (h)	V_G, i (ml)	V_W, i (ml)	$\sum V_W$, i (ml)	$^1C_{H2}$, i (%)	$^2C_{H2}$, i (%)	$^{total}V_{H2}$,i (ml/day)	V_{H2},i (ml)	n_{H2},i (mmol)	pH	ORP	TS_o (g/l)	TS_f (g/l)
0	340	0	0	0	0	0	0	0	6.2		26.65	
15	340	640	640	44.576	19.21	436.8448	436.8448	17.29667	5.69	-307		
44	342	710	1350	32.55	18.75	276.7278	713.5726	28.25359	5.85	-228		
65	344	250	1600	28.098	13.024	102.4021	815.9747	32.30815	5.56	-112		
86	346	240	1840	17.311	17.311	56.37942	872.3541	34.54047	5.6	-181		
110	348	260	2100	20.737	20.737	65.83868	938.1928	37.14732	5.72	-305		
135	350	120	2220	27.794	27.794	58.0523	996.2451	39.44588	5.89	-153		
157	352	10	2230	12.824	12.824	1.2824	997.5275	39.49666				1.67

Table A.35 Raw data for experimental point of A_4; PN= 180, TS_o = 14 g/l, T=45 ºC

Time (h)	V_G, i (ml)	V_W, i (ml)	$\sum V_W$, i (ml)	$^1C_{H2}$, i (%)	$^2C_{H2}$, i (%)	$^{total}V_{H2}$,i (ml/day)	V_{H2},i (ml)	n_{H2},i (mmol)	pH	ORP	TS_o (g/l)	TS_f (g/l)
0	340	0	0	0	0	0	0	0	6.07		15.18	
15	340	670	670	45.853	25.703	463.1153	463.1153	18.33684	5.91	-281		
44	342	720	1390	25.707	14.33	185.1041	648.2194	25.66596	5.81	-219		
65	344	195	1585	23.726	13.402	78.58794	726.8073	28.77761	5.84	-111		
86	346	70	1655	17.303	17.303	25.60956	752.4169	29.79161	6.09	-131		
110	348	25	1680	14.433	14.433	3.60825	756.0251	29.93448	6.25	-182		0.23

Table A.36 Raw data for experimental point of A_5; PN= 180, TS_o = 20 g/l, T=51 ºC

Time (h)	V_G, i (ml)	V_W, i (ml)	$\sum V_W$, i (ml)	$^1C_{H2}$, i (%)	$^2C_{H2}$, i (%)	$^{total}V_{H2}$,i (ml/day)	V_{H2},i (ml)	n_{H2},i (mmol)	pH	ORP	TS_o (g/l)	TS_f (g/l)
0	340	0	0	0	0	0	0	0			19.32	
20	340	150	150	17.335	6.936	84.9415	84.9415	3.197136	6.1	26		
46	342	460	610	37.969	23.5	280.7903	365.7318	13.76587	5.4	-15		
67	344	390	1000	26	15.248	110	475.7318	17.90619	5.46	-37		
96	346	630	1630	35.706	24.168	295.7325	771.4642	29.03735	5.67	-53		
120	348	310	1940	42.464	20.771	195.3085	966.7727	36.38861	5.68	-89		
140	350	80	2020	25.318	25.318	36.1689	1002.942	37.74999	5.87	-104		
164	352	95	2115	34	34	62.86064	1065.802	40.11601	6.04	-102		
186	354	50	2165	35.565	35.565	23.3226	1089.125	40.99386	6.19	-123		
218	356	90	2255	32.015	32.015	28.8135	1117.938	42.07838				0.83

Table A.37 Raw data for experimental point of A_6; PN= 180, TS_o = 20 g/l, T=39 ºC

Time (h)	V_G, i (ml)	V_W, i (ml)	$\sum V_W$, i (ml)	$^1C_{H2}$, i (%)	$^2C_{H2}$, i (%)	$^{total}V_{H2}$,i (ml/day)	V_{H2},i (ml)	n_{H2},i (mmol)	pH	ORP	TS_o (g/l)	TS_f (g/l)
0	340	0	0	0	0	0	0	0	5.85		19.32	
23	340	500	500	26.386	9.643	221.6424	221.6424	8.663321	5.24	-170		
48	342	550	1050	30.89	13.125	242.5597	464.2021	18.14424	5.65	-110		
74	344	315	1365	27.987	12.041	139.2843	603.4865	23.58843	5.58	-103		
98	346	245	1610	25.0507	10.167	106.3878	709.8742	27.7468	5.82	-122		
121	348	50	1660	20.932	20.932	47.9282	757.8024	29.62017				0.34

Table A.38 Raw data for experimental point of F_1; PN= 240, TS_o = 30 g/l, T=55 ºC

Time (h)	V_G, i (ml)	V_W, i (ml)	$\sum V_W$, i (ml)	$^1C_{H2}$, i (%)	$^2C_{H2}$, i (%)	$^{total}V_{H2}$,i (ml/day)	V_{H2},i (ml)	n_{H2},i (mmol)	pH	ORP	TS_o (g/l)	TS_f (g/l)
0	340	0	0	0	0	0	0	0	5.81		29.95	
13	340	880	880	30.234	7.793	368.8548	368.8548	14.60464	6	-150		
37	342	980	1860	46.372	16.685	586.3858	955.2406	37.82232	5.6	-152		
65	344	630	2490	23.127	11.443	167.8606	1123.101	44.46869	5.97	-196		
87	346	360	2850	19.498	11.738	98.0631	1221.164	48.35145	5.58	-126		
115	348	310	3160	27.423	27.423	139.5951	1360.759	53.87866	5.75	-135		
137	350	130	3290	32.596	32.596	60.4803	1421.24	56.27335	5.93	-143		
156	352	90	3380	36.7	36.7	47.47608	1468.716	58.15314	6.1	-132		
182	354	70	3450	27.604	27.604	19.3228	1488.039	58.91822	6.2	-139		0.565

Table A.39 Raw data for experimental point of F_2; PN= 240, TS_o = 30 g/l, T=35 ºC

Time (h)	V_G, i (ml)	V_W, i (ml)	$\sum V_W$, i (ml)	$^1C_{H2}$, i (%)	$^2C_{H2}$, i (%)	$^{total}V_{H2}$,i (ml/day)	V_{H2},i (ml)	n_{H2},i (mmol)	pH	ORP	TS_o (g/l)	TS_f (g/l)
0	340	0	0	0	0	0	0	0	5.8		31.65	
13	340	115	115	29.701	9.047	135.1396	135.1396	5.35079	5.58	-142		
37	342	300	415	54.601	12	319.5977	454.7372	18.00512	5.69	-149		
65	344	640	1055	15.756	13.882	113.759	568.4963	22.50936	5.58	-127		
87	346	270	1325	20.484	7	78.14972	646.646	25.60366	5.75	-110		
115	348	600	1925	17.533	17.533	141.8528	788.4988	31.22026	5.62	-114		
137	350	580	2505	37.225	37.225	284.827	1073.326	42.49786	5.78	-131		
156	352	150	2655	35.588	35.588	53.382	1126.708	44.61149	5.88	-115		1.25

Table A.40 Raw data for experimental point of F_3; PN= 240, TS_o = 10 g/l, T=55 ºC

Time (h)	V_G, i (ml)	V_W, i (ml)	$\sum V_W$, i (ml)	$^1C_{H2}$, i (%)	$^2C_{H2}$, i (%)	$^{total}V_{H2}$,i (ml/day)	V_{H2},i (ml)	n_{H2},i (mmol)	pH	ORP	TS_o (g/l)	TS_f (g/l)
0	330	0	0	0	0	0	0	0	6.01		8.27	
18	330	860	860	31.737	17.82	377.6703	377.6703	15.45549	5.52	-75		
42	332	170	1030	32.237	15.916	102.6673	480.3376	19.65697	6.03	-129		
74	334	65	1095	20.647	20.647	29.22209	509.5597	20.85283	6.34	-184		
94	336	10	1105	8.935	8.935	0.8935	510.4532	20.88939				0.16

Table A.41 Raw data for experimental point of F_4; PN= 240, TS_o = 10 g/l, T=35 ºC

Time (h)	V_G, i (ml)	V_W, i (ml)	$\sum V_W$, i (ml)	$^1C_{H2}$, i (%)	$^2C_{H2}$, i (%)	$^{total}V_{H2}$,i (ml/day)	V_{H2},i (ml)	n_{H2},i (mmol)	pH	ORP	TS_o (g/l)	TS_f (g/l)
0	330	0	0	0	0	0	0	0	5.9		8.33	
18	330	740	740	36.483	11.704	390.3681	390.3681	15.97512	5.68	-460		
42	332	70	810	18.208	8.375	34.33888	424.707	17.38038	5.99	-123		
74	334	10	820	21.935	21.935	47.4839	472.1909	19.32358	5.94	-160		
94	336	0	820	10.188	10.188	0	472.1909	19.32358				0.19

Table A.42 Raw data for experimental point of F_5; PN= 120, TS_o = 30 g/l, T=55 ºC

Time (h)	V_G, i (ml)	V_W, i (ml)	$\sum V_W$, i (ml)	$^1C_{H2}$, i (%)	$^2C_{H2}$, i (%)	$^{total}V_{H2}$,i (ml/day)	V_{H2},i (ml)	n_{H2},i (mmol)	pH	ORP	TS_o (g/l)	TS_f (g/l)
0	420	0	0	0	0	0	0	0	5.83		33.5	
18	420	650	650	43.879	4.063	469.5053	469.5053	18.58985	5.94	-194		
42	422	1280	1930	40.278	9.497	668.3857	1137.891	45.05428	5.8	-188		
72	424	680	2610	52.414	19.263	538.3833	1676.274	66.37133	5.72	-189		
95	426	180	2790	22.346	22.346	53.35638	1729.631	68.48395	5.82	-167		
122	428	50	2840	37.417	37.417	83.21238	1812.843	71.77871	5.85	-153		
144	438	80	2920	46.93	46.93	79.21094	1892.054	74.91503	6.1	-136		
166	438	180	3100	51.75	51.75	114.2616	2006.316	79.43917	6.3	-138		
188	438	210	3310	58.217	58.217	150.5812	2156.897	85.40136	5.8	-145		
214	438	40	3350	61.14	61.14	37.25874	2194.155	86.8766	5.6	-166		
237	438	40	3390	58	58	23.2	2217.355	87.7952		-170		1.34

Table A.43 Raw data for experimental point of F_6; PN= 120, TS_o = 30 g/l, T=35 ºC

Time (h)	V_G, i (ml)	V_W, i (ml)	$\sum V_W$, i (ml)	$^1C_{H2}$, i (%)	$^2C_{H2}$, i (%)	$^{total}V_{H2}$,i (ml/day)	V_{H2},i (ml)	n_{H2},i (mmol)	pH	ORP	TS_o (g/l)	TS_f (g/l)
0	360	0	0	0	0	0	0	0	5.98		29.74	
20	360	760	760	44.039	16.456	493.2368	493.2368	19.52949	5.69	-472		
43	362	850	1610	31.302	12.343	319.8095	813.0463	32.1922	5.79	-116		
62	364	250	1860	36.924	20.336	181.7848	994.8312	39.38989	5.56	-117		
86	366	430	2290	27.823	11.912	147.0413	1141.872	45.21193	5.53	-113		
116	368	830	3120	35.072	14.622	376.3264	1518.199	60.1124	5.58	-159		
139	370	110	3230	24.42	24.42	63.1146	1581.313	62.6114	5.53	-145		
166	372	20	3250	18.464	18.464	3.6928	1585.006	62.75761				1.05

Table A.44 Raw data for experimental point of F_7; PN= 120, TS_o = 10 g/l, T=55 ºC

Time (h)	V_G, i (ml)	V_W, i (ml)	$\sum V_W$, i (ml)	$^1C_{H2}$, i (%)	$^2C_{H2}$, i (%)	$^{total}V_{H2}$,i (ml/day)	V_{H2},i (ml)	n_{H2},i (mmol)	pH	ORP	TS_o (g/l)	TS_f (g/l)
0	360	0	0	0	0	0	0	0	6.17		8.24	
17	360	270	270	28.344	14.672	178.5672	178.5672	7.307546	6.39	-9		
42	362	65	335	43.945	0	134.5325	313.0997	12.81305	5.68	-97		
68	364	65	400	9.319	5.828	39.97851	353.0782	14.4491	5.85	-101		
90	366	40	440	9.556	6.043	17.46688	370.5451	15.1639	6.08	-157		
117	368	80	520	17	17	53.92176	424.4669	17.37055	6.25	-103		
137	370	20	540	7.412	7.412	1.4824	425.9493	17.43122				0.14

Table A.45 Raw data for experimental point of F_8; PN= 120, TS_o = 10 g/l, T=35 ºC

Time (h)	V_G, i (ml)	V_W, i (ml)	$\sum V_W$, i (ml)	$^1C_{H2}$, i (%)	$^2C_{H2}$, i (%)	$^{total}V_{H2}$,i (ml/day)	V_{H2},i (ml)	n_{H2},i (mmol)	pH	ORP	TS_o (g/l)	TS_f (g/l)
0	360	0	0	0	0	0	0	0	5.8		9.17	
15	360	120	120	11.986	5.107	57.5328	57.5328	2.277985	5.62	-502		
42	362	350	470	18.269	9.509	111.5879	169.1207	6.69626	5.77	-287		
66	364	60	530	11.951	5.961	16.05948	185.1802	7.332128	6.12	-233		
87	366	15	545	7.167	4.615	5.48901	190.6692	7.549463	6.25	-188		
109	368	20	565	5.719	5.719	5.20652	195.8758	7.755613	6.34	-136		
133	370	10	575	6.547	6.547	3.7183	199.5941	7.902837	6.36	-130		
155	372	0	575	7.203	7.203	2.44032	202.0344	7.99946				0.46

Table A.46 Raw data for experimental point of C_1; PN= 180, TS_o = 20 g/l, T=45 ºC

Time (h)	V_G, i (ml)	V_W, i (ml)	$\sum V_W$, i (ml)	$^1C_{H2}$, i (%)	$^2C_{H2}$, i (%)	$^{total}V_{H2}$,i (ml/day)	V_{H2},i (ml)	n_{H2},i (mmol)	pH	ORP	TS_o (g/l)	TS_f (g/l)
0	340	0	0	0	0	0	0	0	5.88		20.07	
14	340	430	430	18.762	9.3	144.4674	144.4674	5.720122	5.94	-327		
43	342	510	940	42.282	20.062	328.4366	472.904	18.72442	5.61	-189		
65	344	900	1840	43.967	30.716	477.9362	950.8402	37.64809	5.63	-137		
94	346	90	1930	29.749	29.749	26.7741	977.6143	38.7082	5.86	-151		0.85

Table A.47 Raw data for experimental point of C_2; PN= 180, TS_o = 20 g/l, T=45 ºC

Time (h)	V_G, i (ml)	V_W, i (ml)	$\sum V_W$, i (ml)	$^1C_{H2}$, i (%)	$^2C_{H2}$, i (%)	$^{total}V_{H2}$,i (ml/day)	V_{H2},i (ml)	n_{H2},i (mmol)	pH	ORP	TS_o (g/l)	TS_f (g/l)
0	340	0	0	0	0	0	0	0	6.19		23.04	
15	340	540	540	41.992	22.235	369.5296	369.5296	14.63136	6.07	-181		
44	342	820	1360	33.683	16.559	315.3528	684.8824	27.11761	5.93	-374		
65	344	210	1570	21.164	10.089	60.2856	745.168	29.50459	5.57	-107		
86	346	160	1730	16.092	16.092	46.51758	791.6855	31.34643	5.72	-106		
110	348	75	1805	21.664	21.664	35.63856	827.3241	32.75753	5.9	-135		
135	350	30	1835	19.625	19.625	5.8875	833.2116	32.99064	5.99	-151		0.98

Table A.48 Raw data for experimental point of C_3; PN= 180, TS_o = 20 g/l, T=45 ºC

Time (h)	V_G, i (ml)	V_W, i (ml)	$\sum V_W$, i (ml)	$^1C_{H2}$, i (%)	$^2C_{H2}$, i (%)	$^{total}V_{H2}$,i (ml/day)	V_{H2},i (ml)	n_{H2},i (mmol)	pH	ORP	TS_o (g/l)	TS_f (g/l)
0	340	0	0	0	0	0	0	0	6.2		22.32	
15	340	650	650	43.75	18.653	433.125	433.125	17.14939	6.07	-181		
44	342	800	1450	30.698	9.945	286.7779	719.9029	28.50423	5.69	-250		
65	344	270	1720	33.555	10.574	171.8169	891.7198	35.30725	5.6	-114		
86	346	140	1860	14.994	14.994	36.2848	928.0046	36.74393	5.85	-136		
110	348	80	1940	24.285	24.285	51.76068	979.7653	38.79337	601	-540		
135	350	20	1960	19.255	19.255	3.851	983.6163	38.94585	6.11	-127		0.34

A.2 Abbreviations

AHWS	Acid hydrolyzed wheat starch
A_x	Axial points in Box-Wison statistical experiment design
CHV	Cumulative hydrogen gas volume
COD	Chemical oxygen demand
C_x	Center points in Box-Wison statistical experiment design
DNA	Deoxyribonucleic acid
EDTA	Ethylenediaminetetraacetic acid
Fd_{ox}	Oxidized ferredoxin
Fd_{rd}	Reduced ferredoxin
Fe(II)/C	Ferrous to carbon ratio
FHL	Formate:hydrogen lyase
F_x	Factorial points in Box-Wison statistical experiment design
h	Hour
HPR	Hydrogen production rate
IEA	International Energy Agency
N/C	Nitrogen to carbon ratio
NAD^+	Nicotinamide-adenine dinucleotide
NFOR	NADH:ferredoxin oxidoreductase
O.D.	Optical density
OLRs	Organic loading rates
ORP	Oxidation-reduction potentials
P/C	Phosphorous to carbon ratio
PFL	Pyruvate:formate lyase
PFOR	Pyruvate:ferredoxin oxidoreductase
PN	Particle number
R	Diameter of particles
T	Temperature
TS_f	Final total sugar concentration
TS_o	Initial total sugar concentration
TVFA	Total volatile fatty acid
VFAs	Volatile fatty acids

X_x	Independent variables in Box-Wison statistical experiment design
Y_{H2}	Hydrogen yield
[TS]	Total sugar concentration
$[TVFA]_0$	Initial total volatile fatty acid concentration
$[TVFA]_f$	Final total volatile fatty acid concentration
$[TVFA]_{produced}$	Total volatile fatty acid concentration produced during fermentation